Life cycle assessment of battery electric vehicles and hydrogen fuel cell vehicles

By

Dipankar Khanna

A thesis submitted in partial fulfillment of the requirements for the degree of

Master of Science

in

Engineering Management

Department of Mechanical Engineering

University of Alberta

Abstract

The global road transportation sector is a major greenhouse gas (GHG) emitting sector. In 2021, the sector generated 28% of the world's GHG emissions, mainly due to the direct burning of fossil fuels. In order to reduce the adverse impacts of climate change caused by human activities, the global community aims to cut GHG emissions from 2005 levels by 2030. A significant GHG emission contributor, the transportation sector has a crucial role to play in achieving this target. Decarbonizing the sector by fuel switching (replacing conventional diesel vehicles [CDVs] with battery electric vehicles [BEVs] and hydrogen fuel cell vehicles [HFCVs]) can make it more sustainable and environmentally friendly. BEVs and HFCVs are emerging as important options as they can significantly reduce GHG emissions, especially when coupled with a decarbonized power sector. The GHG emission savings of BEVs and HFCVs have been estimated in many studies. However, the environmental benefits of BEVs and HFCVs rely considerably on driving behavior and the climatic conditions of a given location. The global use of BEVs and HFCVs increased by 70% in 2018 from 2017 and is projected to increase further in the coming decades. Several studies have evaluated the environmental performance of BEVs and HFCVs, but few consider the impact of the key parameters that affect performance: climatic condition, drag coefficient, rolling coefficient, speed, acceleration, and road type. Nor is the environmental impact of lightweight materials such as carbon fiber reinforced plastic (CFRP) manufactured from bitumen-based asphaltene included in the studies. Mass can be reduced significantly by substituting conventional materials (steel, aluminum, copper, etc.) with lightweight CFRP. That said, CFRP brings its own set of production and economic challenges. This study, therefore, explores the impacts of these parameters on the overall life cycle performance of BEVs and HFCVs. In other words, this study

investigates in depth the influence of these missing parameters on the overall life cycle environmental performance of lightweight BEVs, HFCVs, and conventional BEVs and HFCVs.

Nine operational scenarios for BEVs and two for HFCVs were established based on prevalent road types and climatic conditions. The life cycle GHG emissions for BEVs range from 93 g CO_2 eq/km (city in summer scenario) to 258 g CO_2 eq/km (highway in severe winter scenario) for conventional BEVs, and for CFRP BEVs, from 72 g CO_2 eq/km (city in summer scenario) to 163 g CO_2 eq/km (highway in severe winter scenario). The life cycle GHG emissions for HFCV range from 107 g CO_2 eq/km (city in summer scenario) to 382 g CO_2 eq/km (highway in severe winter scenario) for conventional HFCVs, and for CFRP HFCVs, from 85 g CO_2 eq/km (city in summer scenario) to 254 g CO_2 eq/km (highway in severe winter scenario). The manufacturing emissions for conventional BEVs are 19 g CO_2 eq/km and 22 g CO_2 eq/km for CFRP BEVs. The manufacturing emissions for conventional HFCVs are 18 g CO_2 eq/km and 20 g CO_2 eq/km for CFRP HFCVs.

Often, considerably more energy is required to produce CFRP than to produce conventional raw materials such as steel, aluminum, etc. The operation phase is the largest GHG emissions contributor among the life cycle phases (manufacturing, assembly, maintenance, end of life). The operation emissions for the considered scenarios range from 50 g CO_2 eq/km (city in summer) to 175 g CO_2 eq/km (highway in severe winter scenario) for conventional BEVs and for CFRP BEVs, from 32 g CO_2 eq/km (city in summer scenario) to 102 g CO_2 eq/km (highway in severe winter scenario). The operation emissions for conventional HFCVs range from 78 g CO_2 eq/km (city in summer scenario) to 353 g CO_2 eq/km (highway in severe winter scenario), and for CFRP HFCVs, from 54 g CO_2 eq/km (city in summer scenario) to 223 g CO_2 eq/km (highway in severe winter scenario). However, the environmental performance of both CFRP BEVs and CFRP HFCVs depends highly on the CFRP production method. For HFCVs, the hydrogen production process

and the efficiency of the fuel cell highly influence production. For all the considered scenarios, however, the life cycle GHG emissions decreased significantly when conventional raw materials were replaced with CFRP for both BEVs and HFCVs. The GHG savings from the use of CFRP were highest in the highway in severe winter scenario and lowest in the city in summer scenario for both BEVs and HFCVs. This information is beneficial to those making investments and policy decisions related to BEVs and HFCVs.

Preface

This thesis is an original work by me under the supervision of Dr. Amit Kumar. Chapter 2 of this thesis is expected to be submitted as D. Khanna, E. Gemechu, and A. Kumar, "Life cycle assessment of an electric vehicle: The impact of driving pattern and climatic conditions on environmental performance" to *Applied Energy*. Chapter 3 is expected to be submitted as D. Khanna, N. Mahbub, and A. Kumar, "The development of life cycle environmental footprint of a carbon fiber-based hydrogen fuel cell vehicle for colder climate" to *Applied Energy*. I was responsible for the concept formulation, data analysis, scenario development, energy consumption quantification, greenhouse gas emissions calculations, and manuscript composition. Drs. E. Gemechu and N. Mahbub contributed by reviewing the paper and providing useful feedback. Dr. A. Kumar is the supervisory author and is involved with the concept formulation, data analysis, scenario development, energy consumption estimates, greenhouse gas emissions calculations, and manuscript composition.

Acknowledgements

I would like to acknowledge my supervisor, Dr. Amit Kumar, for his continuous support and guidance throughout my research project. His insight, expertise, and steady feedback played a significant role in my successfully completing this work. I would also like to express my gratitude to Future Energy Systems for providing the financial support to carry out this research.

It is my pleasure to thank Dr. Eskinder Gemechu for his continuous support and inspiration throughout the study period. He reviewed the research and provided valuable feedback to improve it. I am also thankful to Drs. Abayomi Olufemi Oni and Nafisa Mahbub for reviewing the work and providing feedback, as well as to Astrid Blodgett for editing it. Last but not the least, I would like to recognize my colleagues in the Sustainable Energy Research Group for their continuous support and useful discussions that helped widen my knowledge on energy research and create a productive research environment.

I am greatly thankful to my parents (Dipti Ram Khanna, Arjun Khanna, Reena Khanna, Rajan Karir)**,** my brother (Shiv Khanna, Anirudh Kembre), my sisters (Shikha Insan, Renu Kohli, Aastha Bassi), and my friends (Parth Shah, Anuj Saini) for their endless support and encouragement that helped me to achieve this level of knowledge and successfully perform this research work.

Table of Contents

List of Tables

List of Figures

Abbreviations

BEV: Battery electric vehicle

CO_2 eq: Carbon dioxide equivalent

CFRP: Carbon fiber reinforced plastic

GFRP: Glass fiber reinforced plastic

GHG: Greenhouse gas

HFCV: Hydrogen fuel cell vehicle

ICE: Internal combustion engine

ISO: International Organization for Standardization

Km: Kilometer

kW: Kilowatt

kWh: Kilowatt hour

LCA: Life cycle assessment

MJ: Mega joules

NMC: Nickel manganese cobalt

PHEV: Plug-in hybrid electric vehicle

WLTC: World harmonized light-duty vehicle test cycle

ICEV: Internal combustion engine vehicle

HVAC: Heating ventilation and air conditioning

Chapter 1

1. Introduction

1.1. Background

The transportation sector is responsible in large part for the steady increase in anthropogenic CO_2 emissions. Between 1990 and 2020, growth in the sector increased global energy demand by 22% and greenhouse gas (GHG) emissions by 25% [1, 2]. Diesel and gasoline vehicle ownership is expected to increase dramatically in the coming years, contributing to extreme dependence on fossil fuels [3]. Fossil fuel combustion emits GHGs and increases the average temperature of the earth's surface [4]. The road transportation sector, therefore, is unsustainable [4, 5]. To counter these issues, researchers and policy makers are looking for sustainable means of decarbonizing the sector [2, 6]. Some suitable options are smart vehicle design, driving efficiency, and smart fuel choices (biofuel-fueled vehicles, electrification of vehicles, and hydrogen-fueled vehicles) [3, 7, 8]. Among these, smart fuel choice (especially battery electric vehicles [BEVs] and hydrogen fuel cell vehicle [HFCVs]) could be realistic and strategic option, as it can significantly reduce GHG emissions, especially when coupled with decarbonizing the power sector [3, 8]. Unlike internal combustion engine vehicles (ICEVs), BEVs and HFCVs do not produce GHG emissions during their operation [9]. However, the energy consumption of the operation phase depends on the composition of the fuel mix, driving range, battery type, and the efficiency of electricity grid mix for BEVs [10-12]. For HFCVs, the amount of GHG emissions in the operation phase depends on the hydrogen production process and the efficiency of the fuel cell [13, 14]. The battery is the powerhouse of BEVs and the fuel cell is the powerhouse of HFCVs [11, 13].

There is a scarcity of research studies on how the battery electric vehicles (BEVs) and hydrogen fuel cell vehicles (HFCVs) perform under extreme climatic conditions, different type of roads particularly in Canada, Alberta. Maintenance and recycling phases of both BEVs and HFCVs needs a lot of exploration [15]. This research considers evaluating the environmental performance of BEVs and HFCVs using life cycle assessment (LCA) approach, considering Alberta, Canada as the base geographic location. The prime phases of this study includes raw material extraction, vehicle assembly, vehicle operation, vehicle maintenance, and end of life. The prime objective of this work focuses on evaluating the environmental performance of BEVs and HFCVs under different climatic conditions and road patterns. The prime factors that affect the energy efficiency of BEVs and HFCVs are drag coefficient, rolling coefficient, driving pattern, climatic condition, and vehicle mass [16]. The drag and rolling forces are greater for heavier and larger BEVs and HFCVs, hence the driving energy consumption is higher than for smaller and lighter BEVs [16, 17]. Weight and size play a major role in determining the energy efficiency and environmental performance of both vehicles [12] and are highly relevant to both, given that the electric motor, traction battery, electronic controller, fuel cell, hydrogen storage tank (for HFCVs), and other electronic components make these vehicles heavier than similar internal combustion engine vehicles (ICEVs) [18]. A 15% weight reduction in a BEV increases its driving range by 20% and the efficiency of the fuel cell by 6% [19]. Substituting conventional raw materials such as steel, copper, aluminum, etc., with lightweight materials like carbon fiber reinforced plastic (CFRP) can increase the energy efficiency and environmental performance of BEVs and HFCVs considerably [20]. CFRPs are fibers with 92 wt. % carbon. The carbon fibers are formed by spinning a carbon precursor to align the carbon atoms parallel to the longer axis of the fiber. This process is followed by controlled pyrolysis to remove nearly all the non-carbon atoms. Thousands of filaments 5 to 15

μm in diameter are bundled together to form a carbon fiber tow, which can be used by itself or woven into fabrics. CFRP is a strong, durable, and lightweight composite material used in manufacturing automobile bodies [20]. However, manufacturing it is complex and time consuming, making it incompatible for the mass production of CFRP vehicle parts [21]. Thus, the environmental benefits of using CFRP highly depend on the precursors and manufacturing process [21]. The most generic precursor is polyacrylonitrile (PAN); more than 90% of CFRP is produced from PAN [22]. PAN is produced through a chain of processes (crude oil production, crude oil refining to produce naphtha, ammonia production, propylene production, acrylonitrile production, polyacrylonitrile production) that depends on conventional crude oil or natural gas-based processes using either propylene or propane as a raw material [22, 23]. Asphaltenes are non-volatile and non-polar components of crude oil that dissolve in aromatics [24]. The main process of asphaltene production includes the production of bitumen, the separation of asphaltene from bitumen, and the production of asphaltene [22]. Asphaltenes from oil sands are becoming more cost effective than PAN [24]. They consist of polar components from condensed aromatics and naphthenic rings. Processed asphaltene can produce carbon fiber with high modulus and strength [20]. Given their lower mass and higher carbon percentage, bitumen-based asphaltenes are extensively used in the production of CFRPs [24]. The GHG emissions from background processes (those designated to provide the raw materials to produce the precursor) are lower in the asphaltene pathway because it has fewer energy-consuming processes (precursor and carbon fiber production) [25]. PAN production requires the recovery of solvent used for dope production. This operation consumes 83% of the total energy consumption of the process and is responsible for 73% of the GHG emissions from PAN production [23]. The asphaltene-based precursor does not require solvent recovery operations like in the production of PAN, thus the difference in GHG emissions from

precursor production between the pathways [24]. The economic value of asphaltene is low, and in current oil sand operations it is stockpiled. Because of their high carbon content and low value, bitumen-derived asphaltenes are a promising precursor for making carbon fibers [23].

1.2. Literature review and research gap

Several studies suggest that BEVs have lower GHG emissions and operating costs than internal combustion engines (ICEs) and include a wide range of estimates on the potential GHG emissions savings from replacing ICEVs with BEVs [26-29]. A few studies determined that a BEV's GHG emissions should be evaluated based on battery storage capacity, rather than considering battery life, which might lead to inconsistent results [10, 11, 30]. Thus battery life, in terms of drive range, plays a vital role in determining the operation efficiency of the battery [10]. Most recent studies conduct life cycle comparisons of BEVs, plug-in hybrid electric vehicles (PHEVs), hybrid electric vehicles (HEVs), and ICEVs, considering different phases like raw material extraction, vehicle assembly, operation, and end of life to evaluate environmental performance in terms of GHG emissions savings [31-33]. Some LCA studies consider only specific and core components of BEVs such as traction battery and traction motor, leaving out the details of the fluids, auxiliary battery, and electronic controller (minor components) while formulating life cycle inventories [2, 12, 34]. Leaving out descriptions of minor components during inventory formulation can lead to difficulties in computing the exact amount of each material used in manufacturing a BEV [18, 35, 36]. Most of the reviews discuss lithium-ion batteries as having lithium iron phosphate and lithium manganese oxide as precursors, the most used precursors [37-40]. Few studies consider the next-generation precursor nickel manganese cobalt oxide (NMC).

BEVs have grown and adapted remarkably in different countries. Recently, Hedegaard et al. assessed the environmental impacts of EV adaption in Denmark, Finland, Norway, Sweden, and Germany [41]. De Tena and Preggers provided deep insight into the adaption of EVs in Germany in the context to EV growth and the generation of renewable energy sources [42]. Most LCA studies focus on the use phase because it is considered that vehicle assembly, maintenance, and end of life are not significant as together they contribute to only 10% of the total life cycle emissions [10, 11, 43, 44]. But without these phases we do not learn the actual GHG emissions saving potential of BEVs, because of the incomplete quantification of inventory data and raw material production data [10, 11]. Bellocchi et al. show a positive correlation between BEVs and different renewable sources of energy (wind, solar, hydro, etc.), with the aim of reducing GHG emission generation while producing electricity for EV charging, in Italy [45]. The environmental performance or GHG emissions of an EV depend mostly on the type of energy source producing electricity for the grid mix for the considered geographic location (for the operation phase) [46], [15]. EVs do not reduce GHG emissions if the grid mix is composed of high GHG-emissive energy sources like coal and natural gas [15]. McCarthy et al.'s study assessed the impacts of BEV performance based on California's electricity grid mix in a well-to-wheel (WTW) analysis that included different phases like fuel extraction, processing, distribution, storage, and use [47]. A few studies analyzed other environmental issues, such as non-exhaust particulate emissions and noise [9]. Some studies discussed the impacts of crucial parameters like driving pattern (speed and acceleration, drag coefficient), type of road (flat, hill), and climatic conditions (summer, winter) on the overall environmental performance of EVs [9, 12, 17].

Candelaresi et al. conducted a comprehensive comparative life cycle assessment of ICEVs and HFCVs and provided a wide range of estimates on the potential GHG emissions savings in

different environmental and road conditions [48]. Other studies explored the energy requirement and GHG emissions in the production of the prime components of HFCVs such as the powertrain, chassis, fuel cell, body, etc. [49]. Mehmeti et al. determined the efficiency and effectiveness of conventional and emerging technologies used for hydrogen production [50]. The efficiency of hydrogen production from coal gasification ranges from 50% to 80%, depending on the technology, quantity and quality of coal used. The efficiency of hydrogen production from natural gas ranges from 65% to 80% depending on the composition of the fuel mix. Ptasinski et al. stressed the importance of producing hydrogen from biomass because it is renewable source [51]. Valente et al. discussed the role of hydrogen as fuel in every life cycle phase of HFCVs (especially the operation phase), considering different hydrogen production pathways. They predicted that the choice of hydrogen production pathway significantly impacts the overall life cycle performance of the HFCV. The hydrogen production pathways considered were water electrolysis, biomass conversion, coal gasification, natural gas reforming, and steam methane reforming (SMR). SMR was identified as the preferred production pathway [52]. Pehnt et al. discussed the theoretical and real efficiency of the fuel cell considering transportation losses, auxiliaries losses, and hydrogen storage losses [53].

Several studies indicate that lightweight vehicles can be fabricated with CFRP, which is both light and mechanically strong and durable [54]. Reducing a vehicle's weight will increase driving efficiency, reduce energy consumption (especially during operation), and increase overall environmental performance [19], [55], [56]. Witik et al. conducted detailed life cycle and techno-economic assessments of different lightweight materials such as CRFP and glass fiber reinforced plastic (GFRP) [57]. Das et al. estimated that enhanced vehicle lightweighting could save 66.1 billion Gj of primary energy by 2050 [58]. Belingardi et al. reduced the weight of a passenger

ICEV by 55% by substituting steel and aluminum (conventional raw materials) with CFRP [59]. However, weight saving and strength are not fully reliable factors while examining the environmental performance of vehicles [21]. Recent studies found that compared to conventional raw materials (steel, aluminum, etc.), CFRP generally increases the environmental impact during the vehicle production phase because of CFRP's high cumulative energy demand [21]. Ghosh et al. studied the impact of carbon nanofiber composites through life cycle analysis and noted the challenges associated with the production of carbon nanofiber and the lack of inventory data for these lightweight materials [20]. In commercial vehicles, CFRP is used to manufacture the powertrain, transmission, chassis, etc., to reduce its overall weight and improve environmental performance [60].

Geographic location plays a vital role in determining the overall environmental performance of both BEVs (especially the performance of the battery) and HFCVs (especially the fuel cell and hydrogen production process) [28]. Few studies consider the impact of severe temperature conditions (like those in Alberta, Canada) on the life cycle performance of BEVs and HFCVs.

1.3. Research motivation

The following statements best summarize the factors that motivated this research:

1. There is very limited research on determining the environmental performance of BEVs and HFCVs in public domain.
2. There is no comprehensive, bottom-up data-intensive models nor customized data sets; these are required to understand the environmental feasibility of BEVs and HFCVs.
3. The need for a cradle-to-grave life cycle analysis to examine the GHG emissions of BEVs and HFCVs throughout their life cycle.
4. There is very limited on research on the impact of life cycle GHG emissions of BEVs and HFCVs considering the impact of driving pattern and climatic conditions.
5. There is very limited research on the life cycle GHG emissions of BEVs and HFCVs with light weight material such as carbon fiber.

1.4. Research objectives

The prime objective of this research is to develop a life cycle framework to examine the environmental impacts and determine the GHG footprints of BEVs and HFCVs considering the driving patterns and climatic conditions. The specific objectives are as follows:

1. To develop an LCA framework to estimate the total energy consumption and life cycle GHG footprint of conventional BEVs and HFCVs throughout their life cycle.

2. To develop the life cycle GHG emissions of BEVs and HFCVs considering the driving patterns and climatic conditions.
3. To compare in detail conventional BEVs and HFCVs with CFRP BEVs and HFCVs in order to identify the impacts of a weight decrease on overall and individual life cycle phase environmental performance.
4. To conduct detailed sensitivity and uncertainty analyses to determine and predict the crucial input parameters that significantly impact energy consumption and overall GHG emissions.
5. To calculate the total energy requirement of conventional and CFRP BEVs and HFCVs throughout their life cycle, including computing energy indices like net energy ratio.
6. To identify the key components and processes in every life cycle phase that produce GHG emissions.

1.5. Scope and limitations of the thesis

This research focuses only on BEVs and HFCVs. The study evaluates the life cycle performance of BEVs and HFCVs in Alberta, Canada. Only the major greenhouse gases like CO_2, CH_4, and N_2O are considered to compute GHG emissions. In the sensitivity and uncertainty analyses, only the more sensitive parameters are considered. The scope and limitations of this study are discussed further in chapters 2 and 3. In this study, conventional (manufactured from steel, aluminum, copper, etc.) vehicles and CFRP BEVs (manufactured from CFRP) as well as conventional and CFRP HFCVs were compared to investigate the

impacts of a weight decrease on the environmental performance of each life cycle phase, especially the operation phase. The base geographic location for this study is Alberta, Canada.

1.6. Organization of the thesis

This thesis is in a paper-based format and is organized in such a way that each chapter can be read independently. Because of this, some background information is repeated in the chapters. There are four chapters. Chapters 2 and 3 are independent papers.

Chapter 2, The life cycle assessment of a battery electric vehicle (BEV): The impact of driving pattern and climatic conditions on environmental performance. A comprehensive LCA framework of a conventional BEV was developed to evaluate its environmental impacts in different driving and climatic conditions and road types, and to compare it with a CFRP-based BEV. The assumptions and data requirement of the considered life cycle phases are explained in detail. The research includes battery replacement and the factors impacting it such as driving range and depth of discharge. The chapter also explains how the climatic conditions, types of roads, use of CFRP, and the dynamic aspect of Alberta's electricity grid mix impact the overall environmental performance of BEVs. The work includes sensitivity and uncertainty analyses for transparent results.

Chapter 3, the life cycle assessment of a hydrogen fuel cell vehicle (HFCV): The impact of driving pattern and climatic conditions on environmental performance. A comprehensive LCA framework of a conventional HFCV was developed to evaluate its environmental impacts considering different driving conditions, hydrogen production pathways, fuel cell efficiency, climatic

conditions, and road types and compared it with a CFRP-based HFCV. The assumptions and data requirement of all the considered life cycle phases are explained in detail. The chapter also explains how climatic conditions, road type, CFRP use, hydrogen production pathways, and fuel cell efficiency impact the overall environmental performance of the HFCV. This chapter includes sensitivity and uncertainty analysis for transparent results.

Chapter 4, Conclusions and recommendations for future work. This chapter concludes the thesis with the main findings and significant observations. It also identifies key areas where further investigation can be conducted along with some recommendations to refine the current model.

Chapter 2

2. Life cycle assessment of an electric vehicle: The impact of driving pattern and climatic conditions on environmental performance

2.1. Introduction

The global transportation sector is among the major greenhouse gas (GHG)-emitting sectors and is responsible for almost 14% of emissions [61]. The largest portion of GHG emissions is from fossil fuels use in road transportation, which accounts for 72% of the sector's GHG emissions [61]. In 2018, 90% of the vehicles operating on the road globally were gasoline- and diesel-fueled [62]. As a result of the steady growth of the transportation sector, energy demand increased by 9.3% and GHG emissions by 20% from 2015 to 2020 [63]. In response to the threats of climate change, governments around the world are making combined efforts under the Paris Agreement, which aims to restrict the temperature rise of the earth's surface to well below 2 C^o [64]. Deep decarbonization of the transportation sector could play a critical role in achieving this target [65-67]. Some of the best approaches to decarbonizing the road transportation sector are technology efficiency improvement, electrification, and a shift to low-carbon fuel [68, 69]. Electrification of vehicles is emerging as one of the key options [69, 70], as it can significantly reduce GHG

emissions compared to gasoline vehicles and serves as a long-term solution especially when coupled with the decarbonized power sector [69, 71]. Unlike conventional internal combustion engine (ICE) vehicles, battery electric vehicles (BEVs) do not directly emit carbon dioxide during operation. However, BEVs could have significant GHG emissions depending on how the electricity stored in the battery is sourced (from renewable energy or a fossil fuel-dominated grid mix) [33]. In addition to the grid mix, other factors such as energy efficiency, battery type and size [71], driving range [71], and driving conditions and pattern also influence the overall performance of an EV [72, 73].

The amount of energy recovered by regenerative braking strongly affects the energy performance of BEVs, especially on steep uphill and downhill roads. Aggressive driving patterns cannot provide the desired outcome of regenerative braking in terms of energy savings, because of the sudden acceleration and deceleration [11]. The energy required by auxiliary systems for heating and air conditioning also affects the energy efficiency of a BEV. Unlike internal combustion engine (ICE) vehicles, which use waste heat from the engine, BEVs draw energy from the battery. Depending on the climate conditions, the heating could increase energy consumption by up to 40% in extremely cold weather compared to normal conditions [31, 46].

Vehicle size and weight are other key factors that affect energy efficiency. Rolling and air resistance are greater for large and heavy vehicles, hence the driving energy consumption is higher for light and small vehicles [11, 33]. Reducing the weight by using alternative materials can improve energy efficiency and GHG performance. This is more relevant for BEVs since the requirement of batteries and additional electrical components makes them heavier than similar ICE vehicles. A 10% weight reduction in a BEV increases its driving range by 13.7% [74]. Using lightweight materials such as carbon fiber reinforced plastic (CFRP) or glass fiber reinforced

plastic (GFRP) can improve energy efficiency in BEVs [75]. CFRP is a composite material produced by impregnating carbon fibers with a thermosetting resin. CFRP is one-quarter the weight and ten times stronger than conventional steel [74]. CFRP is used in a wide range of vehicle structural and non-structural components [76]. However, the net environmental benefits of CFRP use in BEVs are highly dependent on the precursors used and the manufacturing process involved in CFRP production. Polyacrylonitrile (PAN) is the most widely used precursor; it accounts for around 90% of current carbon fiber production. Asphaltene from the oil sands process recently emerged as a cost-effective alternative to PAN. Asphaltenes are heavy fractions of bitumen and crude oil that are soluble in n-heptane. Because of their high carbon content and low value, bitumen-derived asphaltenes are promising precursors for carbon fiber manufacturing. Recently Loreto et al. developed a process model to evaluate the life cycle GHG emissions and cost of asphaltene-based carbon fiber [77].

Studies on BEVs mainly compare their environmental performance with internal combustion engine vehicles (ICEVs), plug-in hybrid electric vehicles (PHEVs), and hybrid electric vehicles (HEVs) through life cycle assessment (LCA) [2, 5, 9, 31, 66, 78, 79]. A wide range of estimates on the potential energy and GHG emissions savings is reported in the literature. For example, Hawkins et al. found that BEVs can reduce GHG emissions by 9 and 29% compared to ICEVs in an average European Union (EU) electricity mix [44]. Garcia et al., on the other hand, found a GHG reduction of 30-39% when they considered the electricity mix and climate conditions in Portugal [80]. The GHG emission savings from BEVs highly depend on climatic conditions, roads, and driving patterns. Vehicle and battery lifetime are also important parameters that significantly affect life cycle GHG emissions [15, 44, 80-82]. Depending on driving patterns and climatic conditions in a particular geographic location, a BEV's battery may need to be replaced several

times [15, 82, 83]. Hence, the overall environmental performance of BEVs is highly dictated by electricity mix, driving patterns, and climatic conditions.

Several BEV LCA studies have been conducted for specific jurisdictions. Weis et al. computed the effects of BEV charging on cost and GHG emissions in the US [84], and Onat et al. conducted a state-based comparative energy and carbon footprint in the US [85]. The latter study concluded that BEVs are the least energy-intensive options in 24 of 50 states. The production of the electricity by low emission energy sources leads to lower GHG emissions in 24 of 50 states. Recently, Andersson and Börjesson evaluated the impacts of renewable fuel use on the life cycle GHG performance of electric vehicles in the EU [86]. Renewable fuels appear to offer higher GHG reduction than a low carbon electricity mix.

On the material side, only a few studies demonstrate replacing conventional materials with lightweight alternatives such as CFRP as an effective strategy to enhance vehicle efficiency, reduce vehicle weight, and reduce overall environmental impacts. CFRP provides necessary mechanical strength and significant weight reduction compared to conventional materials such as steel and aluminum [76]. While using CFRP instead of steel and aluminum offers weight-saving and strength, the GHG emissions associated with the energy and material requirements in the manufacturing of CFRP are problematic. CFRP conversion processes are known to be energy- and GHG-intensive [21]. Hence, it is important to look at the environmental benefit from the full life cycle perspective. Furthermore, the life cycle GHG effect of environmental asphaltenes-based carbon fiber CFRP has not yet been explored in the literature. This study, therefore, primarily aims to address these knowledge gaps. The overall aim of the paper is to develop an LCA framework to evaluate the impacts of asphaltene-based CFRP use, driving conditions, and climate factors on the overall GHG performance of a lightweight BEV. The specific objectives are:

- To develop an LCA framework to estimate the total energy consumption and life cycle GHG footprint of a conventional BEV throughout its life cycle.
- To study the GHG emission footprint of BEVs based on climatic conditions, roads, and driving patterns.
- To compare in detail a conventional BEV with a CFRP BEV in order to identify the impacts of a weight decrease on overall and individual life cycle phase environmental performance.
- To conduct detailed sensitivity and uncertainty analyses to determine and predict the crucial input parameters that can significantly impact the energy consumption and overall GHG emissions.
- To calculate the total energy requirement of the conventional and CFRP EVs throughout their life cycle, including computing energy indices like net energy ratio.
- To identify the key components and processes in every life cycle phase that produce GHG emissions.

2.2. Method

This section presents the method followed to evaluate the environmental performance of a carbon fiber-based lightweight battery electric vehicle (BEV) and a conventional BEV. We used LCA, an internationally standardized approach (as per the International Organization for Standardization [ISO]), to evaluate the environmental impacts of the BEV systems [87, 88]. LCA, according to the ISO framework, has four phases: goal and scope definition, life cycle inventory analysis, life cycle impact assessment, and interpretation of results [88, 89]. LCA is implemented to define the goal and scope of a project; compile all the relevant energy of the required raw materials, and quantify

the associated GHG emissions produced in each of the considered life cycle phases [90, 91]. Each stage of the LCA is discussed below in detail.

2.2.1. Goal and scope definition

The primary goal of this study is to evaluate the life cycle GHG emissions of a lightweight BEV vehicle produced using carbon fiber from bitumen-based asphaltene. This study also compares the GHG performance of a lightweight BEV with a conventional BEV (steel- and aluminum-based BEV). 1 km is used as a functional unit, a measured performance of a product that can be used as a reference unit [90, 91]. The life cycle GHG emissions are expressed in terms of g CO_2 eq/km. The lifetime of a vehicle depends on factors such as survival rate (defined by the manufacturer [92]), climatic conditions, driving patterns, and road conditions [93]. A mid-size five-seat passenger car with a lifetime driving distance of 200,000 km is considered in this study. The choice of vehicle lifetime is based on specific climate and driving conditions and three studies [9, 71, 94]. Alberta, Canada, is used as the location for a case study. LCA uses a cradle-to-grave system, including different product phases such as raw material extraction, vehicle production, vehicle assembly, operation, maintenance, recycling, and disposal. Raw material extraction incudes the extraction of different raw materials required to produce BEVs. The emissions factor of the required raw materials is calculated in the GREET model considering Canada as the prime geographic location. The assembly phase involves the use of the different equipment and machinery to assemble the prime components of BEVs to form complete assembled BEV [18]. Indirect inputs include the transportation of the vehicle's equipment from the manufacturing location to the appropriate assembly location, etc. [29]. The operation phase incorporates the calculation of energy consumption for different scenarios formulated based on different road types and seasons in Alberta, Canada. The replacement and maintenance of batteries, tires, fluids,

traction motors, and fluids are considered in the operation and maintenance phases of this study [95]. Recycling and disposal are the two prime categories of the end-of-life phase and are further classified into sorting or dismantling, shredding, transportation, and landfilling [96]. All the above-mentioned life cycle phases include the calculation of equivalent CO_2 emissions.

2.2.2. Alberta and Canada context

Canada's transportation sector is the second-largest contributor to GHG emissions and in 2017 generated 174.3 Mt CO2 eq, mostly from fossil fuel consumption [63]. There is a need to find suitable alternatives that can mitigate the threats from extreme dependence on gasoline and diesel [97]. In 2018, BEV sales in Canada made up to 2.2% of vehicle sales [97]. To promote the growth of BEV sales and ownership, the Government of Canada provides incentives and rebates; the Government of Canada's EV Incentive Program, for example, offers a $2,500 to $5,000 rebate on EV purchases [98]. The federal government has also invested $437 million to build BEV charging infrastructure [99]. In Alberta, 90% of registered vehicles use gasoline and diesel [100] and emit 30.7 Mt CO2 eq of GHG emissions, which accounted for 11% of the province's GHG emissions in 2017 [63]. Alberta's transportation sector generates far more GHG emissions than the other provinces' transportation sectors do. So, there is a need to replace gasoline and diesel engine vehicles with BEVs in Alberta to meet GHG emissions reduction targets.

The highlights from our LCA results is critical for Alberta's Bitumen Beyond Combustion program, which presents technological advancements by creating high-value and non-combustion products from bitumen [101]. The use of carbon fiber as a steel and aluminum alternative is viewed as an environmentally sustainable solution in the transportation sector. However, it is important to quantify the benefit by considering the entire life cycle

from the extraction of resources to vehicle manufacturing, assembly, vehicle operation, maintenance, and end of life [24].

Alberta is unique in its climate. It has cold climate with long winters with several months of below zero temperature [102]. It is critical to understand the GHG performance of the BEVs in these kinds of colder countries.

Figure 1 depicts the system boundary that specifies the life cycle stages and unit processes involved in the product system. A cradle-to-grave analysis was performed. The complete life cycle of a vehicle comprises vehicle production, vehicle use, end of life, and the upstream process. Each life cycle stage along with the data requirements are discussed in the inventory analysis.

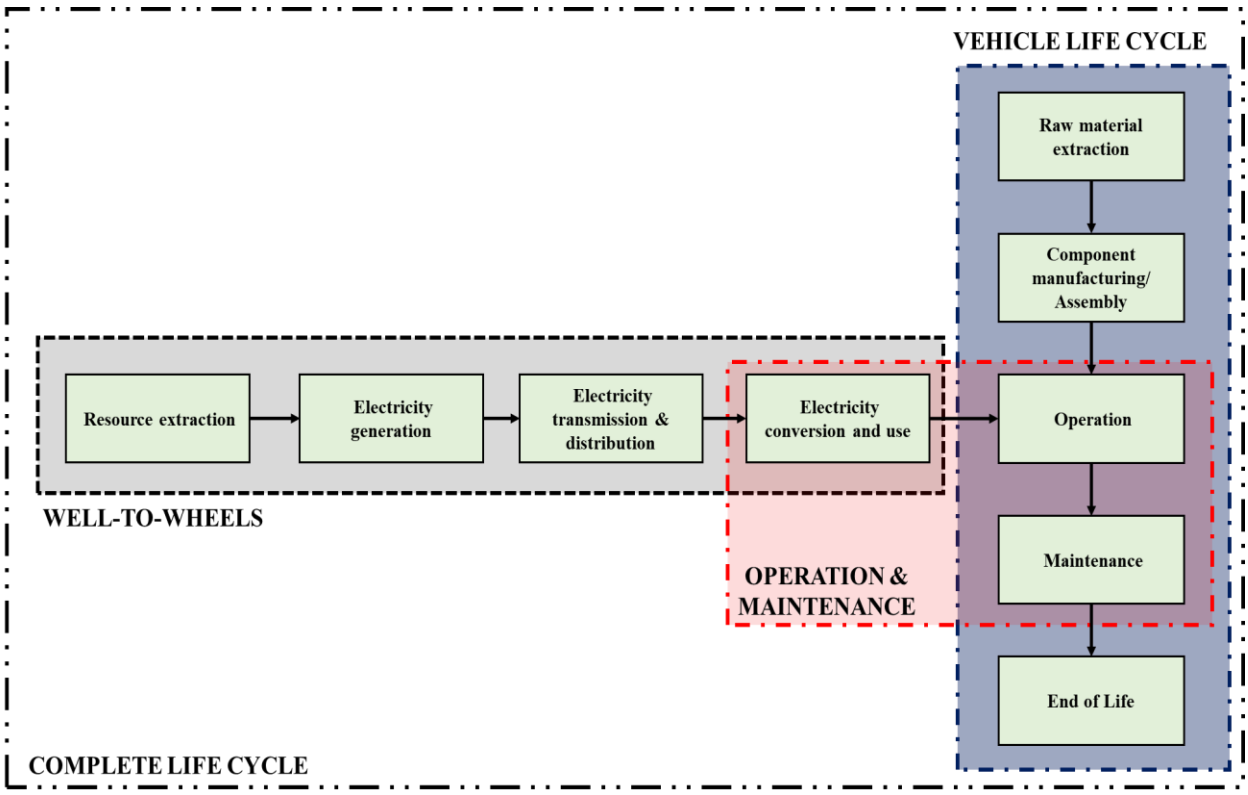

Figure 1: System boundary of a battery electric vehicle life cycle

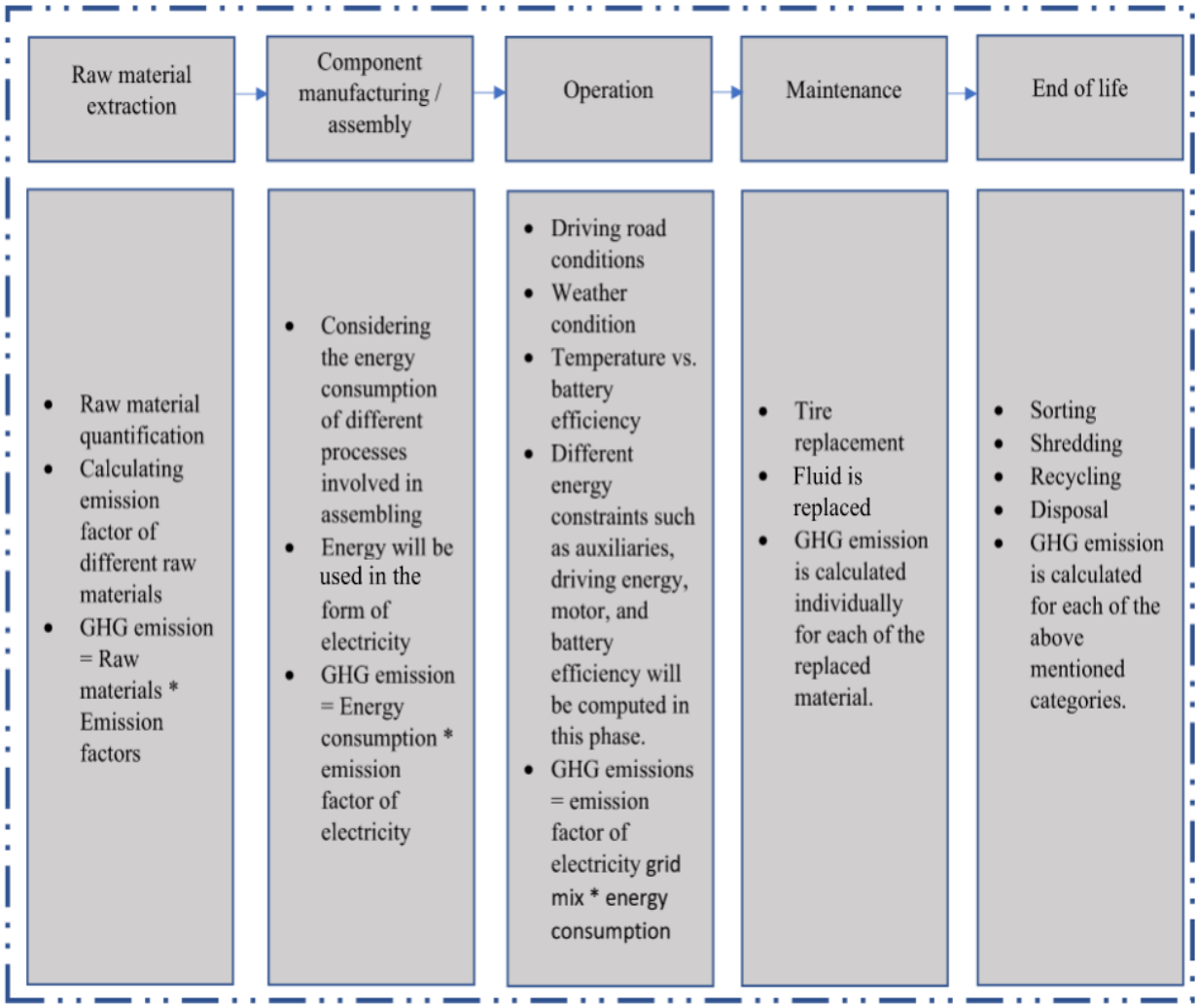

Figure 2: Key parameters and the process for GHG emissions calculations in each life cycle phase

2.2.3. Inventory analysis

2.2.3.1. Vehicle production

Two pathways were considered for vehicle production: a conventional steel and aluminum-based BEV and a carbon fiber-based lightweight BEV made from asphaltene. The main vehicle components in both cases are the body in white, interior and exterior, chassis, controller, powertrain system, traction battery, traction motor, and transmission system [18]. First, we developed the vehicle inventory, which includes the prime components of a BEV mentioned above [18]. The gross mass of a conventional vehicle is 1,511 kg, of which 150 kg is the lithium-ion battery and 1361 kg are for the remaining components. [103-105]. Basic raw materials associated with the manufacturing of the key components of both conventional and carbon fiber BEVs are steel, wrought aluminum, cast aluminum, cast iron, copper, magnesium, rubber, plastic, carbon fiber reinforced plastic, and glass fiber reinforced plastic. The carbon fiber vehicle weighs 877 kg, of which 120 kg is the lithium-ion battery and 757 kg are for the remaining components. The weight can be reduced by around 42% by replacing steel and aluminum with carbon fiber. Table 1 summarizes the materials for the main components of conventional and carbon fiber-based BEVs. Steel and aluminum, the main materials in a conventional vehicle, together account for more than 64% of the total mass contribution. Most of the steel is used to make the body (415 kg), chassis (252 kg), transmission system (44 kg), and traction motor (60 kg). Aluminum is evenly distributed over several components [18]. Average plastic is used to produce most of the body and some of the chassis. CFRP is used mainly in the body interior and the body in white. A significant portion is also used in the chassis. Carbon fiber makes up 26% of the total

mass of the carbon fiber-based lightweight vehicle [55]. Table 2 lists the mass distribution by key components. CFRP and plastic materials constitute a high mass fraction in the carbon fiber-based vehicle.

Table 1: Bill of materials for conventional and carbon fiber reinforced plastic (CFRP)-based BEVs based on raw materials [18]

Materials	**Conventional vehicle**		**CFRP-based vehicle**	
	Mass, kg	**Mass, %**	**Mass, kg**	**Mass, %**
Steel/cast iron	735	48	67	8
Aluminum	241	16	80	9
Copper/brass	92	6	40	5
Magnesium	4	0	4	0
Glass	32	2	32	4
Average plastic	159	11	159	18
Rubber	92	6	92	11
Carbon fiber	0	0	225	26
Glass fiber	0	0	20	2
Others	156	10	152	18
Total	**1511**	**100**	**877**	**100**

Table 2: Bill of materials for conventional and carbon fiber reinforced plastic (CFRP)-based BEVs based on components [18]

Components	**Conventional vehicle**		**CFRP-based vehicle**	
	Mass, kg	**Mass, %**	**Mass, kg**	**Mass, %**
Transmission system	72	5	20	2
Body (body in white, interior, exterior)	623	41	282	32
Chassis (without battery)	439	29	253	29
Powertrain system	70	5	46	5
Traction motor	56	4	56	6
Electronic controller	69	5	69	8
Fluids	25	2	25	3
Battery Li ion	151	10	120	14
Battery Pb acid	6	0	6	1
Total	**1511**	**100**	**877**	**100**

A lithium nickel manganese cobalt oxide (Li-NMC) battery with 86.4 MJ or 24 kilowatt-hours (kWh) and an efficiency of 90% is assumed [18, 103, 105]. Li-NMC is among the most efficient alternatives and has a higher energy density and lower environmental burden than traditional batteries currently used in EVs [39, 40]. Carbon fiber, aluminum, steel, glycol insulation, graphite, lithium, Nickel manganese cobalt (NMC) precursor (powder), and coolant are the major components in the battery. A conventional (Li-NMC) battery with a mass of 151 kg (manufactured from conventional metals) and battery capacity of around 24 kilowatt-hours (kWh) and an efficiency of 90% is considered [15, 18, 105]. A Li-NMC battery produces fewer toxic elements or metals (i.e., iron, copper, manganese) after disposal [15, 39, 40]. We calculated energy consumption and GHG emissions for each of the key components of the battery. A lightweight lithium nickel manganese cobalt oxide battery with a mass of 120 kg, battery capacity of 24 kWh, and efficiency of 90% is considered in this study [18]. The weight of the Li-NMC battery can be reduced by around 21% by replacing steel and aluminum with carbon fiber [18, 55]. Table 3 below shows the detailed percentage mass composition comparison and the key components for both conventional and carbon fiber-based Li-NMC batteries.

Table 3: Mass distribution of lithium NMC battery by key components for conventional and CFRP-based BEVs [18, 74]

Components of Li-NMC battery	**Conventional vehicle**		**CFRP-based vehicle**	
	Mass, kg	**Mass, %**	**Mass, kg**	**Mass, %**
Active material (MNC powder)	39	26	39	32
Graphite/carbon	24	16	24	20
Binder (PVDF)	3	2	3	3
Copper	18	12	0	0
Wrought aluminum	37	24	0	0
Electrolyte: ethylene carbonate	7	5	7	6
Electrolyte: dimethyl carbonate	7	5	7	6
Plastic: polypropylene	2	1	2	1
Plastic: polyethylene	1	0	1	1
Plastic: polyethylene terephthalate	0	0	0	0
Steel	1	1	0	0
Thermal insulation	1	1	1	1
Coolant glycol	7	4	7	5
Carbon fiber	0	0	25	21
Electronic parts	6	4	6	5
Total	**151**	**100**	**120**	**100**

2.2.3.2. BEV assembly

This phase is the assembly of the key components mentioned above. The assembly stage requires different processes such as paint production, vehicle component assembly, painting, heating, ventilation and air conditioning (HVAC) and lighting, heating, material handling, welding, and lithium-ion and lead-acid battery assembly [106]. We calculated the energy consumption and GHG emissions for each process with information based on Burnham et al. [18].

2.2.3.3. Vehicle operation

Unlike internal combustion engine vehicles, BEVs use electricity to propel the wheels. The operational-related environmental performance is, hence, highly dependent on the greenness of the grid mix where the vehicle is operated. Because the electricity mix is one of the critical parameters in modeling life cycle GHG emissions, it is important to consider a grid mix that reflects the actual current situation as well as the potential change in the future [11]. In this study, Alberta is used as a reference location. Alberta's current grid mix is highly dominated by fossil fuels, which account for nearly 90% of the total electricity; renewable energy sources make up only 10% [107]. Moreover, the province generates around 60% of Canada's electricity sector GHG emissions [108]. Currently, there is a focus on phasing out coal and increasing shares of renewables such as solar and wind to ensure the transition to a low-carbon grid system. The composition of Alberta's grid mix will change significantly in the coming years, and this change will lead to a change in grid mix GHG emissions factors for the years considered in this study. The dynamic aspect of the electricity-mix and associated GHG intensities in

Alberta is, hence, considered in the analysis. The analysis allows us to accurately estimate the overall GHG emissions generated by a BEV throughout its lifetime during its operation phase. The electricity GHG emission intensity values were derived from Davis et al. [108, 109]. We used the Low Emissions Analysis Platform (LEAP) model to incorporate the dynamic aspect of GHG emission factors based on Alberta's grid mix for the 11 years between 2020 and 2030. This will help to precisely estimate the overall GHG emissions generated by the vehicle throughout its lifetime, during its operation phase. The low emission analysis platform (LEAP) is a widely used software tool for energy policy analysis and climate change mitigation assessment [109].

Table 4: GHG emission factors of Alberta's electricity grid mix for the considered years [109]

Year range	**Emission factors (g CO2 eq/MJ)**
1	151
2	141
3	134
4	110
5	114
6	122
7	117
8	113
9	100
10	92
11	85

All the use phase energy requirements are based on the regulations of the world harmonized light-duty vehicle test cycle (WLTC) [110]. The WLTC takes into consideration different climatic conditions, driving behavior, regenerative charging, type of road, and energy loss during charging to compute the net energy required to operate a BEV feasibly [111]. Energy is mainly required to drive the wheels but also for auxiliary activities such as air conditioning, heating, lighting, and so on. The net energy requirement per km travelled is the sum of all the energy consumed. However, the value of energy constraints for a particular scenario will be different from other scenarios because of the differences in specifications and characteristics of driving [29]. The amount of energy consumed by each energy constraint mentioned above depends on factors such as speed, acceleration, drag coefficient, rolling coefficient (which in turn depends on the type of road [rural, urban, highway]), and the prevalent climatic conditions (severe winter, mild winter, summer) [29]. Based on the type of road and climatic conditions in Alberta, Canada under which the vehicle is assumed to operate, nine scenarios were developed. These are city in summer, highway in summer, rural in summer, city in severe winter, highway in severe winter, rural in severe winter, city in mild winter, highway in mild winter, and rural in mild winter. A fundamental science-based equation was used in each operational scenario to compute the energy consumption and GHG emissions of the driving force to propel the vehicle. The equation of force is a combination of three forces: linear force, drag force, and rolling force. The total force is multiplied by the average travel distance to get the net energy consumption of our vehicle [29]. Linear force depends on acceleration and mass and speed of operation. The greater the value of the force, the higher the energy consumption [12].

The mass of the car is the same in each scenarios, so the scenario in which the car operates at a higher speed will correspond to a higher value of linear force. Because we travel at much higher speeds on highways than in cities and rural areas [12], energy consumption due to linear force will be higher on highways than in cities and rural areas. Drag force depends on the speed, drag coefficient, density of air, and mass of the car. The higher the speed, the greater the drag coefficient. There is more drag force on highways than in cities and rural roads, so drag force will consume more energy on highways than on cities and rural roads [17]. Rolling depends on rolling friction or the coefficient of road, mass, and acceleration due to gravity; these are the same in each scenario [17]. The rolling coefficient depends on road conditions; icy and snowy roads have more rolling coefficient than dry roads. Alberta, the considered geographic location, is covered with snow most of the winter. So, the rolling force energy consumption will be greater in severe winter scenarios than in mild winter conditions and will be lowest in summer [12]. Drag and rolling coefficient values for both conventional BEVs and CFRP BEVs are shown below in Table 6 and Table 7. A bottom-up energy requirement model was developed for each scenario. The key parameters are summarized in Table 5. The equations used to determine the drag force and rolling force are discussed in the supporting information (section 2).

Table 5: Scenarios and key parameters for the BEV energy requirement model

Scenarios	Key parameters
City in summer: City_Summer	• Operational time [112] • Temperature 15ºC to 35ºC [15, 106, 107] • Drag coefficient [10] • Rolling coefficient[106, 108] • Average speed and acceleration [25, 106]
City in mild winter: City_Mild_Winter	• Operational time [112] • Temperature -14ºC to 14ºC [15, 112, 113] • Rolling coefficient [10, 114] • Drag coefficient [10, 114] • Average speed and acceleration [27, 112]
City in severe winter: City_Severe_Winter	• Operational time [112] • Temperature -40ºC to -15ºC [15, 112, 113] • Rolling coefficient [10, 114] • Drag coefficient [112, 114] • Average speed and acceleration [27, 112]
Highway in summer: Highway_Summer	• Operational time [106] • Temperature 15ºC to 35ºC [15, 112, 113] • Rolling coefficient [10, 114] • Drag coefficient [10, 114] • Average speed and acceleration [10, 27]
Highway in mild winter: Highway_Mild_Winter	• Operational time [112] • Temperature -14ºC to 14ºC [15, 112, 113] • Rolling coefficient [10, 114] • Drag coefficient [10, 114] • Average speed and acceleration [27, 112]
Highway in severe winter: Highway_Severe_Winter	• Operational time [112] • Temperature -40ºC to -15ºC [15, 112, 113] • Rolling coefficient [10, 114] • Drag coefficient [10, 114] • Average speed and acceleration [27, 112]
Rural area in summer: Rural_Summer	• Operational time [112] • Temperature -40ºC to -15ºC [15, 112, 113] • Rolling coefficient [10, 114] • Drag coefficient [10, 114] • Average speed and acceleration [27, 112]

Scenarios	Key parameters
Rural area in mild winter: Rural_Mild_Winter	• Operational time [112] • Temperature -40ºC to -15ºC [15, 112, 113] • Rolling coefficient [10, 114] • Drag coefficient [10, 114] • Average speed and acceleration [27, 112]
Rural area in severe winter: Rural_Severe_Winter	• Operational time [112] • Temperature -40ºC to -15ºC [15, 112, 113] • Rolling coefficient [10, 114] • Drag coefficient [10, 114] • Average speed and acceleration [27, 112]

Table 6: Values of drag and rolling coefficients for conventional BEVs [16]

Scenarios	Drag Coefficient	Rolling Coefficient
City in severe winter	0.29	0.00175
City in mild winter	0.29	0.00315
City in summer	0.29	0.007
Highway in severe winter	0.67	0.0025
Highway in mild winter	0.45	0.0025
Highway in summer	0.35	0.0076
Rural in severe winter	0.29	0.00175
Rural in mild winter	0.29	0.00315
Rural in summer	0.29	0.005

Table 7: Values of drag and rolling coefficients for CFRP BEVs [16, 55]

Scenarios	Drag Coefficient	Rolling Coefficient
City in severe winter	0.24	0.00155
City in mild winter	0.24	0.0028
City in summer	0.24	0.00623
Highway in severe winter	0.34	0.00223
Highway in mild winter	0.30	0.00223
Highway in summer	0.31	0.00676
Rural in severe winter	0.25	0.00155
Rural in mild winter	0.25	0.0028
Rural in summer	0.25	0.00445

The efficiencies of the electric motor and the controller are supposed to be 85 and 95%, respectively [27]. The efficiency of the motor and controller differs by scenario. The efficiency of the motor and controller are highest in city in summer and lowest in highway in severe winter because less energy is used to maintain the thermal comfort of the motor and the controller in summer than in severe winter where considerable energy is used to maintain the thermal comfort of the motor and controller. The eddy current and friction loss of the motor is directly proportional to its rotational speed. The rotational speed of the motor is directly proportional to the translational speed of the vehicle. The rotational speed of the motor is higher on highways than in cities, so more eddy current and friction loss occurs on highways than in cities. Motor and controller efficiency values for each scenario for both conventional BEVs and CFRP BEVs are shown below in Table 8.

Table 8: Motor and controller efficiency values for both conventional and CFRP BEVs [29]

Scenarios	Efficiency of motor	Efficiency of controller
City in severe winter	85	93
City in mild winter	87	93
City in summer	90	95
Highway in severe winter	82	87
Highway in mild winter	84	89
Highway in summer	85	90
Rural in severe winter	83	88
Rural in mild winter	84	90
Rural in summer	87	93

The maximum rating demands for the AC and heat are assumed to be 1.40 kW and 2.30 kW, respectively. The rolling and drag coefficient values for each condition were compiled from the literature [16, 94, 115]. The drag and rolling coefficients increase with an increase in the weight of the vehicle. So, the rolling and drag coefficient values for a conventional BEV will be relatively higher than for a lightweight carbon fiber-based BEV, for a particular scenario. The total mass of a carbon fiber-based BEV is 955 kg, constituting a deadweight of 875 kg and a passenger weight of 80 kg [27, 116], and for the conventional BEV the value is 1585 kg, constituting a deadweight of 1505 kg. The operational time required to travel 50 km is different in every scenario because of varying traffic rules and speed limits. Operational time is highest for a city in severe winter and lowest for a highway in summer (75 minutes and 35 minutes, respectively) [112, 117, 118]. The energy required to drive or provide the required torque to the wheel varies by scenario depending on speed, acceleration, drag coefficient, rolling coefficient, and the slope of the road. We developed a model to estimate the highest energy of 0.83

MJ/km for a highway in severe winter and the lowest energy of 0.25 MJ/km for a city in summer for a carbon fiber EV. The corresponding energy requirements for a conventional EV are 1.58 MJ/km on a highway in severe winter and 0.40 MJ/km in a city in summer [29]. AC and heat energy constraints will be different for each scenario because of the different climatic conditions and will be reflected by the average power demand [29]. The AC or heater average power demand is expressed as a % of max rating and is lowest in summer and highest in severe winter, or 75% and 25% of max rating, respectively: and it is the same for both conventional and carbon fiber BEVs [29]. The auxiliaries' energy consumption is determined by summing the energy required for the LED light, radio & navigation, and preheating. The auxiliaries' energy consumption is highest in city in severe winter and lowest in city in summer, or 0 MJ/km and 0.02 MJ/km, respectively; and is the same for both conventional and carbon fiber BEVs [29, 55]. Stopping at traffic signals, aggressive braking, and uneven roads dissipate energy, the amount of which will vary by scenario depending on traffic maps, the frequency of stops or traffic lights, and the type of road [11]. Dissipated energy is highest in city and lowest in highway in severe winter (0.09 MJ/km and 0.02 MJ/km, respectively,) and is the same for both conventional and carbon fiber EVs [11]. The energy required to provide the necessary wheel torque will also vary for each scenario depending on the speed, acceleration, drag coefficient, rolling coefficient, and slope of the road. This energy constraint is highest for highway in severe winter and lowest for city in summer for both conventional and carbon fiber BEVs [10]. But the range of values of drive energy for a carbon fiber BEV is lower than for a conventional BEV because there is less applicable drag and rolling force due to the lower weight of a carbon fiber BEV.

The drive energy for conventional and carbon fiber BEVs ranges from 0.32 MJ/km to 0.98 MJ/km and 0.20 MJ/km to 0.54 MJ/km, respectively [10].

The energy consumption in vehicle operation is the sum of the energy consumption of each activity. AC consumption will be greater in summer than in severe and mild winter. Energy consumed in LED lighting, radio, and navigation will be almost the same in each scenario [10]. The energy dissipated in stopping and braking at traffic signals will be higher in city scenarios than in highway and rural ones because there are more traffic lights or stops in cities than on rural roads and highways [119]. Net energy consumption is computed by summing each of the above energy constraints for a considered scenario and is usually expressed in terms of kWh/km. Energy consumption and GHG emissions are highest in highway in severe winter and lowest in city in summer (1.50 MJ/km and 0.43 MJ/km for conventional EVs and 0.88 MJ/km and 0.28 MJ/km for carbon fiber EVs) [29].

The battery is the powerhouse of a BEV and stores energy from the grid mix to propel the engine and for other activities. The battery can be recharged after traveling a certain distance. Each scenario developed here considers a different number of battery replacements depending on battery lifetime and performance [120]. The battery performance and its driving range (the number of kilometers traveled by the vehicle on one full battery charge) depends on driving pattern, speed, acceleration, type of road, and prevalent climatic conditions. The cooler the ambient temperature, the shorter the driving range of the vehicle. Under the same climatic conditions, the drive range of a BEV will be longer in a city than on a highway or a rural road because the drive range is shorter when the operational speed is higher. Among the scenarios, the drive range of

a BEV is highest in a city in summer and lowest on a highway in severe winter, 200 km, and 66 km, respectively [111, 121].

The other two factors that significantly affect battery performance are the depth of discharge and the number of charging cycles. Depth of discharge refers to the portion of the energy stored in a battery that can be used feasibly. For initial cycles, the depth of discharge is 100%, after which it decreases to 95%, 85%, and so on. For this study, 80% was considered the lowest depth of discharge under which a BEV can operate [11, 122] as it is not technically feasible to use the battery once its depth of discharge falls below 80% [122]. Charging cycles refer to the number of times the battery can be charged after being fully or partially drained. 800 charging cycles were assumed in this study [119]. One of the critical factors that influence the performance of EVs is drive range. Drive range is the number of kilometers travelled by a BEV on one full battery charge and is dependent on the ambient temperature, type of road, speed, and acceleration. The cooler the ambient temperature, the shorter the drive range of the BEV, which implies that the drive range of BEVs in summer is considerably greater than in mild and severe winter conditions [71]. Under the same prevalent climatic conditions, the drive range of an EV will be greater in the city than on highways and rural roads, because the drive range is shorter when the operational speed is higher [12]. Of all the considered scenarios, the drive range of an EV will be highest in the city in summer and lowest in the highway in severe winter: 200 km and 66 km, respectively [12]. Drive range values for both conventional BEVs and CFRP BEVs are shown below in Table 9. The number of battery replacements will be higher in severe winter scenarios than in mild winter and summer scenarios. The number of battery replacements is highest in the highway in severe winter

scenario, 8 times, and lowest in the city in summer (2 times) for conventional BEVs. The battery lifetime and replacement rate were calculated for each scenario. More information is available in the supporting information (section 3).

Table 9: Detailed values of drive range for both conventional BEVs and CFRP BEVs [121]

Scenarios	**Drive range (Conventional BEV) [km]**	**Drive range (CFRP BEV) [km]**
City in severe winter	83	121
City in mild winter	117	180
City in summer	200	281
Highway in severe winter	66	89
Highway in mild winter	75	114
Highway in summer	93	140
Rural in severe winter	77	93
Rural in mild winter	92	132
Rural in summer	143	203

2.2.3.4. Maintenance of an EV

Some essential components like batteries, fluids, and tires lose their peak performance after being operated for a certain number of kilometers and need to be serviced or replaced to maintain the vehicle's desired performance and fuel economy. The replacement interval of different components or fluids varies because of differences in specifications and applications. For example, tires, brake fluid, and powertrain coolant are assumed to be replaced three times over the life cycle of an EV [9, 123]. For windshield fluids and engine oil, 19 and 39 replacements are considered, respectively [44, 123]. GHG emissions for each serviced or replaced component were estimated from earlier work [123].

2.2.3.5. End of life

Recycling and disposal are the two prime categories of the end-of-life phase. The recycling phase is uncertain because we do not know how the recycled product will be used (either open-loop or closed-loop recycling). So, for clear and transparent results, the recycling phase is omitted from this study. Only the disposal portion is examined in the end-of-life phase [9]. The disposal phase of a vehicle includes sorting or dismantling, shredding, transportation, and landfilling [96]. The disposed portion of the vehicle is classified as glider or battery; the techniques involved in battery disposal are very different from those used for the disposal of the glider. It is assumed that all parts of the glider and battery are disposed of in the same manner. Sorting or dismantling is assumed to take place in Vancouver, BC, 40 km from the shredding facility [96]. Dismantled components are transported by heavy truck to a shredding facility. Energy requirements and GHG emissions for sorting, dismantling, and transportation were extracted from a study conducted by the City of Vancouver on the disposal of BEVs [96]. For the shredding phase, data for the calculation of energy requirement and GHG emissions was gathered from literature [120]. The disposal of the glider was formulated from several studies [96, 120, 124]. The energy requirement and GHG emissions for the disposal of Li-ion batteries were modeled according to literature [124, 125]. This phase is described in detail in the tables below.

Table 10: Steps involved in the end-of-life phase for both conventional and CFRP BEVs [95]

Steps included in end of life	Description
Disassembly of the vehicle	This step includes dismantling the car into different portions such as the powertrain, residual car body, motor, battery. etc.
Recycling of the battery	This step includes recycling the case material, battery management system, battery cells, critical materials (e.g., lithium).
Recycling of the electric motor	This step includes recycling metals, recycling or reusing magnets, recycling scarce materials (e.g., rare earth metals).
Recycling of power electronics	This category includes power electronics, non-propulsion electrical systems: recycling cables, electronics, and valuable materials.
Recycling of wheels and tires	This category includes recycling the wheels and tires.
Shredding of residual car body	This step includes shredding, separation, and treatment of the heavy and light fractions, respectively.
Use of transport services	This category includes the transport of the residual car body by truck to a shredder facility.
Waste flows	This step includes the waste flows during sorting and processing. Waste is separated from the recyclable portion.
Powertrain	This category includes the battery, electric motor, electronic controller (inverter, converter), and powertrain system (PDU, cables, and charger).
Glider	This category includes the remaining components of BEVs except the powertrain.

2.3. Results and discussion

This section presents the GHG emissions estimates of conventional and CFRP-based BEVs. The GHG emissions are evaluated in g CO_2 eq per km assuming a lifetime of 200,000 km. First, the GHG emissions from the manufacturing of major vehicle components are discussed, followed by the operational emissions for the nine scenarios. The life cycle GHG emissions for each scenario are compared later. The climatic and road conditions and the driving behaviors are normalized to selected provinces in Canada to understand the overall GHG emission performances of conventional and CFRP-based EVs. Finally, the sensitivity analysis results are discussed.

2.3.1. Vehicle production GHG emissions

Figures 3 and 4 show the manufacturing GHG emission contributions by key components and materials, respectively. A conventional vehicle emits 12.4% fewer GHGs than CFRP-based vehicles. In both cases, the highest GHG emissions are due to the production of the body (body in white, interior, and exterior) and the chassis, which together account for more than 76% of vehicle production emissions. For a conventional vehicle, the materials with high GHG contributions are steel and aluminum, 49%, and 22%, respectively. The high GHG emissions are in proportion to the materials' large mass contributions as well as the energy-intensive processes in their supply chains. Plastic, rubber, and copper also have important GHG emissions contributions. In the case of the CFRP-based vehicle, the largest contribution is from the use of carbon fiber, which alone accounts for around 64% of the manufacturing emissions. Carbon fiber production involves a series of energy-intensive processes that result in high GHG emissions per kg of carbon fiber.

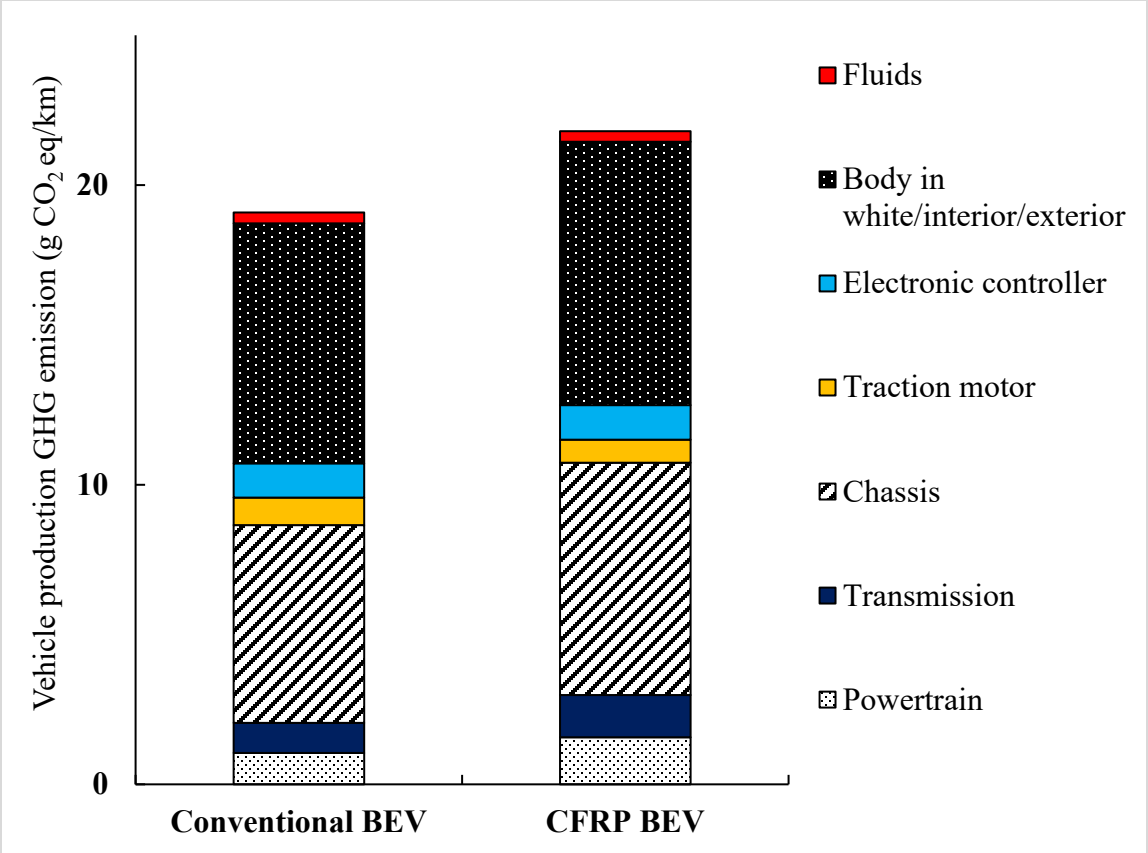

Figure 3: Vehicle production GHG emissions contribution by key components: conventional vs. CFRP BEVs

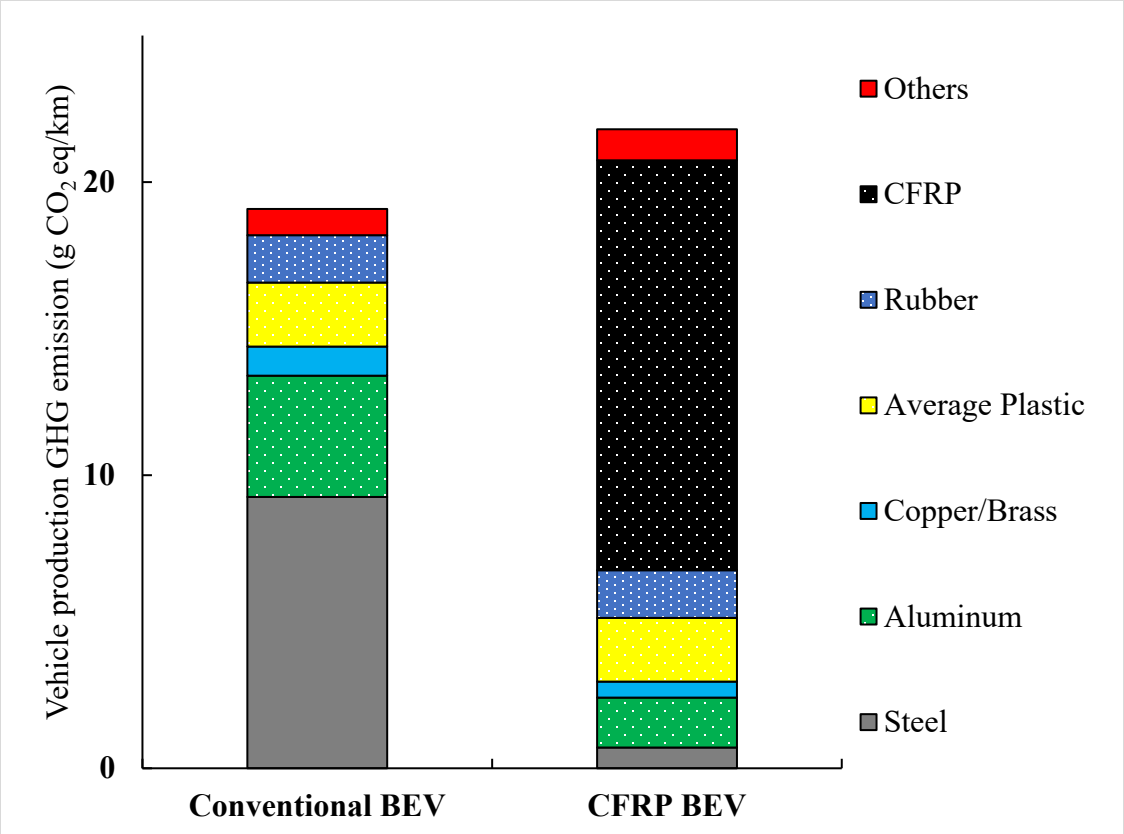

Figure 4: Vehicle production GHG emissions contribution by key raw materials: conventional vs. CFRP BEVs

2.3.2. GHG emissions due to battery requirements

Figure 5 depicts the GHG emissions associated with battery requirements in the life cycle of the vehicles for each scenario. Battery manufacturing GHG emissions for a Li-NMC battery are 1.32 g CO_2 eq/km per battery for conventional BEVs and 2.01 g CO_2 eq/km per battery for CFRP EVs. The emission differences are due to differences in the number of battery replacements. Compared to conventional vehicles, a CFRP-based EV requires fewer replacements in every scenario because the lightweight CFRP results in less drag and rolling force, more gradual degradation of the depth of discharge, and longer battery life compared to a conventional EV [55]. The battery replacement rate is highest in the highway in severe

winter scenario. The battery lifetime is computed based on its energy consumption. Battery energy consumption and battery replacement are higher in severe winter than in mild winter and summer because of the internal battery loss, battery degradation, and rapid loss of depth of discharge in severe winters [12]. Similarly, battery energy consumption and battery replacement are higher in highways than in rural areas or cities because more energy loss occurs at high speed, acceleration, and aggressive driving behavior on highways; more energy is dissipated in the battery at high speeds [12]. So, from the above statements it is concluded that highway in severe winter requires the most batteries and the city in summer requires the least. The most battery replacements are in highway in severe winter and the least in city in summer: 8 and 2 for conventional and 1 and 4 for CFRP BEVs, respectively. The GHG emissions due to battery requirements range from 2.02 to 8.04 g CO_2 -eq/km for a CFRP-based BEV and from 2.7 to 10.6 g CO_2 eq/km for a conventional BEV.

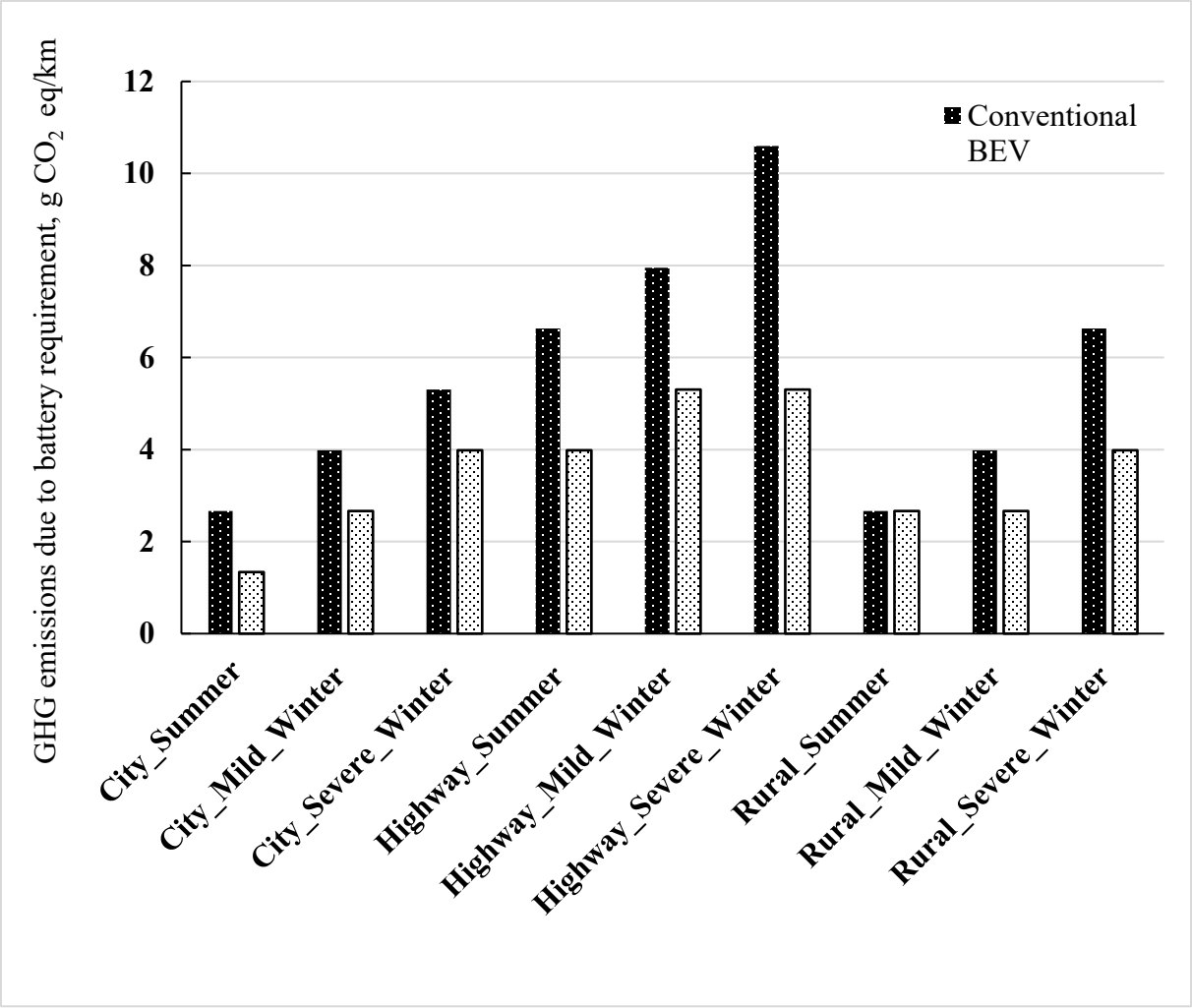

Figure 5: GHG emissions due to battery requirements in the life cycle of the BEV: conventional vs. carbon fiber reinforced plastic

2.3.3. Operating GHG emissions

GHG emissions during the operational phase are due to the upstream emissions in the production of electricity [12]. The emission variations among the scenarios for both conventional and CFRP-based vehicles are a result of differences in energy requirements, which are influenced by climatic conditions, road type, and driving behaviors [55]. The key energy-consuming activities are providing the required wheel torque, heating and air conditioning, and miscellaneous auxiliary activities. Energy demand is modeled by

considering the mass, acceleration, drag coefficient, rolling coefficient, density, velocity, traveling distance, and frontal area of the EV [29]. The coefficients differ by scenario depending on road and climatic conditions. The overall emissions in the summer scenarios are lower than in the mild and severe winter scenarios because there is less internal battery loss. Based on the type of road, the percentage contribution of operation emissions is higher in cities than in rural areas and on highways [29]. The overall operational and life cycle emission in cities is lower than on rural and highway roads because of calm driving speeds and acceleration [12].

The energy consumed by heaters and air conditioning (AC) is calculated by multiplying the highest heater/AC demand, operational time, and average use of the maximum power of the heater and AC. The maximum power demand of the heater and AC is the same in each scenario, 2.30 KW and 1.40 KW, respectively [126]. Operational time is defined as the time required to travel the considered travelling distance, 50 km/day [29]. Operational time differs by scenario because of different climatic conditions, road, and traffic. Operational time on highways is lower than on rural and city roads because on highways the speed limit is higher and traffic obstructions fewer. Operational time ranges from 50 minutes on highways to 75 minutes in cities [11, 111]. The average use of the maximum power of AC and heaters is calculated based on the thermal drive cycle and is usually expressed in percentage (%). The thermal drive cycle defines the temperature range for each scenario taking into account the prevalent climatic conditions of Alberta, Canada. The temperature ranges are -35ºC to – 15ºC in severe winter, -14ºC to 10ºC in mild winter, and 11ºC to 35ºC in summer [31]. The comfortable temperature inside the EV is from 18ºC to 22ºC; this range and the range of climatic conditions are incorporated as input values to compute the average

demand of AC or heat in each scenario. For each temperature value applicable to a particular climatic condition, the use of AC or heat is calculated in terms of a % of maximum power demand using a basic thermal equation from the World harmonized Light Duty Vehicle Test Cycle (WLTC) [31]. All the % values are plotted, and the final average value is computed using regression analysis defined by the Urban Dynamometer Driving Schedule (UDDS). The % average heat demand is highest in severe winter; AC's % average is highest in summer and in both cases is independent of road type. The % average demand of the heater or AC ranges from 25% to 75% [121]. So, the average consumption of AC or heat is computed by multiplying the three variables defined above and then dividing the result by the lifetime of EV to express the consumption in MJ/km. The average consumption of AC/heat ranges from 0.03 MJ/km city in summer to 0.16 MJ/km city in severe winter. The average consumption of AC/heat is directly proportional to operational time, and operational time is higher in cities given the higher traffic obstructions and lower speed limits, leading to more energy consumption than on highways and rural roads [121]. The GHG emission values for the energy consumed by AC/heaters for all the considered scenarios are shown below in Table 11.

Energy consumed by auxiliaries includes the energy consumption of LED lights used for lighting, radio, and navigation, and seat preheating (mostly used in severe climatic conditions) [29]. The rating of conventional and power LED lights is 140W and 50W, respectively . The rating of radio navigation and preheating devices is 20W and 70W, respectively [29]. The calculation of energy consumption for each device is similar to that of the AC/heater consumption, in that the drive cycle for each temperature value to compute the % average demand of LED lights, radio navigation, and preheating device is considered.

The total energy consumed by auxiliaries is the sum of the energy consumed by LED lights, radio navigation, and the preheating devices [29]. The energy consumption of the auxiliaries ranges from 0 MJ/km in city in summer to 0.02 MJ/km in city in severe winter. The energy consumption of radio navigation is almost the same in every scenario, but the energy consumption of LED lights and the preheating device is higher in severe winter than in mild winters and summer because of the cold climatic conditions and early sunset in Alberta, Canada. The GHG emission values of the energy consumed in auxiliaries for all the considered scenarios is shown below in Table 12.

Energy lost in the motor and controller is defined as the energy loss for maintaining the desired temperature of the internal circuit and also considers the eddy current and inefficiency loss. The efficiencies of the electronic controller and traction motor are considered to be 95% and 85%, respectively, as per the study by Müller et al. [127]. The efficiency of the motor and controller depends on the scenario [29]. The efficiency of the motor and controller will be highest in city in summer and lowest in highway in severe winter because less energy is dissipated in maintaining the thermal comfort of the motor and controller in summer than in severe winter, where considerable energy is lost to the surroundings to maintain the thermal comfort of the motor and controller [29]. The eddy current and friction loss of the motor are directly proportional to its rotational speed [95]. The rotational speed of the motor is directly proportional to the translational speed of the vehicle. The rotational speed of the motor is higher on highways than in cities, so more eddy current and friction loss occurs on highways than in cities [95]. Motor and controller efficiency values for each scenario for both conventional BEVs and CFRP are shown in Table 8. Energy lost by the motor and controller is calculated by multiplying the

inefficiency loss of each, 15% and 5%, by the energy consumed to obtain the required wheel torque [95]. Energy lost in the motor and controller ranges from 0.06 MJ/km in city in summer to 1.18 MJ/km on the highway in severe winters for conventional BEVs. The energy lost in the motor and controller is directly proportional to the energy requirement to obtain the desired wheel torque for driving the car [29]. The energy requirement to obtain the desired torque for city summer is far less given the lower speed load and for highway in severe winter it is because of the high speed load compared to other scenarios [29]. Based on the above explanation, the energy lost in the motor and controller will be lowest for city scenarios and highest for highway scenarios and in between for rural scenarios. The energy lost in the motor and controller will be lowest in summer scenarios and highest in severe winter scenarios and in between for mild winter scenarios because less energy is dissipated in maintaining the thermal comfort of the motor and controller in summer than in severe winter where considerable energy is lost to the surroundings in maintaining the thermal comfort of motor and controller [29]. GHG emissions lost in the motor and controller range from 8 g CO_2 eq/km in city in summer to 45 g CO_2 eq/km in highway in severe winter for conventional BEVs to 6 g CO_2 eq/km in city in summer to 35 g CO_2 eq/km for CFRP BEV. The GHG emissions values for the energy lost in the motor and controller for all the considered scenarios are shown below in Table 13.

Energy is lost in each scenario because of curves, sudden braking or stopping, the frequency of traffic signals, traffic obstructions, and speed limits. Energy dissipation is represented as the percentage of driving energy required to obtain the desired wheel torque [29]. The % of energy dissipation is different for city and highway or rural roads in Alberta, Canada because of the difference in the number of curves, traffic signals, and traffic obstructions

[15]. The % energy dissipation factor for city and highway / rural is considered to be 25% and 20% as per the WLTC based on the driving patterns of Alberta, Canada [12, 15]. Regenerative braking is one of the most crucial accessories of the EV considered in this study [128]. This study thus considers regeneration efficiency, which recovers some portion of dissipated energy. A regeneration efficiency of 69% is considered for every scenario; in other words, 69% of energy dissipated is recovered, for every scenario [29]. The greater the dissipated energy, the greater the energy recovery from the regenerative braking. The net energy dissipated is the difference between the original energy dissipation without regenerative efficiency and the energy recovered by regeneration efficiency [12]. The net energy dissipation ranges from 0.02 MJ/km in city in summer to 0.09 MJ/km in highway in severe winter. The GHG emissions values for the dissipated energy for every scenario is shown below in Table 15.

The equation used to compute the energy consumption required to provide the required torque to the wheels is the basic physics energy equation reflecting the relation between energy and different forces applicable while driving an EV; the equation is shown below in section 2 in the supporting information. But the value of the parameters in the energy equation differs by scenario because the driving patterns, climatic conditions, and battery performance differ [12]. The parameters included in the energy equation are mass, acceleration, drag coefficient, rolling coefficient, density, velocity, travelling distance, and frontal area of the EV [12]. The mass, air density, travelling distance, and frontal area are the same for each scenario with values of 1511 kg, 1.2 kg/m^3, 50 km/day, 2.27 m^2, respectively [12]. The remaining parameters (i.e., acceleration, speed, rolling coefficient, and drag coefficient) vary based on the scenario's prevalent road and climatic conditions

[12]. Acceleration, for instance, varies with road type, climatic conditions, traffic signals etc., and is greater on highways than in cities and on rural roads because speed limits are higher and there are fewer traffic obstructions on highways [12]. Acceleration ranges from 0.14 m/sec^2 in city in summer to 0.52 m/sec^2 in rural areas in severe winter considering all the factors mentioned above [12].

Operation speed depends on the type of road and is minimally affected by climatic conditions. The operation speeds for each considered road are taken from the Alberta Household Travel Survey (AHTS) considering applicable road and climatic conditions for each scenario [129]. The operational speed is higher on highways than in cities and on rural roads because there are fewer traffic obstructions and higher speed limits. The operational speed is 12.50 m/sec in cities and 25 m/sec on highways [12]. The operational speed for each scenario is determined by considering road and climatic conditions applicable [12]. The drag coefficient depends on the speed, density of air, and mass of the car. Operational speed differs by road type, thus leading to the differences in drag coefficient values [16].

The drag coefficient ranges from 0.29 in all city road scenarios to 0.77 in all highway road scenarios [17]. Drag and rolling coefficient values are given in Tables 6 and 7. The drag coefficient value is greater on hilly roads than flat roads because of the greater air resistance on hilly roads [17]. The rolling coefficient depends on the type of road, climatic conditions, mass of the EV, density of air, frontal area of the EV, and acceleration due to gravity [16]. Icy and snowy roads have a lower rolling coefficient than dry roads because they generate less static and kinetic friction than dry roads do, indicating that the rolling coefficient value will be higher in summer than in mild and severe winter [16]. Possible rolling coefficient values are 0.001 in severe winter and 0.0076 in summer [16].

The energy required to provide the desired torque to the wheels is the sum of all three forces multiplied by the travelling distance [10]. The energy required to provide the desired torque ranges from 0.34 MJ/km to 0.92 MJ/km. In winter and on highways, the energy required to achieve desired torques is higher than in summer and in the city because of the higher speed loads and greater friction from snowy roads [16].

The net energy consumption is the sum of all the energy constraints mentioned above. The net energy consumption of the operations phase ranges from 0.51 MJ/km to 2.51 MJ/km. The GHG emissions values of the dissipated energy for all the considered scenarios is shown below in Table 14. Figure 6 shows the net energy consumption of operation phase for all the scenarios in a graph. The GHG emissions for the operation phase are calculated by multiplying the net energy consumption with the relevant emission factor of Alberta's grid mix.

Figure 6 shows the GHG emission results for all scenarios. A CFRP-based BEV emits fewer GHG emissions than a conventional BEV in every scenario. A CFRP-based BEV has 42% less mass than a conventional BEV. The lower mass enables a CFRP-based BEV to operate at high efficiency as the total energy demand in the powertrain is lower. A CFRP-based BEV emits 30-45% fewer total operational GHG emissions. The highest reduction is in the case of highway in severe and mild winter scenarios. The largest portion of the energy saving is from the energy required to drive the powertrain, followed by the losses from the motor and controller. Energy in the powertrain accounts for 58-79% of demand in all cases. Among the scenarios, highway in severe winter shows the highest operational GHG emissions, 200.4 g CO_2 eq/km for the conventional EV. The lowest operational emissions

are observed in the case of the CFRP-based EV when operated in a city in summer, 36.8 g CO_2 eq/km.

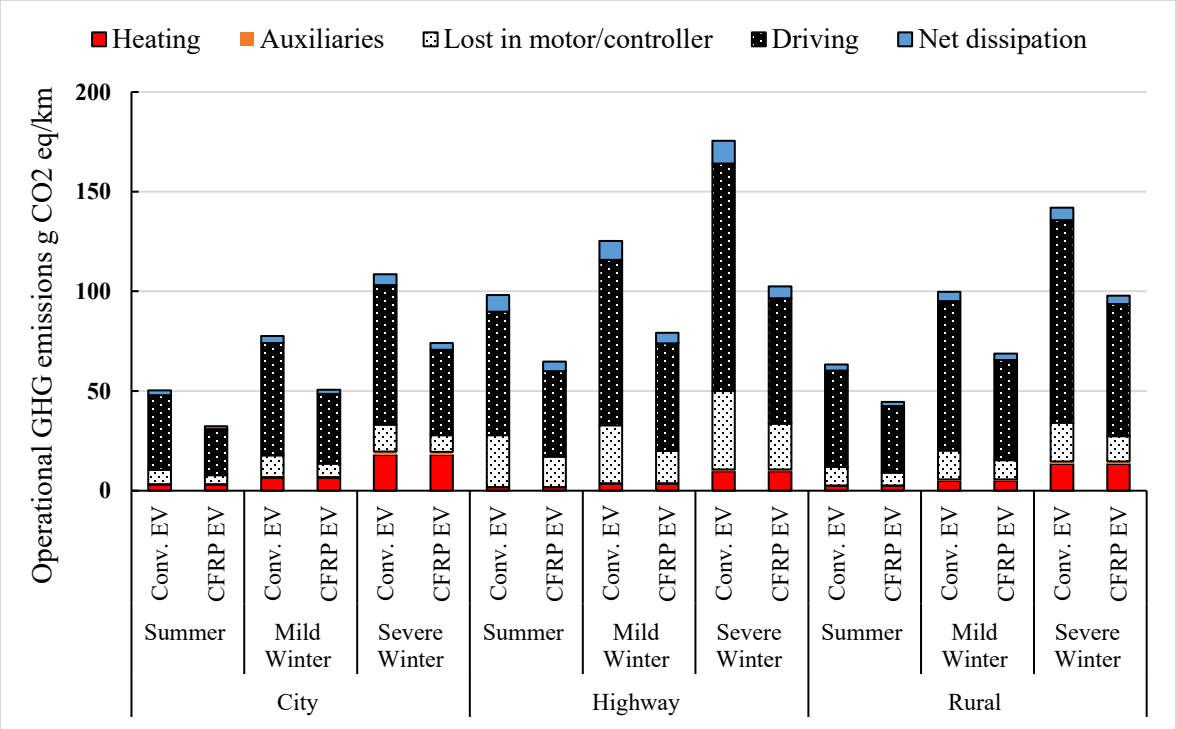

Figure 6: Operational GHG emissions for all scenarios: conventional vs. carbon fiber reinforced plastic (CFRP)

Table 11: GHG emissions of AC/heater consumption for both conventional and CFRP BEVs [29]

Scenarios	**GHG emissions (g CO_2 eq/km) (conventional)**	**GHG emissions (g CO_2 eq/km) (CFRP)**
City in severe winter	20	20
City in mild winter	7	7
City in summer	3	3
Highway in severe winter	11	11
Highway in mild winter	4	4
Highway in summer	2	2
Rural in severe winter	15	15
Rural in mild winter	6	6
Rural in summer	3	3

Table 12: GHG emissions of auxiliaries' consumption for both conventional and CFRP BEV [29]

Scenarios	**GHG emissions (g CO_2 eq/km) (conventional)**	**GHG emissions (g CO_2 eq/km) (CFRP)**
City in severe winter	1.98	1.98
City in mild winter	0.61	0.61
City in summer	0.34	0.34
Highway in severe winter	1.12	1.12
Highway in mild winter	0.36	0.36
Highway in summer	0.21	0.20
Rural in severe winter	1.49	1.49
Rural in mild winter	0.99	0.99
Rural in summer	0.29	0.29

Table 13: GHG emissions of energy lost in the motor and controller for both conventional and CFRP BEV [29]

Scenarios	**GHG emissions (g CO_2 eq/km) (conventional)**	**GHG emissions (g CO_2 eq/km) (CFRP)**
City in severe winter	15	9
City in mild winter	12	8
City in summer	8	5
Highway in severe winter	45	26
Highway in mild winter	33	18
Highway in summer	30	17
Rural in severe winter	22	15
Rural in mild winter	17	11
Rural in summer	11	7

Table 14: GHG emissions of energy consumed in driving for both conventional and CFRP BEVs [11]

Scenarios	**GHG emissions (g CO_2 eq/km) (conventional)**	**GHG emissions (g CO_2 eq/km) (CFRP)**
City in severe winter	80	49
City in mild winter	64	40
City in summer	43	26
Highway in severe winter	130	72
Highway in mild winter	95	62
Highway in summer	71	49
Rural in severe winter	116	75
Rural in mild winter	85	57
Rural in summer	55	38

Table 15: GHG emissions of energy dissipated for both conventional and CFRP BEVs [11]

Scenarios	GHG emissions (g CO_2 eq/km) (conventional)	GHG emissions (g CO_2 eq/km) (CFRP)
City in severe winter	6	4
City in mild winter	4	2
City in summer	3	1
Highway in severe winter	13	7
Highway in mild winter	11	6
Highway in summer	10	5
Rural in severe winter	7	5
Rural in mild winter	5	4
Rural in summer	4	2

Table 16: Total GHG emissions of the operation phase [11, 12]

Scenarios	GHG emissions (g CO_2 eq/km) (conventional)	GHG emissions (g CO_2 eq/km) (CFRP)
City in severe winter	124	84
City in mild winter	88	58
City in summer	57	37
Highway in severe winter	200	117
Highway in mild winter	143	90
Highway in summer	112	74
Rural in severe winter	162	111
Rural in mild winter	114	78
Rural in summer	72	51

2.3.4. End of life

For this phase, Vancouver, British Columbia is considered as the geographic location. The end-of-life has four parts: sorting, shredding, recycling, and disposal [120]. For each of these, the EV is divided into the glider and the powertrain (battery, motor, controller, powertrain system cables, and charger), then summed to compute the energy demand for whole EV for each category [96]. This study computes disposal and recycling energy

separately. The energy required for sorting or dismantling the glider or powertrain is the product of three parameters: 1) The distance travelled to take our vehicle from the place of operation to the shredding facility, 2) the energy required to transport the vehicle to the shredding facility, and 3) The mass of the glider. The values of these parameters are from Kukreja's report [96]. Thus, the energy required to sort, dismantle, and transport the glider is 73.39 MJ [96]. After this value has been calculated, every component of the glider is either disposed or recycled based on the technical considerations. The energy required to dispose or recycle the sorted portion of glider can be calculated by multiplying the total energy by the fraction of the disposed or recycled portion of glider [120]. The energy required to sort, dismantle, and transport the disposed and recycled portions of the glider are 52.23 MJ and 21.16 MJ [96]. The energy required to sort, dismantle, and transport the disposed or recycled portions of the powertrain is calculated in the same way and are 4179.10 MJ/km and 691 MJ/km, respectively [130].

The shredding energy required to shred the glider at shredding facility can be calculated as the product of energy required to operate the shredder and the mass of the glider, which is 322.09 MJ [130]. This shredding energy is categorized into the recycled and disposed portions using their respective mass fractions. The shredding energy required to shred the disposed or recycled portions of glider is computed as 259 MJ and 62 MJ [130]. Similarly, the energy required to shred the disposed or recycled portions of powertrain is computed as 112 MJ and 18MJ, respectively. The energy consumption and GHG emissions for the disposed and recycled portions of the battery or glider are computed on the basis of the recycled value of each metal per kg, taken from Kukreja's study, and the disposed portion can be calculated by subtracting the recycled portion from the original bill of material of

each metal [130]. The energy required to dispose and recycle a glider is calculated by the product of the mass fraction of the disposed or recycled glider and the total energy required to treat (either dispose or recycle) the glider [130]. Based on the above statement, the energy required to dispose or recycle a glider is 1344 MJ or 326 MJ, based on Kukreja's net values of recycling and disposing of a glider [130].

Similarly, for the powertrain, the energy required to dispose or recycle the glider (all the components of the BEV except the battery) is 4179 MJ or 691 MJ, respectively, based on Kukreja's net values of recycling and disposing a powertrain of 4870 MJ [96]. The values for all four categories – sorting, shredding, disposal, and recycling – taken from Kukreja's study were summed to calculate the net GHG emissions involved in this phase.

Similarly, the GHG emissions calculations for the end of life of CFRP BEVs are categorized into four stages and the powertrain and glider are considered separately [55].

Table 17: Values of the parameters involved in end of life for conventional and CFRP BEVs [55, 96, 130]

Parameter	Value (conventional BEV)	Unit	Value (CFRP BEV)	Formulas used
Distance travelled to take our vehicle to shredding facility	40	km	40	Referred
Energy required to transport vehicle to shredding facility and sorting and dismantling	1.5	MJ/ t.km	1.5	Referred
Mass of vehicle	1511	kg	877	Referred
Mass of glider	1160	kg	580	Mentioned above in vehicle production phase
Mass of powertrain	351	kg	297	Calculated above in vehicle production phase
Mass of glider that is disposed	520.14	kg	205	Total mass of glider - mass of recovered glider
Mass of glider that is recovered or recycled	482.77	kg	375	Mass of raw materials recovered (shown in table 12) * mass of glider
Mass of powertrain that is disposed	301.80	kg	268	Total mass of powertrain - mass of recovered glider
Mass of powertrain that is recovered or recycled	49.82	kg	29	Mass of raw materials recovered (shown in table 13) * mass of powertrain
Energy required to operate the shredder	0.37	MJ/kg	0.37	Referred
Energy required for only recycling and disposal of glider	1297.33	MJ	1568	Referred
Energy required for only disposal of glider	672.83	MJ	756	Total energy required for recycling and disposal of glider * (disposed mass of glider/ total mass of glider)
No. of batteries base case (city in summer)	1	Unit less	1	Mentioned in supporting section 3
Weight of powertrain	351.62	kg	297	Mentioned above in vehicle production phase

Table 18: Energy consumption and GHG emissions of parameters involved in end of life for conventional and CFRP BEVs [55, 74, 96, 120]

Parameter	Value (CFRP BEV)	Value (conventional BEV)	Unit	Formulas used
Net energy required to transport glider to shredding facility along with sorting and dismantling	42.14	60.17	MJ	Distance travelled to take our vehicle to shredding facility * Energy required to transport vehicle to shredding facility and sorting and dismantling * Mass of glider
Net energy required to transport disposed portion of glider	21.22	31.21	MJ	Net energy required to transport glider to shredding facility along with sorting and dismantling * (mass of disposed glider/ total mass of glider)
Net energy required to operate the glider at shredder and sorting, dismantling	223.43	371.08	MJ	Energy required to operate the shredder * mass of glider
Net energy required to sort, dismantle, and shred the disposed portion of glider	123.43	192.45	MJ	Net energy required to operate the glider at shredder and sorting, dismantling * (mass of disposed glider/ total mass of glider)
Energy required to transport the powertrain to shredding facility along with sorting and dismantling	13.24	21.10	MJ	Distance travelled to take our vehicle to shredding facility * Energy required to transport vehicle to shredder facility and sorting and dismantling * Mass of powertrain
Energy required to transport the disposed portion of the powertrain to shredding facility	11.23	18.11	MJ	Energy required to transport disposed portion of powertrain to shredding facility * (Mass of powertrain that is disposed/ Mass of powertrain)
Energy required to operate the powertrain at shredder and sorting facility	67.87	130.10	MJ	Mass of powertrain * Energy required to operate the shredder

Parameter	Value (CFRP BEV)	Value (Conventional BEV)	Unit	Formulas used
Energy required to operate the disposed powertrain at shredder and sorting facility	56.98	111.67	MJ	Energy required to operate the powertrain at shredder and sorting facility * (Mass of powertrain that is disposed / Mass of powertrain)
Emissions in transportation	25.6	43.1	kg	Distance travelled to take our vehicle to the shredding facility * Mass of vehicle * Emission factor of transportation
Energy required to only dispose and recycle the powertrain	3814	4870.10	MJ	[74, 96]
Energy required to only dispose the powertrain	3457	4180.10	MJ	Energy required to only dispose and recycle the powertrain * (Mass of powertrain that is disposed/ Mass of powertrain)
Emissions generated during disposal and recycling of the glider	42.14	53.51	kg CO_2 eq	[74, 96]
Emissions in shredding, sorting, and dismantling of car	29	20	kg CO_2 eq	[74, 96]
Emissions generated in the disposed portion of glider during its transportation, shredding, sorting, dismantling, and recycling	157	234	kg CO_2 eq	(Emissions in shredding, sorting, and dismantling of car + Emissions in transportation) * (Mass of glider that is disposed / Mass of vehicle) + Emission generated during disposal and recycling of glider * (Mass of glider that is disposed/ Mass of glider)
Emissions required to only dispose powertrain	0.58	0.76	Kg CO_2 eq/ kg of powertrain	[74, 96]

Table 19: Raw material recovery of glider for conventional and CFRP BEVs [96]

Material recovered per kg of glider	**Units**	**Value**
Aluminum scrap	kg	0.0042
Copper scrap	kg	0.0066
Ferrous scrap	kg	0.654
Plastic	kg	0.155
Residue	kg	0
Electronic components scrap	kg	0
CFRP	kg	0

Table 20: Raw material recovery of powertrain for conventional and CFRP BEVs [96]

Material recovered per kg of powertrain)	**Units**	**Value**
Aluminum scrap	kg	0.27
Copper scrap	kg	0.125
Ferrous scrap	kg	0.411
Plastic	kg	0
Residue	kg	0
Electronic components scrap	kg	0.194

2.3.5. Life cycle GHG emissions

Figure 7 shows life cycle GHG emissions. The emissions for a CFRP-based BEV range from 72.7 g CO_2 eq/km in the city summer to 165.7 g CO_2 eq/km in the highway severe winter scenarios. The corresponding values for a conventional BEV are 93.0 g CO_2 eq/km

and 258.3 g CO_2 eq/km. In all cases, operation emissions have the largest contribution (51% to 78%), followed by the manufacturing GHG emissions (11% to 33%). The impacts from other life cycle stages are below 10%. Although manufacturing GHG emissions for CFRP-based BEVs are higher than for conventional BEVs in all scenarios, mainly because of the high emissions intensity of carbon fiber processing compared with steel and aluminum, there is a large trade-off with operational stage emissions. The life cycle GHG emission savings with the replacement of CFRPs are more prominent in the cases where operational emissions are significant either because of climatic conditions, topography, or grid electricity emission factors. Among the nine scenarios considered, the highest GHG emissions reduction is observed in the highway in severe and mild winter scenarios. The advantage of CFRP over conventional is marginal in the city and rural summer conditions cases. The end-of-life phase comprises the energy requirements for transporting the used vehicle to a recycling facility, dismantling, sorting, shredding, and disposal of non-recyclable components. Due to the high uncertainty in the end of life of the vehicle, recycling and using the same scrap metals in vehicle manufacturing were not considered in the analysis for either CFRP or conventional vehicles. The GHG emissions associated with the end of life of BEVs account for 2% to 4% of the total emissions. The use of recycled metals is presumed to reduce the GHG emissions from the manufacturing phase depending on the recycling process. Similarly, using recycled CFRP instead of virgin carbon fiber would significantly affect manufacturing emissions. However, because the technology and

applications are still emerging, large-scale carbon fiber recycling facilities are not yet well established.

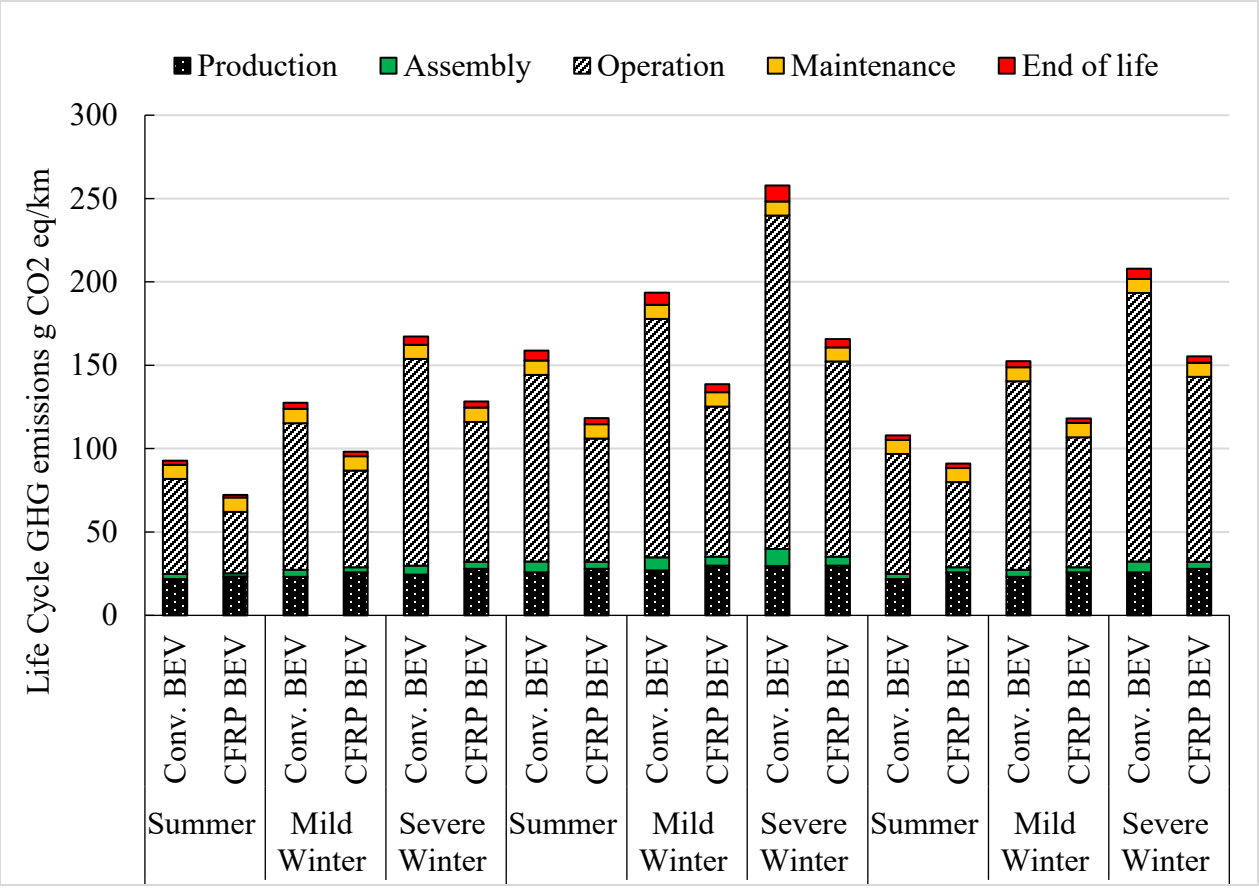

Figure 7: Life cycle GHG emissions: conventional vs. carbon fiber reinforced plastic (CFRP)-based BEVs

To evaluate the relevance of the GHG performance of conventional vs. CFRP-based EVs in a particular city, the life cycle emissions from all nine scenarios were normalized to the climatic and road conditions of two cities. For severe and mild winter climates, the city of Edmonton was used, and for broader summer and moderate climate conditions, the city of Vancouver was used in a case study [15, 102, 129]. Data on annual average climate were obtained from Literature [12, 130-132] and household road driving patterns from household survey data from the literature [12, 132, 133]. The normalized results are presented in Figure 8. In both Edmonton and Vancouver, the CFRP-based BEV emits fewer life cycle GHGs.

BEVs emit fewer GHGs in Vancouver than in Edmonton, which can be explained by the lower grid GHG intensity (an average of 40 g CO_2 eq/kWh) due to a high share of hydropower. Furthermore, Vancouver is characterized by a short winter and long summer climates, which result in low operational emissions compared with jurisdictions with long, severe, or mild winter climates. GHG emissions savings from the use of a CFRP-based EV vs. conventional steel and aluminum-based BEV in Vancouver are minimal compared with the use of a CFRP in Edmonton. Substituting steel and aluminum with lightweight carbon fiber has a significant advantage in Edmonton and can reduce life cycle GHG emissions by 30%.

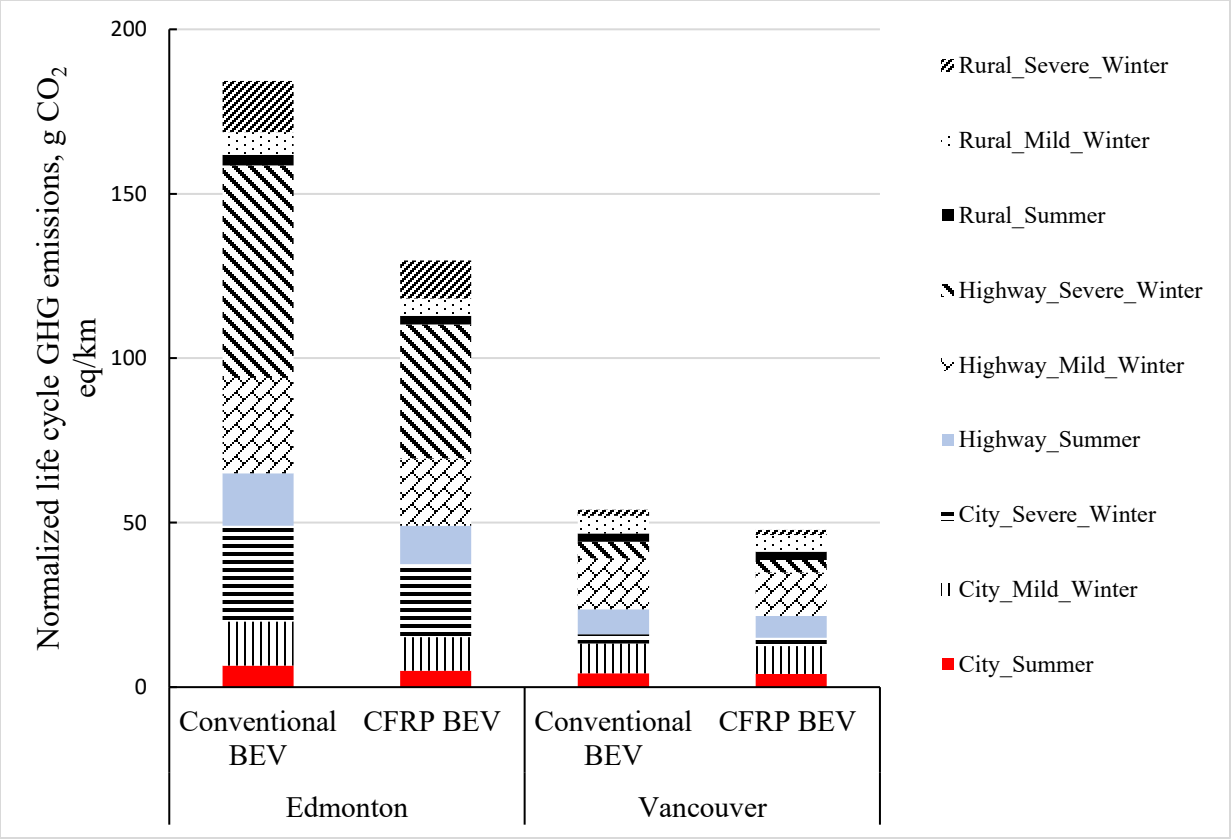

Figure 8: Normalized life cycle GHG emissions

2.3.6. Sensitivity and uncertainty analyses

The LCA study involves several modeling procedures and assumptions that could affect the certainty of the output results used as a decision support tool. Uncertainty in LCA results arises from different sources. They are broadly categorized as parameter-related uncertainty (related to the use of data to model the life cycle inventory), uncertainty due to modeling choice (associated with the choice of allocation rules, the definition of the functional unit, setting the system boundary), and uncertainty due to temporal and spatial variabilities in the inventor and impact assessments [134, 135]. To avoid any misleading conclusions in an

LCA study-based decision, the robustness of the results needs to be evaluated through sensitivity and uncertainty analyses. The Regression, Uncertainty, and Sensitivity Tool (RUST) model, an Excel-based tool developed by Di Lullo et al. [135], was used in this study. A sensitivity analysis was conducted to identify the key parameters that have significant impacts on the model output results. Morris's statistical method was implemented for this purpose [136]. Morris's method identifies important parameters from a high number of model inputs, as in this case. Once key sensitive input parameters were identified, an uncertainty analysis was run using a Monte Carlo simulation to provide the likely range of life cycle GHG emissions for each scenario, for both CFRP and conventional BEVs.

The Morris plot for the city in the summer scenario is shown in Figure 9; all the scenarios show similar trends. Parameters with high Morris mean and standard deviation values (those far from the origin of the plot) are the most sensitive ones. The lifetime of the vehicle, mass, average travel distance per day, efficiency of the controller, rolling, and dragging coefficients appear to be the most critical parameters dictating the energy required for driving the wheel. The parameters in the red box (closer to the origin of the plot) appears to have a negligible effect on the output results and hence were ignored.

The data for the most sensitive parameters were refined to include the maximum and minimum values in determining the uncertainty ranges. Table 21 summarizes the key parameters with their corresponding maximum and minimum values considered. Figure 10 shows the box plot of the life cycle GHG emissions for all scenarios for both CFRP and conventional EVs. The GHG emissions for the highway in severe winter scenarios range

from 257^{+99}_{-65} g CO_2 eq/km for conventional BEVs to 163^{+48}_{-34} g CO_2 eq/km for CFRP-based BEVs. For the city in summer case, the emissions range from 93^{+25}_{-18} g CO_2 eq/km for conventional to 72^{+17}_{-12} g CO_2 eq/km for CFRP-based BEVs, respectively.

Table 21: Range of values for sensitive parameters

Parameters	**Minimum**	**Maximum**	**Reference**
Vehicle lifetime, km	100000	220,000	[9, 44]
Average distance per day, km/day	20	80	[15, 112, 113]
Efficiency of motor, η	75	95	[115]
Efficiency of controller, η	85	98	[115]
Rolling coefficient (city in summer for conventional)	0.00235	0.76	[16, 94, 115]
Rolling coefficient (highway in severe winter for conventional)	0.00175	0.00448	[16, 94, 115]
Rolling coefficient (city in summer for conventional)	0.00235	0.76	[16, 94, 115]
Rolling coefficient (highway in severe winter for conventional)	0.00175	0.00448	[16, 94, 115]
Drag coefficient (city in summer in severe winter for conventional	0.2	0.524	[94, 137]
Drag coefficient (highway in severe winter for conventional)	0.2	0.812	[94, 137]
Drag coefficient (city in summer for CF)	0.2	0.524	[94, 137]
Drag coefficient (highway in winter CF)	0.2	0.812	[94, 137]
Average speed (city), km/hr	30	55	[112, 137]
Average speed (highway), km/hr	70	100	[112, 137]`
Average acceleration (city) m/sec^2	0.1	0.4	[112, 137]

Parameters	Minimum	Maximum	Reference
Average acceleration (highway) m/sec^2	0.14	0.67	[112, 137]
Steel conventional mass, kg	283	803	[18, 34, 94, 138]
CFRP emission factor, kg CO_2 eq/kg	15.25	34.4	[18, 94, 139]
Frontal area, m^2	1.5	3.5	[130, 140]
Density, kg/m^3	1	1.4	[130, 140]
Rating power heater, kW	1	3.4	[12]

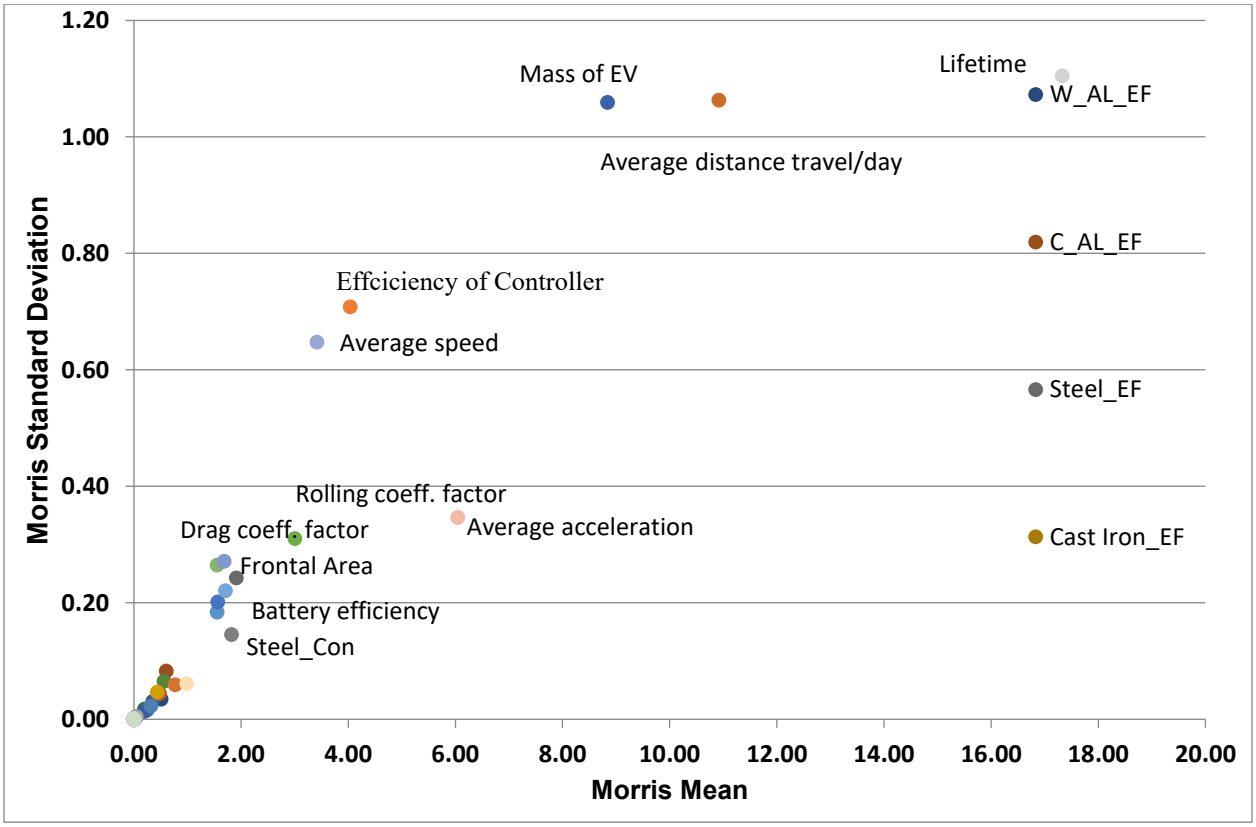

Figure 9: Morris plot for city in summer scenario

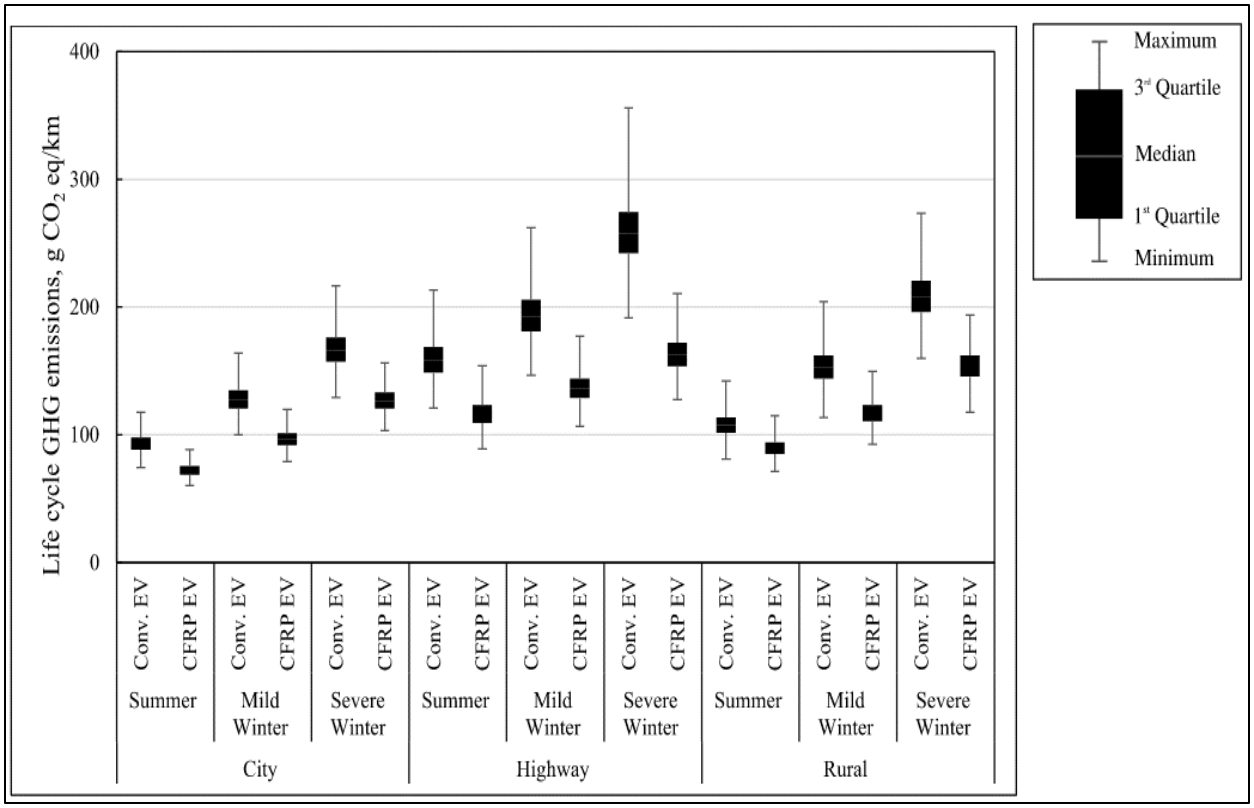

Figure 10: Life cycle GHG emissions: Uncertainty results

2.4. Conclusion

The study was conducted to evaluate the environmental benefits of using carbon fiber to produce a lightweight electric vehicle. The life cycle GHG emissions of a carbon fiber reinforced plastic (CFRP)-based EV produced using carbon fiber made from asphaltene were compared with those from a conventional steel and aluminum vehicle. The study focused on understanding the environmental trade-offs along the life cycle of an EV from the extraction of resources to the vehicle's end of life. Nine scenarios based on climatic and driving conditions were developed: operation in city in summer, operation on highway in summer, operation in rural area in summer, operation in city in severe winter, operation on highway in severe winter, operation in rural area in severe winter, operation in city in mild winter, operation on highway in mild winter, and operation in rural area in mild winter.

The results highlight that substituting steel and aluminum in the key components of EVs by CFRP has a GHG emissions advantage. The magnitude of emissions saving differs among the scenarios. A high GHG emission reduction is observed in the scenarios with relatively high operational emissions. The highway in severe winter scenario shows life cycle GHG emissions of 258.3 g CO_2 eq/km for a conventional vehicle and 165.7 g CO_2 eq/km for a CFRP. The lowest GHG emissions are in the city in summer scenario, 93.0 g CO_2 eq/km and 72.7 g CO_2 eq/km for conventional and CFRP-based EVs, respectively. The operational phase has a high GHG contribution in all cases, followed by the manufacturing phases. The impacts from other vehicle phases are minimal.

The study highlights that the use of a CFRP-based EV has a high GHG advantage in the City of Edmonton, which is characterized by severe or mild long winters. Sensitivity and uncertainty analysis are performed to determine the most sensitive parameters and deduce a possible range of

GHG emissions in all cases. The life cycle GHG emissions range from 72^{+17}_{-12} g CO_2 eq/km for a CFRP-based EV in the city in summer scenario to 257^{+99}_{-65} g CO_2 eq/km for a conventional EV in the highway in severe winter scenario.

The results of this study provide guidelines for technology developers on the process conditions that should be improved to obtain relatively low GHG emissions at a commercial scale. The results also help stakeholders make informed decisions on the suitability of producing asphaltene-based carbon fiber.

Chapter 3

3. The development of life cycle environmental footprint of a carbon fiber-based hydrogen fuel cell vehicle for colder climate

3.1. Introduction

Of the energy-consuming sectors, the transportation sector contributes most to global GHG emissions and generated about 28% of anthropogenic CO_2 emissions in 2021 [11, 19, 141]. Road transportation makes up about 72% of direct GHG emissions through the consumption of fossil fuels [141].. Because of the steady growth in the transportation sector, global energy demand increased by 2.6% and GHG emissions by 23% between 2014 and 2022 [142], leading to both the degradation of urban air quality and the immense increase in the average temperature of the earth's surface [62]. The road transportation sector, therefore, is unsustainable [65].. Decarbonizing the road transportation sector can significantly reduce the sector's overall GHG emissions [143] and thus has become essential in many countries in order to meet the objectives of Paris Agreement [35].

Some of the main alternatives to decarbonizing the road transportation sector are a modal shift to a low-carbon system and renewable fuels through fuel switching (battery electric vehicles [BEVs],

hydrogen fuel cell vehicles (HFCVs), biofuels), improving driving efficiency, and smart and light vehicle design [8]. Of these, the HFCV is an attractive option [14, 48].

Hydrogen can be produced in abundance from many sources of renewable energy and combined with oxygen in a fuel cell to power vehicles, releasing only water vapour (i.e., no direct carbon emission) [144]. Therefore, HFCVs can significantly reduce the GHG emissions and fossil fuel dependence of the transportation sector [145]. That said, HFCVs can generate considerable GHG emissions, depending on the way in which the hydrogen used to propel the vehicle is produced [144]. Hydrogen does not occur naturally on earth and hence is considered an energy carrier, not an energy source [146]. The basic methods of producing hydrogen are natural gas reforming, electrolysis of water, steam methane reforming (SMR), water splitting by photo catalysis, biomass conversion, and coal gasification [50, 147]. SMR is the most generic way to produce hydrogen [146]. Each process has its own production, storage, and delivery characteristics [148], and the environmental impact of each differs depending on the resource availability [144].

In addition to the hydrogen production process, driving pattern, climatic conditions, and fuel cell efficiency can significantly influence the overall environmental performance of HFCVs [111, 149]. In an HFCV, electricity is produced by the continuous reaction of hydrogen (H_2) and oxygen (O_2) in the proton exchange membrane embedded in the fuel cell. The fuel cell is an energy converter (with a performance efficiency of 50%) generating electric energy from the chemical reaction of hydrogen and oxygen [48]. Unlike gasoline-fueled vehicles that use waste heat from the engine, HFCVs draw electrical energy from the fuel cell, enabling the reaction of hydrogen and oxygen to form water and producing electricity and heat in the process [48]. The produced electricity is used to propel the vehicle and charge the electric battery to store extra energy [150].

Battery electric vehicles (BEVs), like HFCVs, do not emit any direct carbon emissions during operation. The basic difference between BEVs and HFCVs is the supply source of the electric energy to the electric motor [48]..

The vehicle type, size, and mass significantly affect its environmental performance and corresponding life cycle emissions [11]. The rolling coefficient (frictional force) and drag coefficient (air resistance force) values are directly proportional to the mass of the vehicle [16]. Hence, the rolling and drag coefficient values are high for heavy and large vehicles, leading to higher energy consumption and GHG emissions than for light vehicles [11, 33]. Lightweight vehicles, according to recent studies, generate fewer GHG emissions than heavy vehicles because drag and rolling force are lower [19, 54, 55]. When conventional materials (steel, aluminum) are replaced with lightweight materials (like CFRP) during manufacturing, there is a high potential to considerably decrease a vehicle's overall GHG emissions [21].. This is significant for HFCVs since the requirement of a fuel cell stack, hydrogen storage tank, battery, electric motor, and additional electrical components makes them heavier than gasoline- and diesel-fueled vehicles [19]. Reducing the weight of an HFCV by 15% increases its driving range by 22% [19]. Hence, using lightweight materials such as CFRP can significantly improve environmental performance and mitigate the GHG emissions of HFCVs [75].

Some studies examine the environmental and economic impacts of asphaltene-based carbon fiber through life cycle assessment (LCA), an environmental accounting and management approach [22, 23]. Most studies on HFCVs evaluate the vehicle's environmental performance and compare it with BEVs and ICEVs (internal combustion engine vehicles) through LCA [13, 35, 48, 95, 145, 151]. A. Granovskii et al. [6] and Hussein et al. [152] compared ICEVs and HFCVs, in particular the impact of fuel cell efficiency on the overall life cycle results, and concluded that HFCVs perform

better than ICEVs when the efficiency of the fuel cell is more than 25%. Pouria et al. [13] predicted that HFCVs can significantly reduce volatile organic compounds (VOCs) and GHG emissions by almost 90% (compared to ICEVs) in all Canadian provinces. Briguglio et al. [153] developed a simulation model to evaluate the viability of renewable hydrogen vehicles in Messina, Italy, considering hydrogen production by electrolysis using electricity produced from wind turbines. Jiang and Nigro [154] concluded that the transparency and validity of diversified LCA study results are affected by vehicle type, climatic condition, geographic location, and resource availability. Staffell et al. [155] discussed the drawbacks of HFCVs, i.e., low fuel cell efficiency, lack of suitable refueling station infrastructure, and high cost of maintaining the fuel cell stack and powertrain system. Collela et al. [156] analyzed the impact of three ways of producing hydrogen – water electrolysis using wind energy, steam reforming of natural gas, and coal gasification – on overall life cycle GHG emissions. Miotti et al. [157] and Simons and Bauer [158] developed an original and unique life cycle inventory for HFCVs considering the enormous disaggregation of prime components (in terms of sub-components and raw materials) such as the powertrain system, fuel cell on-board storage, chassis, and body.

None of these studies assesses the life cycle environmental impacts of the operation phase of the HFCV life cycle. Comparative life cycle studies of energy consumption have been conducted; there are more for BEVs and ICEVs than for HFCVs [2, 13, 150]. The environmental impacts of HFCVs depend considerably on driving pattern, road type, and climatic conditions [159]. Furthermore, the vehicle's and fuel cell's lifetime significantly affect their overall life cycle emissions [13, 18]. HFCV component use, aggressive driving patterns, and extreme weather conditions lead to frequent replacements of HFCV components, especially tires and fluids [81, 82, 95, 123, 146, 148].

To assess the life cycle impacts of an HFCV, we quantified and evaluated its indispensable phases (manufacturing, assembly, operation, maintenance, and end of life). The life cycle of hydrogen fuel (i.e., a well-to-wheel analysis) is outside the scope of this study and has been reviewed based on existing literature.

There is an increasing demand to manufacture vehicles by replacing conventional raw materials (aluminum, steel, etc.) with lightweight materials like CFRP to reduce vehicle weight, enhance vehicle efficiency, and reduce the overall environmental impact [19, 55, 56]. Commercially, some passenger vehicles use CFRP to manufacture the hood and internal structure [21, 56]. CFRPs are used in applications that require more strength, stiffness, and higher resistance to corrosion and fatigue [160]. Although CFRP is light and durable, it is highly energy intensive, and it is difficult to estimate its energy consumption, material requirement, and GHG emissions [160]. As several studies have noted, there is no GHG and energy consumption life cycle analysis of asphaltene-based CFRP. This study, therefore, developed an LCA framework to evaluate the energy consumption and GHG emissions of asphaltene-based CFRP considering CFRP use, driving conditions, and climatic aspects on the life cycle performance of a lightweight HFCV. The specific objectives of this study are:

- To develop an LCA methodological framework to evaluate the net energy consumption and the life cycle GHG emissions of a conventional HFCV throughout its life cycle.
- To conduct a detailed life cycle assessment model of conventional HFCVs and CFRP HFCVs.
- To perform a comparative analysis of conventional HFCVs and CFRP HFCVs to understand the effect of weight decrease on the overall environmental performance.

- To perform comprehensive sensitivity and uncertainty analysis to identify the input parameters that most impact energy consumption and the life cycle GHG emissions.
- To calculate the net energy consumption and net energy ratios of conventional HFCVs and CFRP HFCVs throughout their life cycles.
- To identify and analyze the key components and the main processes (raw material quantification, operations parameters, disposal phase parameters) in each life cycle phase that contribute most to GHG emissions.

3.2. Method

The prime description of goal and scope is same as discussed in chapter 2. Each stage of this LCA is discussed below in detail.

3.2.1. Goal and scope definition

The prime goal of this research is to examine the life cycle GHG emissions and energy consumption of a CFRP-based HFCV produced using carbon fiber from bitumen-based asphaltene. This study also aims to compare the environmental performance of a CFRP-based HFCV with a conventional HFCV (manufactured from steel, aluminum, copper, etc.). Rest of the assumptions are mentioned in chapter 2.

3.2.2. Alberta and Canada context

Canada's transportation sector is the second-largest global contributor to GHG emissions and generated about 205.34 Mt CO_2 eq in 2021 because of the fossil fuel consumption.

Almost 90% of Canada's transportation sector relies on fossil fuels [97]. Hence, it is essential to find a fuel substitute. HFCVs have a small share of the transportation market but are gaining increased attention in several countries (i.e., Italy, the United States, and China) because they do not generate direct carbon emissions during operating, have low energy consumption, and have fast charging times compared to BEVs and ICEVs [35]. Presently, there are 15 hydrogen refuelling platforms in China [35]. According to a Chinese travel survey, there will be over 1 million HFCV operating on the road by 2037 [35]. The federal government in China has invested $156 million to build efficient HFCV infrastructure for hydrogen refueling stations [155, 158].. Moreover, insights from this LCA could be used to enhance government programs, which proposes technical developments in generating non-combustible and premium products from bitumen [161]. Substituting conventional raw materials with CFRP is considered an environmentally sustainable option for the global transportation sector [19]. More details on and explanation of the decarbonisation of the transportation sector is mentioned in section 2.2.2.

Figure 11 shows the system boundary indicating the individual life cycle stages along with flows and unit processes in each stage. We performed a cradle-to-grave analysis. The complete life cycle of a vehicle consists of vehicle production (raw material extraction, assembly), operation, maintenance, end of life (disposal), and the upstream process. Each life cycle stage is explained below in the inventory analysis section with all the data requirements and the relevant assumptions aligning with the goal and scope of this study.

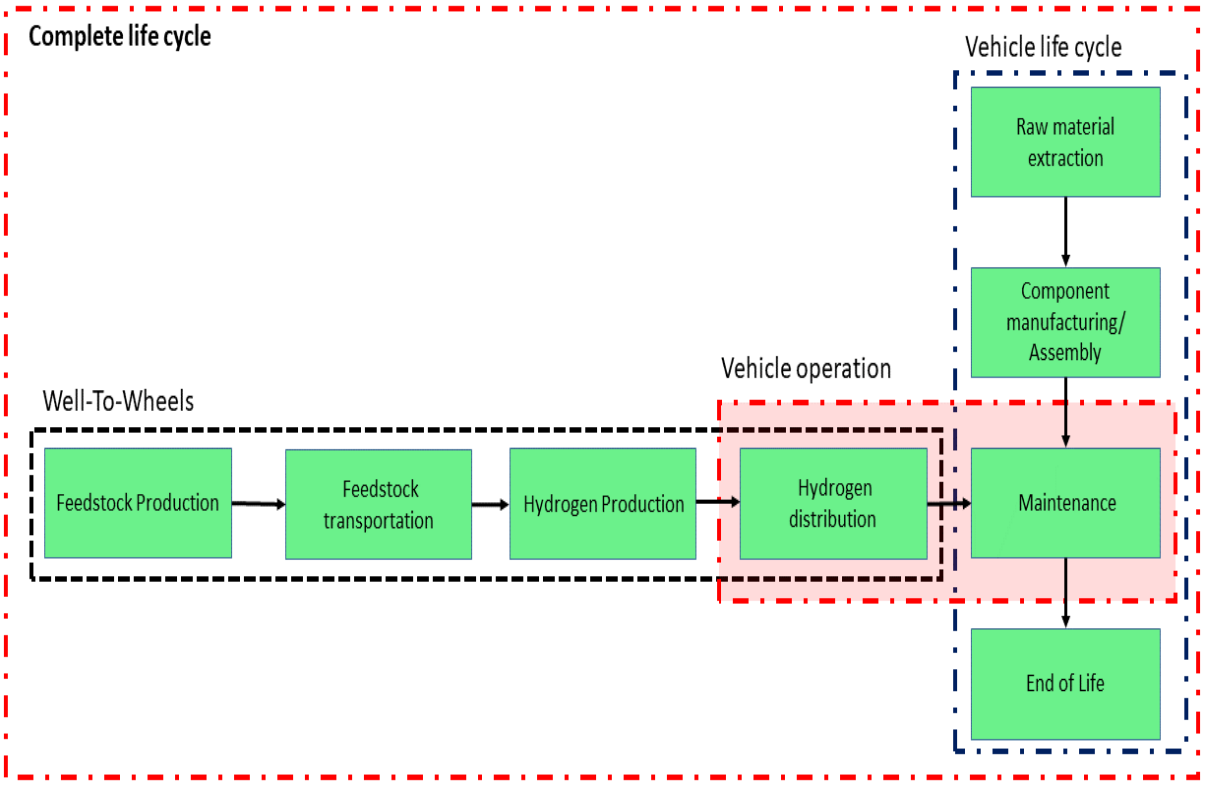

Figure 11: System boundary of a hydrogen fuel cell vehicle life cycle

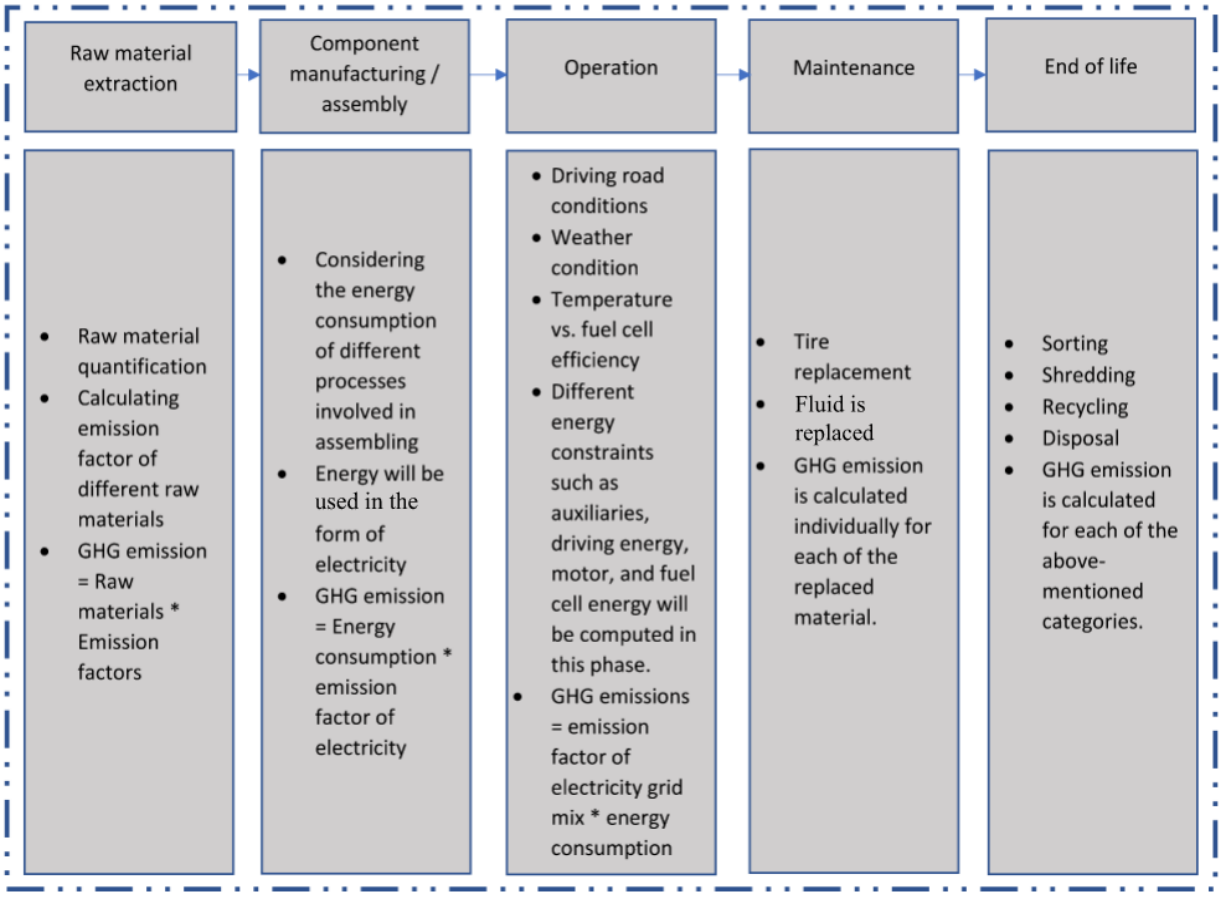

Figure 12: Key parameters and the process for GHG emission calculations in each life cycle phase

3.2.3. Inventory analysis

3.2.3.1. Vehicle manufacturing

Two pathways are considered for vehicle manufacturing, a carbon fiber-based lightweight HFCV made from asphaltene and a conventional HFCV manufactured from steel and aluminum. The primary vehicle components considered in both cases are the hydrogen fuel cell on-board storage, chassis, transmission system, traction motor, powertrain system, body in white, interior and exterior, controller, and traction battery [18, 105]. We developed detailed life cycle inventories for both a conventional HFCV

and a CFRP HFCV, which include the breakdown of prime components of HFCVs [35, 106].

The total mass of a conventional HFCV is 1,778 kg, of which 136 kg is the hydrogen fuel cell on-board storage and 48 kg is the lithium-ion battery [18, 35, 106]. The main raw materials used in the production of prime components of conventional HFCV and CFRP HFCVs are carbon fiber reinforced plastic (CFRP), cast aluminum, copper, steel, aluminum, rubber, glass fiber reinforced plastic (GFRP), cast iron, wrought aluminum, and plastic [18, 105]. The total mass of a CFRP HFCV is 1000 kg, of which 117 kg is hydrogen fuel cell on-board storage and 32 kg is the lithium-ion battery. The total mass is reduced by 44% by substituting steel and aluminum with CFRP [18-21, 35, 106]. Table 22 shows the bill of materials for the key components of both conventional HFCVs and CFRP HFCVs. Steel and aluminum are the main raw materials used in manufacturing a conventional HFCV, and together they account for more than 63% of the total mass contribution [18, 35]. Steel is primarily used to manufacture the body (507 kg), chassis (330 kg), powertrain system (65 kg), and traction motor (24 kg) [18, 35, 106]. Aluminum is uniformly distributed over all the components of a conventional HFCV [18, 35, 105, 106]. Plastic is used largely to produce a significant portion of the body (18%) and some of the powertrain system (17%) for a conventional HFCV [18, 105]. CFRP is primarily used in manufacturing the body (body in white, interior, exterior; 32%) and chassis (25%) for a CFRP-based HFCV [19, 20, 55, 56]. CFRP makes up 30% of the total mass contribution of a CFRP-based HFCV [19, 21, 55, 56, 162]. Table 23 shows the mass contribution of all the components of a CFRP-based

HFCV. CFRP (30%) and plastic (18%) make up most of the mass in a CFRP-based HFCV [19, 21, 56].

Table 22: Bill of materials for conventional and carbon fiber reinforced plastic (CFRP)-based HFCVs [18]

Materials	**Conventional vehicle**		**CFRP-based vehicle**	
	Mass, kg	**Mass, %**	**Mass, kg**	**Mass, %**
Steel/cast iron	1007	57	85	9
Aluminum	101	6	62	6
Copper/brass	64	4	45	5
Magnesium	0	0	0	0
Glass	37	2	37	4
Lead	14	1	14	1
Average plastic	182	10	181	18
Rubber	92	5	92	9
Carbon fiber	89	5	295	30
Glass fiber	10	1	9	1
Others	182	10	179	18
Total	**1778**	**100**	**1000**	**100**

Table 23: Mass distribution of key components used for conventional and CFRP-based HFCVs [18]

Components	**Conventional vehicle**		**CFRP-based vehicle**	
	Mass, kg	**Mass, %**	**Mass, kg**	**Mass, %**
Transmission system	44	2	12	1
Body (body inwhite, interior, exterior)	721	41	327	33
Chassis (without battery)	452	25	199	20
Powertrain system	130	7	67	7
Traction motor	66	4	66	7
Electronic controller	58	3	58	6
Fluids	103	6	103	10
Fuel cell on-board storage	136	8	117	12
Li ion battery	48	3	32	3
Pb acid battery	20	1	20	2
Total	**1778**	**100**	**1000**	**100**

We considered a lithium nickel manganese cobalt oxide (Li-NMC) battery with a capacity of 86.4 MJ (24 kWh) and an efficiency of 90% to store extra electrical energy that can be used when hydrogen is not available [37, 120, 163]. Li-NMC has a better energy density and less environmental burden than the traditional batteries used in HFCVs [7, 164]. Thermal insulation, glycol, steel, CFRP, aluminum, graphite, lithium,

coolant, and NMC powder (precursor) are the key components of the battery [18, 105, 106, 164].. A conventional Li-NMC battery with a mass of 48 kg and a CFRP-based Li-NMC battery with a mass of 32 kg and 90% efficiency were considered in this study. When conventional raw materials are replaced with CFRP, the weight of the Li-NMC battery is reduced by 33% [19, 21, 56, 165]. Table 24 presents the percentage mass distribution of both a conventional and a CFRP-based Li-NMC battery.

Hydrogen fuel cell on-board storage and the powertrain system are the only components that distinguish an HFCV from a BEV; the remaining components (chassis, body, battery, motor, controller; mass composition different) are the same [18, 105, 106]. A compressed hydrogen tank system, fuel cell, water supply system, air supply system, cooling system, and the piping system are the prime components of fuel cell on-board storage [18, 35, 106]. We considered a fuel cell on-board storage system with a mass of 136 kg for a conventional HFCV and 117 kg for a CFRP-based HFCV and reduced the weight of the HFCV by 14% when we substituted conventional raw materials with CFRP [18, 19, 21, 35, 106]. CFRP is the raw material most used for manufacturing fuel cell on-board storage system for both conventional HFCVs (65%) and CFRP-based HFCVs (80%) [13, 14, 19, 21].

In this study, the fuel cell is considered an energy converter (with a performance efficiency of 50%), generating electric energy from the chemical reaction of hydrogen and oxygen with the help of the proton exchange membrane [13, 14, 166]. To determine the efficiency of the fuel cell, we considered all the losses (auxiliary, hydrogen production, transportation and storage, and dissipated energy) [13, 14, 166]. The SMR process, with an emission factor of 11.35 (kg CO_2 eq/kg of grey hydrogen), is used for

hydrogen production; the stored hydrogen is compressed up to pressure of 700 bar [167-169]. Hydrogen is stored and HFCVs are charged in the special hydrogen refueling stations and, afterwards, hydrogen is stored in the storage tank (with a volume of 5 liters, in this study) at the compression pressure of 700 bar [35, 106, 168, 170]. We determined fuel consumption based on the calorific value of hydrogen (142 MJ/kg of hydrogen) and the efficiency of the fuel cell (50%) [35, 106, 168, 170].

Table 24: Mass distribution of a lithium NMC battery by key components for both conventional and CFRP HFCVs [18]

Components of a Li-NMC battery	**Conventional vehicle**		**CFRP-based vehicle**	
	Mass, kg	**Mass, %**	**Mass, kg**	**Mass, %**
Active material (NMC powder)	8	17	8	25
Graphite/carbon	4	8	4	12
Binder (PVDF)	0	1	0	0
Copper_B	11	23	0	0
Wrought aluminum	10	21	0	0
Electrolyte: Ethylene carbonate	1	4	1	3
Electrolyte: Dimethyl carbonate	2	4	2	6
Plastic: Polypropylene	1	2	1	3
Plastic: Polyethylene	0	1	0	0
Plastic: Polyethylene terephthalate	0	0	0	0
Steel	0	1	0	0
Thermal insulation	0	1	0	0
Coolant glycol	3	7	3	9
Carbon fiber	0	0	8	25
Electronic parts	5	10	5	16
Total	**48**	**100**	**32**	**100**

Table 25: Mass distribution of hydrogen fuel cell on-board storage by raw materials for both conventional and CFRP HFCVs [18]

Components of a Li-NMC battery	Conventional vehicle		CFRP-based vehicle	
	Mass, kg	Mass, %	Mass, kg	Mass, %
CFRP	89	66	94	80
Glass fiber	6	4	6	5
Wrought aluminum	0	0	0	0
Average plastic	11	8	11	9
Steel	13	9	0	0
Stainless steel	11	8	0	0
Others	7	5	6	5
Total	**136**	**100**	**32**	**100**

3.2.3.2. Assembly of an HFCV

This phase is the assembling of all the prime components (mentioned above) to form a complete HFCV. The assembly phase includes paint production, vehicle components assembly, painting, HVAC, lighting, heating, material handling, welding, and lithium-ion battery and lead acid battery assembly [18, 106]. The energy consumption and life cycle GHG emissions for each of process was computed using the information from the GREET model [18, 106].

3.2.3.3. Vehicle operation

Unlike ICEVs, HFCVs, like BEVs, use electricity (produced by the chemical reaction of oxygen and hydrogen) to propel the vehicle [13]. The operation phase emissions depend mostly on the process used to produce hydrogen [148, 156]. Since hydrogen is the primary source of electric energy delivered to the electric motor to power the HFCV,

it is important to consider the feasibility and efficiency of the current hydrogen production process as well as the changes needed in the industry [50, 147]. The global annual production of hydrogen is more than 50 million tonnes [50, 147]. Hydrogen is primarily derived from natural gas (48%), refinery waste gases (30%), and coal (18%), and a small amount (4%) from electrolysis and biomass [50, 147]. The basic methods of hydrogen production are natural gas reforming, electrolysis of water, steam methane reforming, water splitting by photo catalysis, biomass conversion, and gasification of coal [50, 147]. Steam methane reforming (SMR) is the most widely used because it can obtain a high level of purity in the produced hydrogen at reasonable cost. In SMR, methane from natural gas is heated with steam and produces a carbon monoxide (CO)/hydrogen mixture that can be used as a fuel [50]. The effectiveness of hydrogen production from SMR ranges from 65% to 80% depending on the fuel mix composition [144, 171, 172]. Because Alberta, Canada is considered the base location for this study, we considered the dynamic aspect of the fuel mix used to produce of hydrogen in Alberta [13, 15, 100]. Considering the dynamic aspect of the fuel mix allowed us to clearly predict the net energy consumption and the life cycle GHG emissions generated throughout the lifetime of an HFCV in its operation phase.

All the operation phase calculations and energy assumptions were implemented as per the directives defined in chapter 2. Drag and rolling coefficient values for both conventional BEVs and CFRP BEVs are shown in Table 6 and Table 7. The key parameters considered for the operation phase are in Table 26. The equations used to determine the rolling force and drag force are in the supporting information.

Table 26: Operational phase scenarios considered and their respective key parameters for an HFCV

Scenarios	Key parameters
City driving in Summer (City_Summer)	• Operational time [112]
	• Temperature 15ºC to 35ºC [15, 106, 107]
	• Rolling coefficient [10, 114]
	• Drag coefficient [10, 114]
	• Average speed and acceleration [27, 112]
Driving on Highway in Severe in Winter (Highway_Severe_Winter)	• Operational time [112]
	• Temperature -40ºC to 14ºC [15, 112, 113]
	• Rolling coefficient [10, 114]
	• Drag coefficient [10, 114]
	• Average speed and acceleration [27, 112]

The details of the energy lost in motor and controller is mentioned in chapter 2. The motor and controller efficiency values for each of the scenario for both conventional HFCVs and CFRP HFCVs are shown in Table 8 incorporated in chapter 2.

The total considered weight of a conventional HFCV is 1858 kg, 1778 kg of which is vehicle weight and 80 kg passenger weight, and for a CFRP-based HFCV the weight is 1080 kg, 1000 kg of which is the vehicle weight and 80 kg passenger weight [18, 19, 35, 158]. The average traveling distance is considered to be 50 km in both scenarios, but the operational time differs given the different speed limits and traffic rules [111, 118, 129]. . The energy consumption for city in summer is 0.96 MJ/km; this is less than highway in severe winter, 4.38 MJ/km for a conventional HFCV [173]. For a CFRP-based HFCV, the energy consumption for city in summer is 0.68 MJ/km and 2.79 MJ/km for highway in severe winter [12, 173]. Heating or AC energy constraints also differ because of the difference in the climatic conditions and is reflected in terms of average power demand [12, 173], expressed as a % of maximum power rating; it is lower for city in summer and

higher for highway in severe winter, 25% and 75% of max rating, respectively (it is the same for both a conventional HFCV and a CFRP HFCV) [12, 173].

We estimated the net energy consumption of auxiliaries by summing the energy required for seat preheating, radio and navigation, and LED lights. The auxiliaries' energy consumption is higher in highway in severe winter than for city in summer (0.01 MJ/km and close to 0 MJ/km, respectively) and is the same for both a CFRP HFCV and a conventional HFCV [111, 173]. Aggressive braking, uneven roads, and intermittent stopping at traffic signals are associated with dissipated energy and values will vary depending on the road characteristics, climatic conditions, and the frequency of traffic lights [34, 173]. The dissipated energy value is higher in highway in severe winter than city in summer (0.1 MJ/km and 0.02 MJ/km, respectively) and is the same for both a conventional HFCV and a CFRP-based HFCV [34, 173]. The energy consumed to provide the desired torque to the HFCV will differ depending on the topography of the road, drag coefficient, speed, rolling coefficient, and acceleration [16].The detailed explanation is mentioned in the chapter 2. The drive energy for a CFRP-based HFCV in city in summer is 0.22 MJ/km and in highway in severe winter is 0.88 MJ/km; for a conventional HFCV, these values are 0.36 MJ/km and 1.67 MJ/km, respectively [16, 19].

We estimated the operation's phase energy consumption by summing each energy constraint mentioned above. AC consumption is higher in the city in summer scenario than the highway in severe winter scenario and for heat consumption, the opposite. Energy consumed in seat preheating, radio and navigation, and LED lighting is almost same for each scenario [10, 19]. The energy dissipated due to aggressive braking, uneven roads, and intermittent stopping at traffic signals is higher in the city in summer scenario than

the highway in severe winter scenario because in the city there are more stops and traffic lights [119].

Net energy consumption is expressed in terms of MJ/km. GHG emissions for highway in severe winter are higher than for city in summer: 54 g CO_2 eq/km and 223 g CO_2 eq/km, respectively, for a CFRP-based HFCV and 78 g CO_2 eq/km and 353 g CO_2 eq/km for a conventional HFCV.

3.2.3.4. Maintenance of an HFCV

Many vital components, like fluids, tires, battery, electric motor, fuel cell, gaskets, and bipolar plates, lose their peak performance after being operated for a certain number of kilometers and need to be inspected, serviced, or replaced to maintain the vehicle's desired performance and fuel economy [18, 95]. The replacement interval of components and fluids differs because of differences in the characteristics and applications [18, 95]. For example, the powertrain coolant, brake fluid, and tires are assumed to be replaced three times throughout the considered lifetime of HFCV [18, 95]. For transmission fluid and adhesives, 2 and 14 replacements are considered [18, 95, 123]. GHG emissions for each replaced component were estimated from Bartolozzi et al.'s work [95, 123].

3.2.3.5. End of Life

Recycling and disposal are the two important aspects of this phase. The recycling phase is completely uncertain because of the high unpredictability about how the product will be recycled (i.e., open loop or closed loop) [120]. So, for clear and transparent results, we omitted this phase; only the disposal emissions were evaluated and quantified. The

disposal phase for both conventional and CFRP based-HFCVs is categorized into several processes: sorting or dismantling, transportation, shredding, and landfilling [96]. The disposed sections of the HFCV are sorted into the glider and powertrain, as the techniques involved in disposing them are different [96, 120]. That said, recent studies proposed that all the parts of the powertrain and glider be disposed of in the same fashion [96, 120].

Sorting or dismantling is considered to be done in Vancouver, BC (this is the only recycling facility of its kind in Canada), 40 km from the shredding facility in Delta, BC [96, 120]. Dismantled portions are transported to the shredding facility in heavy trucks. Energy consumption and GHG emissions for sorting, transportation, and dismantling are directly proportional to the mass of the vehicle, as per the study conducted by the City of Vancouver on the disposal of BEVs [96, 120]. The concepts and techniques involved in disposal are same for both BEVs and HFCVs, and the BEV data from literature [96] was directly used for quantifying the GHG emissions of HFCVs and then modified by taking into account the change in mass and some alterations in the powertrain system (the addition of a hydrogen fuel cell on-board storage system).

For the shredding phase, we used D. Baker's and B. Kukreja's data to calculate energy consumption and GHG emissions [96, 120]. The disposal emissions and energy calculations of the glider were also taken from those studies and one by Nemry et al. [96, 120, 124]. The energy requirement and GHG emissions for the disposal of the Li-ion battery and powertrain system are also from these sources [96, 120, 124]. This phase is described in detail in Chapter 2, whose study takes a similar approach and procedure.

3.3. Results and discussion

The net life cycle GHG emission estimates of conventional and CFRP-based HFCVs obtained in this study are shared here. The GHG emissions are given as g CO_2 eq/km assuming a lifetime of 295,095 km, starting with emissions produced during the production of prime vehicle components, followed by the assembly phase, the operation phase for both scenarios, maintenance, and finally the end of life. The GHG emissions of the two scenarios are compared later, to determine favourable conditions for the operation of an HFCV. The characteristics of road and climatic conditions are normalized for selected provinces in Canada to determine overall performance and compute the net life cycle GHG emissions for both the conventional and the CFRP-based HFCV. Finally, sensitivity and uncertainty analysis are performed for both scenarios.

3.3.1. Vehicle production GHG emissions

Figure 13 and Figure 14 show the GHG emissions generated during HFCV production from prime raw materials and components, respectively. A conventional HFCV generates 9.3% fewer GHG emissions than a CFRP-based HFCV. In both scenarios, the highest GHG emissions are generated in fabricating the body (body in white, exterior, and interior) and the chassis, which in total account for almost 55% of vehicle's manufacturing emissions. For a conventional HFCV, steel and aluminum are the primary GHG contributors (48% and 7%, respectively). The higher % of GHG emissions from steel and aluminum is due to their large mass contributions as well as the energy-intensive processes involved in their production. CFRP, copper, plastic, and rubber also have significant GHG emissions contributions. For the CFRP-based HFCV, CFRP contributes the highest GHG emissions,

accounting for almost 72% of vehicle's total production emissions. CFRP is produced through a chain of highly energy-intensive processes, resulting in considerably higher GHG emissions per kg than conventional raw materials like steel and aluminum.

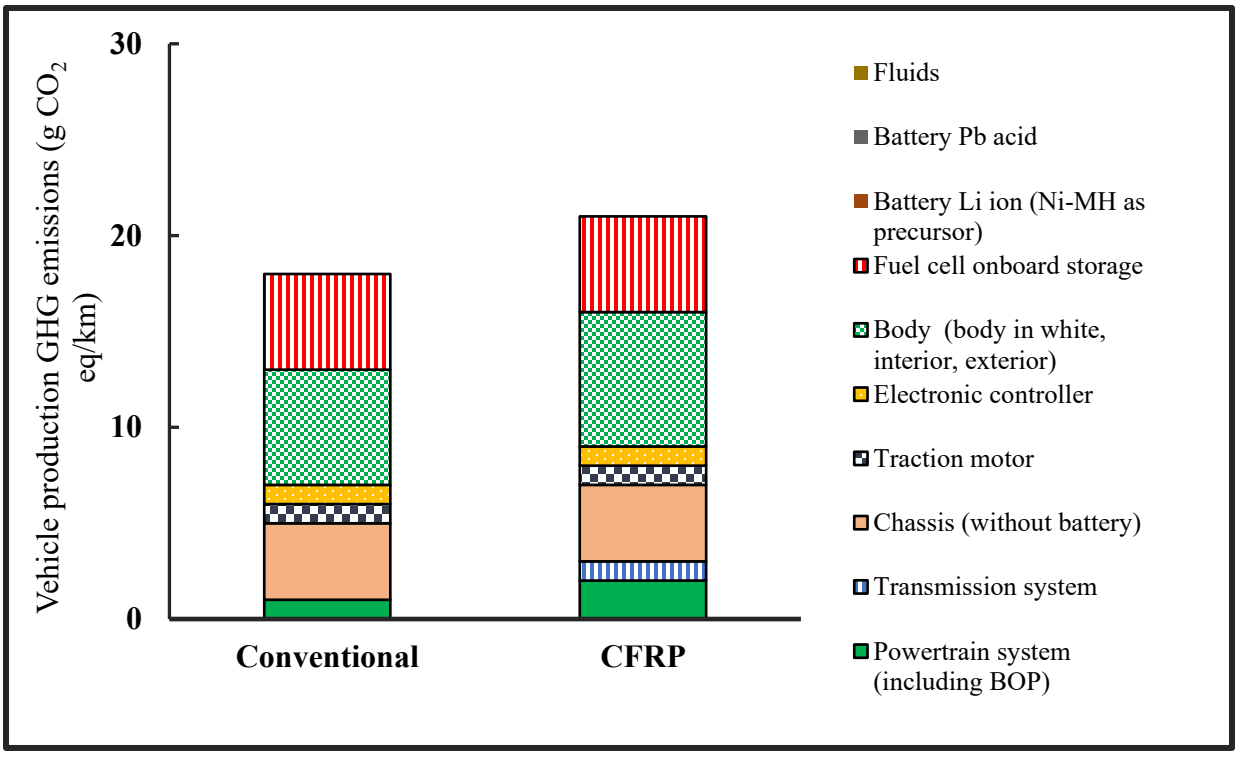

Figure 13: Vehicle manufacturing GHG emissions contribution by key components: conventional vs. carbon fiber reinforced plastic (CFRP) HFCVs

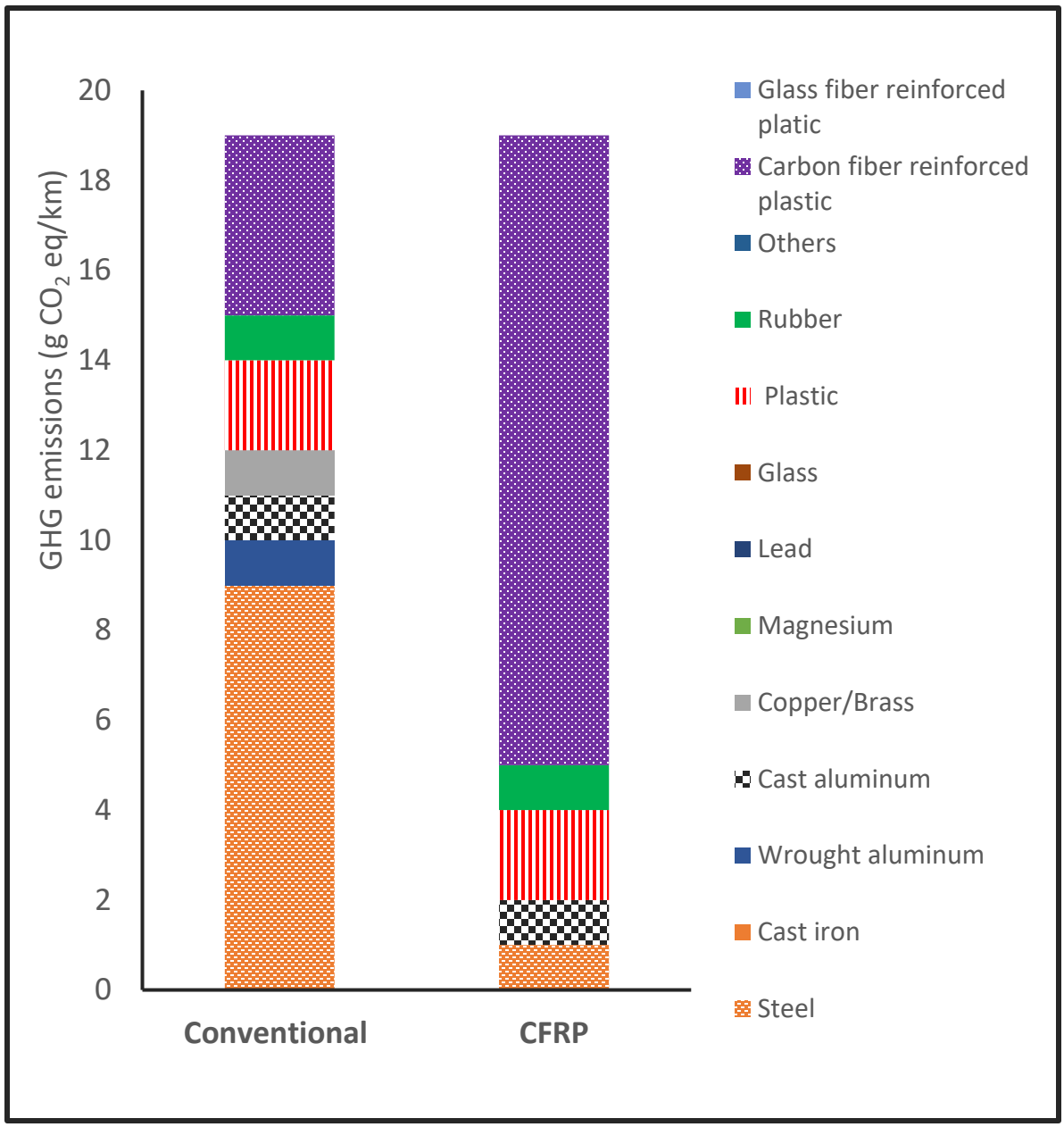

Figure 14: Vehicle manufacturing GHG emission contribution by prime raw materials: conventional vs. carbon fiber reinforced plastic (CFRP) HFCVs

3.3.2. Battery and hydrogen fuel cell on-board storage production:

We used battery production emissions for a Li-NMC battery of 0.46 g CO_2 eq/km for a CFRP-based HFCV and 0.31g CO_2 eq/km for a conventional HFCV. The GHG emissions are higher for the CFRP-based HFCV because CFRP is the material used most in Li-NMC battery manufacturing for this vehicle and, as noted above, is highly energy intensive, unlike steel and aluminum, the material used most in conventional HFCVs. The GHG emissions generated in hydrogen fuel cell on-board storage in both conventional and CFRP-based HFCVs are 4.6 g CO_2 eq/km. This is because CFRP is the primary raw material used, and the respective % mass contributions are almost the same in both cases.

3.3.3. Vehicle operation GHG emissions

The GHG emissions generated in the operation phase are mainly the upstream emissions from hydrogen production [13]. The emissions are different in the considered scenarios (city in summer, highway in severe winter) mainly because of differences in driving patterns, road characteristics, and the prevalent climatic conditions that influence overall operational energy consumption [13]. Heating and air conditioning, dissipated energy loss, auxiliaries' activities, and driving energy are the main energy-consuming parameters. The energy consumption model was developed to consider the rolling coefficient, frontal area, acceleration, speed, drag coefficient, mass, density, and travelling time and distance of an HFCV [12]. However, these parameters will change with climatic conditions and road specifications. The overall emissions in the summer scenarios are lower than in the mild and severe winter scenarios because there is less internal battery loss [10, 12]. Based on the type of road, the percentage contribution of operation emissions is greater in cities than in rural

areas and highways. The overall operational and life cycle emission in cities is lower than in rural areas and highway roads because of calm driving speeds and acceleration [10].

The energy consumed by heaters and AC is calculated by multiplying the highest heater and AC demand, operational time, and average use of the highest power of the heater or AC. The highest power demand of the heater or AC is the same in each scenario, 2.30 KW and 1.40 KW, respectively [29]. Operational time is defined as the time required to travel the considered travelling distance, 50 km/day. Operational time differs among scenarios because of the different climatic conditions, roads, and traffic obstructions [29]. Operational time at highways is shorter than in rural areas and city roads because highways have higher speed limits and fewer traffic obstructions. Operational time ranges from 50 minutes on highways to 75 minutes in cities [29]. The average use of the highest power of AC or heaters is calculated based on the thermal drive cycle and is usually expressed in percentage (%.) The thermal drive cycle defines the temperature range for each scenario taking into account the prevalent climatic conditions of Alberta, Canada [29]. The temperature range is -35 C to – 15 C in for severe winter, -14 C to 10 C in mild winter, and 11 C to 35 C in summer. The comfortable temperature inside the EV is from 18 C to 22 C. This range and the range of climatic conditions are used as input to compute the average demand of AC or heater in each scenario [102]. For each temperature value, the use of AC or heat is calculated in terms of the percent of maximum power demand using a basic thermal equation from the World harmonized Light Duty vehicle Test Cycle). All the % values are plotted, and the final average value is computed using regression analysis defined by the (Urban Dynamometer Driving Schedule (UDDS). The % average demand of heat is highest in severe winter and for AC it is highest in summer and is independent of road type [29]. The % average demand

of the heater or AC is from 25% to 75%. The average consumption of AC or heat is computed by multiplying the three variables defined above and then dividing them by the lifetime of EV to express the consumption in MJ /km [29]. The average consumption of the AC/heater is 0.03 MJ/km city in summer to 0.08 MJ/km in highway in severe winter. The average consumption of the AC/heater is directly proportional to operational time, as the operational time is higher in cities because there are more traffic obstructions and lower speed limits, leading to more energy consumption than on highways and rural roads [29]. The GHG emission values for the energy consumed by AC/heaters for every scenario is shown below in Table 28.

. The GHG emission values of the energy consumed by the auxiliaries of HFCV is calculated in same way as in BEV for every considered scenario and is shown below in Table 29

. The GHG emission values of the energy lost in motor and controller of HFCV is calculated in same way as in BEV for every considered scenario and is shown below in Table 30. The GHG emissions lost in the motor and controller are 3 g CO_2 eq/km in city in summer to 15 g CO_2 eq/km in highway in severe winter for conventional BEVs.

. The % energy dissipation factor for city and highway / rural is considered to be 25% and 20% as per the WLTC based on the driving patterns of Alberta, Canada [12, 15]. Regenerative braking is one of the most crucial accessories of the HFCV considered in this study. This study thus considers regeneration efficiency, which recovers some portion of dissipated energy. A regeneration efficiency of 69% is considered for every scenario; in other words, 69% of energy dissipated is recovered, for every scenario [29].The detailed discussion of regenerative energy savings is discussed in chapter 2. The net energy dissipation ranges from 0.02 MJ/km in city in summer to 0.09 MJ/km in highway in severe

winter. The GHG emissions values for the dissipated energy for every scenario is shown below in Table 31.

The equation utilized to compute driving energy of HFCV is mentioned in chapter 2. The mass, air density, travelling distance, and frontal area are the same for each scenario with values of 1511 kg, 1.2 kg/m^3, 50 km/day, 2.27 m^2, respectively [12]. The remaining parameters (i.e., acceleration, speed, rolling coefficient, and drag coefficient) vary based on the scenario's prevalent road and climatic conditions [12]. Acceleration, for instance, varies with road type, climatic conditions, traffic signals etc., and is greater on highways than in cities and on rural roads because speed limits are higher and there are fewer traffic obstructions on highways [12]. Acceleration ranges from 0.14 m/sec^2 in city in summer to 0.52 m/sec^2 in rural areas in severe winter considering all the factors mentioned above [12].

.

The drag coefficient ranges from 0.29 in all city road scenarios to 0.77 in all highway road scenarios [17]. Drag and rolling coefficient values are given in Tables 6 and 7. Icy and snowy roads have a lower rolling coefficient than dry roads because they generate less static and kinetic friction than dry roads do, indicating that the rolling coefficient value will be higher in summer than in mild and severe winter [16]. Possible rolling coefficient values are 0.001 in severe winter and 0.0076 in summer [16].

The energy required to provide the desired torque to the wheels is the sum of all three forces multiplied by the travelling distance. The energy required to provide the desired torque to

the wheels ranges from 0.34 MJ/km to 0.92 MJ/km [13]. In winter and on highways, the energy required to achieve desired torques is higher than in summer and in the city because of the higher speed loads and greater friction from snowy roads [16].

The net energy consumption is the sum of all the energy constraints mentioned above. The net energy consumption of the operations phase is 0.51 MJ/km for city in summer to 2.51 MJ/km for highway in severe winter. Figure 15 shows the net energy consumption of the operation phase for all the scenarios in a graph. The GHG emissions values of the dissipated energy for all the considered scenarios is shown below in Table 14. Figure 6 shows the net energy consumption of operation phase for all the scenarios in a graph. The GHG emissions for the operation phase are calculated by multiplying the net energy consumption with the relevant emission factor of Alberta's grid mix.

Figure 15 shows the operational GHG emission results for the considered scenarios for both the conventional HFCV and the CFRP-based HFCV. A CFRP-based HFCV produces fewer GHG emissions than a conventional HFCV for both the city in summer and highway in severe winter scenarios. A CFRP-based HFCV weighs 44% less than a conventional HFCV. The lower mass value lowers its overall energy consumption, leading to higher performance and energy efficiency. A CFRP-based HFCV generates 30% (in city in summer) and 37% (in highway in severe winter) fewer operational GHG emissions than conventional HFCV. Most of the saved energy is from the driving energy providing the desired torque to the wheels, followed by the losses produced in the controller and motor. Driving emissions

account for almost 76% of the total operational GHG emission in both cases. The city in summer scenario contributes 78 g eq/km for a conventional HFCV and 54 g CO_2 eq/km for a CFRP-based HFCV. The highway in severe winter scenario contributes 353 g CO_2 eq/km for a conventional HFCV and 223 g CO_2 eq/km for a CFRP-based HFCV.

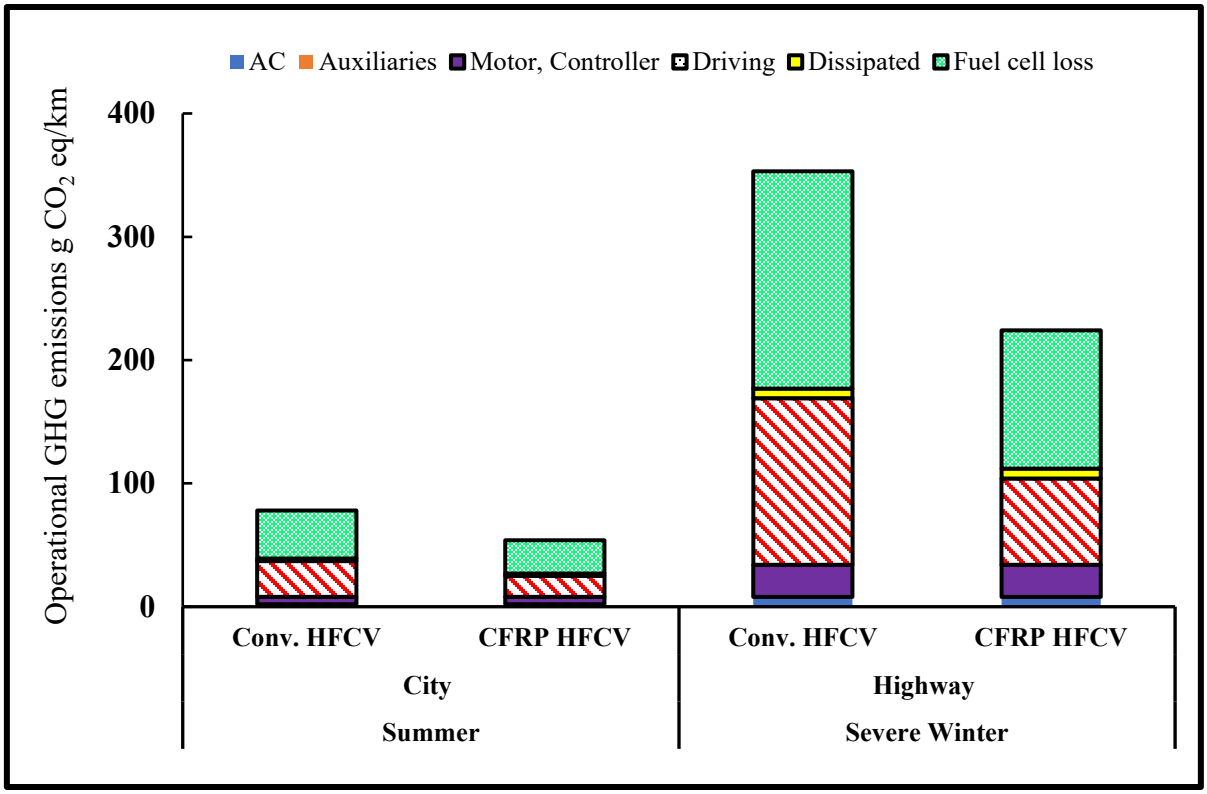

Figure 15: Operational GHG emissions for the considered scenarios: conventional vs. carbon fiber reinforced plastic (CFRP) HFCV

Table 27: GHG emissions of AC/heater consumption for both conventional and CFRP HFCVs [13, 29]

Scenarios	GHG emissions (conventional HFCV)	GHG emissions (CFRP HFCV)
City in summer	1	1
Highway in severe winter	4	4

Table 28: GHG emissions of auxiliaries' consumption for both conventional and CFRP HFCVs [13, 29]

Scenarios	GHG emissions (conventional HFCV)	GHG emissions (CFRP HFCV)
City in summer	0.12	0.12
Highway in severe winter	0.41	0.41

Table 29: GHG emissions of energy lost in the motor and controller for both conventional and CFRP HFCVs [13, 14, 29]

Scenarios	GHG emissions (conventional HFCV)	GHG emissions (CFRP HFCV)
City in summer	3	3
Highway in severe winter	15	15

Table 30: GHG emissions of energy dissipated for both conventional and CFRP HFCVs [13, 29]

Scenarios	GHG emissions (conventional HFCV)	GHG emissions (CFRP HFCV)
City in summer	1	1
Highway in severe winter	5	5

Table 31: GHG emissions of energy consumed for driving for both conventional and CFRP HFCVs [13, 15, 29]

Scenarios	GHG emissions (conventional HFCV)	GHG emissions (CFRP HFCV)
City in summer	18	11
Highway in severe winter	82	43

Table 32: Total GHG emissions of operation phase for both conventional and CFRP HFCVs [13, 15, 29]

Scenarios	GHG emissions (conventional HFCV)	GHG emissions (CFRP HFCV)
City in summer	24	16
Highway in severe winter	107	68

3.3.4. Life cycle GHG emissions

Figure 16 shows the net life cycle GHG emissions for both a conventional HFCV and a CFRP-based HFCV. The emissions for city in summer scenario are 107 g CO_2 eq/km for a conventional HFCV and 85 g CO_2 eq/km for a CFRP-based HFCV. The emissions for highway in severe winter scenario are 382 g CO_2 eq/km for a conventional HFCV and 254 g CO_2 eq/km for a CFRP-based HFCV. The emissions for a conventional HFCV are 26% and 50% higher than those for a CFRP-based HFCV for the city in summer and highway in severe winter scenarios. The operation phase makes the largest contribution to GHG emissions (64% to 92%), followed by the manufacturing phase (4% to 23%) for both scenarios for both conventional and CFRP-based HFCVs. The contribution from the remaining life cycle phases (assembly, maintenance, and end of life) are below 10%, so none of these phases is mentioned in the results and discussion section.

Although manufacturing GHG emissions for a CFRP-based HFCV are relatively higher than for a conventional HFCV, primarily because of the higher emission intensity of carbon fiber processing compared to steel and aluminum, there is large trade-off with operational stage emissions. The life cycle GHG emissions savings obtained on substituting steel and aluminum with CFRP are seen most in the operational phase emissions because the key

parameters of this phase (change in the road type [slope], climatic condition, and driving pattern) can significantly affect the net life cycle emissions. Among the considered scenarios, the life cycle GHG emissions for a conventional HFCV are 26% and 50% higher for city in summer and highway in severe winter than for a CFRP-based HFCV. The benefits of a CFRP-based HFCV over a conventional HFCV are seen most in the highway in severe winter scenario, but the benefits are marginal in the city in summer scenario.

The end-of-life phase incorporates the energy requirements for transporting the used HFCV to the recycling facility, followed by the dismantling, sorting, shredding, and disposal of non-recyclable parts. Given the high uncertainty of this phase, recycling and using the scrap metals in vehicle production were omitted from this study. The disposal GHG emissions associated with this phase range from 0.2% to 1.4% in both scenarios for CFRP-based and conventional HFCVs. Using recycled raw materials is considered to reduce GHG emissions from the production phase depending on the recycling process. Similarly, using recycled CFRP instead of virgin CFRP will significantly impact the manufacturing emissions. However, because the applications and technology are still developing, large-scale CFRP recycling facilities for HFCV have not been developed.

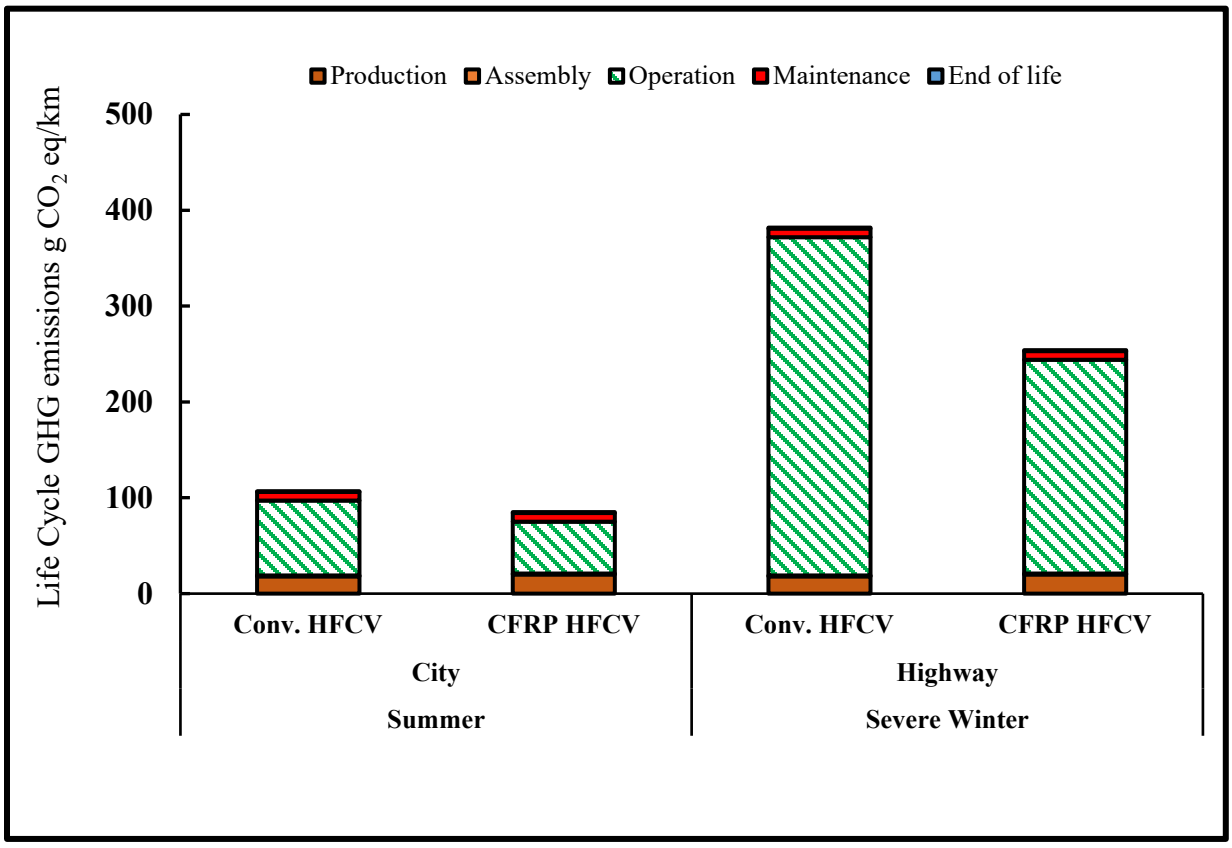

Figure 16: Life cycle GHG emissions: conventional vs. carbon fiber reinforced plastic (CFRP)-based HFCVs

3.3.5. Sensitivity and uncertainty analysis

The sensitivity and uncertainty analysis of the HFCV was conducted in a similar manner and with the same software described in section 2.3.5. Once the key sensitive input parameters ware identified (i.e., those parameters located far from the origin of the plot), we conducted uncertainty analysis using a Monte Carlo simulation to obtain the likely range of life cycle GHG emissions for both conventional and CFRP HFCVs for both considered scenarios.

The Morris plot for highway in severe winter scenario for a CFRP-based HFCV is shown in Figure 17; each scenario showed a similar trend. Parameters that are located far from the origin of the Morris plot and are considered the most sensitive ones. The fuel cell efficiency,

average acceleration, hydrogen emission factor, average speed, frontal area, drag coefficient, motor efficiency, and HFCV lifetime are the parameters that most influence the energy required for driving the wheel. The parameters in the red box (those closer to the origin of the plot) have a negligible effect on the output results and hence were ignored**.**

The data for the most sensitive parameters were refined to their maximum and minimum values to determine uncertainty ranges. Table 34 summarizes these key parameters along with their corresponding maximum and minimum values. Figure 18 shows the box plot of the life cycle GHG emissions for the considered scenarios for both conventional and CFRP-based HFCVs. The GHG emissions for the highway in severe winter scenario are from 254^{+48}_{-34} g CO_2 eq/km for CFRP-based to 382^{+99}_{-65} g CO_2 eq/km for conventional HFCVs. For the city in summer scenario, the emissions range from 85^{+17}_{-12} g CO_2 eq/km for CFRP-based to 107^{+25}_{-18} g CO_2 eq/km for conventional HFCVs, respectively.

Table 33: Range of values for sensitive parameters

Parameters	**Minimum**	**Maximum**	**Source**
Vehicle lifetime, km	200,000	350,000	[13, 18]
Average distance per day, km/day	20	80	[15, 100, 129]
Efficiency of motor, η	75	95	[127]
Efficiency of controller, η	85	98	[127]
Rolling coefficient (city in summer, conventional)	0.00235	0.76	[16, 94, 127]

Parameters	Minimum	Maximum	Source
Rolling coefficient (highway in severe winter, conventional)	0.00175	0.00448	[16, 94, 127]
Rolling coefficient (city in summer, CFRP)	0.00235	0.76	[16, 94, 127]
Rolling coefficient (highway in severe winter, CFRP)	0.00175	0.00448	[16, 94, 127]
Drag coefficient (city in summer, conventional)	0.2	0.524	[13, 94, 174]
Drag coefficient (highway in severe winter, conventional)	0.2	0.812	[13, 94, 174]
Drag coefficient (city in summer, CFRP)	0.2	0.524	[13, 94, 174]
Drag coefficient (highway in severe winter, CFRP)	0.2	0.812	[13, 94, 174]
Average speed (city), km/hr	30	55	[111, 174]
Average speed (highway), km/hr	70	100	[111, 174]
Average acceleration (city), m/sec^2	0.1	0.4	[111, 174]

Parameters	Minimum	Maximum	Source
Average acceleration (highway), m/sec^2	0.14	0.67	[111, 174]
Steel conventional mass, kg	283	803	[18, 93, 94, 138]
CFRP emission factor, kg CO^2 eq/kg	15.25	34.4	[18, 23, 93, 138]
Frontal area, m^2	1.5	3.5	[30, 126, 130]
Density, kg/m^3	1	1.4	[12, 126, 130]
Rating power heater, kW	1	3.4	[12]
Rating power AC, kW	1	2.5	[12]
Efficiency of fuel cell, η	30	60	[48, 148, 150]
Hydrogen emission factor	8	14	[144, 168, 169, 171]

Figure 17: Morris plot for highway in severe winter scenario for a CFRP HFCV

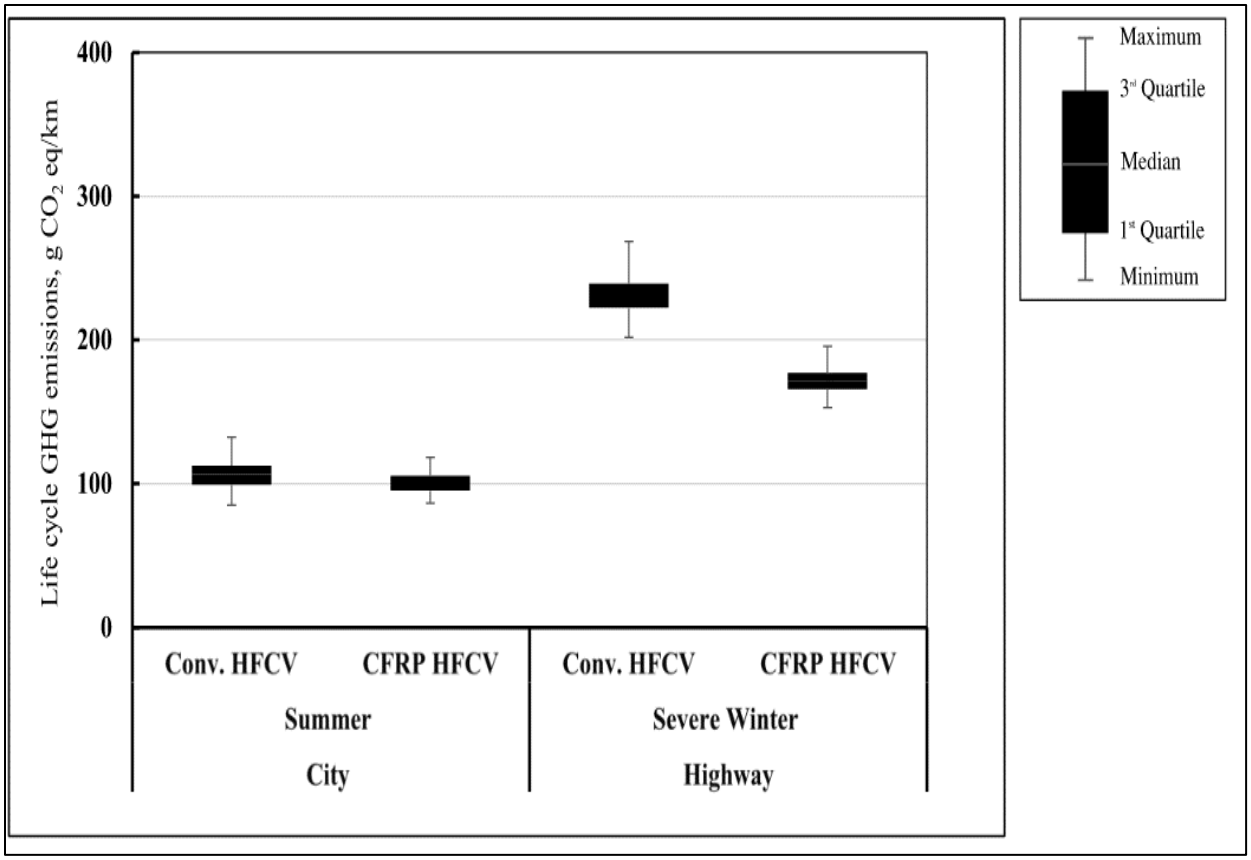

Figure 18: Life cycle GHG emissions: Uncertainty results

3.4. Conclusion

This study examined and quantified the environmental benefits of substituting conventional materials like steel and aluminum with CFRP to produce a lightweight HFCV. The life cycle GHG emissions of a CFRP-based HFCV manufactured from carbon fiber made from asphaltene were compared with those of a conventional vehicle made primarily with steel and aluminum. This study quantified the environmental trade-offs in the life cycle of an HFCV starting from raw material extraction to its end of life (i.e., we conducted a cradle-to-grave analysis). We developed two scenarios, city in summer and highway in severe winter, that consider changes in driving pattern, climatic conditions, and road type.

We found that replacing steel and aluminum with CFRP for manufacturing the key components of an HFCV significantly reduced the overall GHG emissions, by different amounts in each scenario. The most savings are in the operational phase, and, of the scenarios, the highest savings are in highway in severe winter scenario, simply because the most savings will be in the scenario with the highest operational emissions, that is, highway in severe winter scenario. The highway in severe winter scenario has life cycle GHG emissions of 254 g CO_2 eq/km for a CFRP-based HFCV and 382 g CO_2 eq/km for a conventional HFCV and in the city in summer scenario, 85 g CO_2 eq/km for a CFRP-based HFCV and 107 g CO_2 eq/km for a conventional HFCV. The highest emissions are in the operation phase in every scenario, followed by the manufacturing phase. The influence of the other life cycle phases on GHG emissions is marginal.

The results of this study suggest that using a CFRP-based HFCV can significantly reduce GHG emissions in Alberta, Canada, whose climate is characterized by severe, long winters. Sensitivity and uncertainty analysis were performed to determine the most sensitive parameters and estimate emissions ranges for two scenarios. The life cycle GHG emissions for the highway in severe winter

scenario are 382^{+99}_{-65} g CO_2 eq/km for a conventional HFCV and 254^{+48}_{-34} g CO_2 eq/km for a CFRP-based HFCV. The life cycle GHG emissions for the city in summer scenario are 107^{+25}_{-18} g CO_2 eq/km for a conventional HFCV and 85^{+17}_{-12} g CO_2 eq/km for a CFRP-based HFCV.

The results of this study provide insights for decision makers on the process conditions that can be improved to reduce GHG emissions on a commercial scale. These results can also guide stakeholders and technology developers in building infrastructure and facilities for asphaltene-based CFRP production in Alberta, Canada.

Chapter 4

4. Conclusions and Recommendations for Future Work

4.1. Conclusion

In this research, we estimated the environmental impacts of using carbon fiber reinforced plastic (CFRP; made from asphaltene) to manufacture lightweight battery electric vehicles (BEVs) and hydrogen fuel cell vehicles (HFCVs). The objective was to develop a comprehensive LCA framework of CFRP-based BEVs and HFCVs and compare them with conventional steel and aluminum BEVs and HFCVs. There are some challenges associated with current BEV battery technologies and the reduced efficiency of HFCV fuel cells. BEVs and HFCVs incorporate the most advanced technologies and significantly reduce GHG emissions. However, their initial cost and weight negatively impact their mass production. This research determined the environmental performance of each life cycle phase of BEVs and HFCVs from raw material extraction to end of life. Operational phase emissions are the largest contributor of life cycle emissions among all the phases and are significantly impacted by driving pattern, road type, and climatic conditions. We developed nine BEV scenarios based on climatic and driving conditions: operation in city in summer, operation on highway in summer, operation in rural area in summer, operation in city in mild winter, operation on highway in mild winter, operation in rural area in mild winter, operation in city in severe winter, operation on highway in severe winter, operation in rural area in severe winter. Two operational scenarios for HFCVs were developed based on climatic and driving conditions: operation in city in summer and operation on highway in severe winter.

The results indicate that replacing conventional raw materials (steel, aluminum etc.) with CFRP will significantly reduce GHG emissions for both BEVs and HFCVs. The magnitude of emission savings differs among the scenarios. The highest GHG emission savings for CFRP BEVs and HFCVs is achieved in the scenario with the highest GHG emissions in conventional BEVs and HFCVs, highway in severe winter. The highway in severe winter scenario shows life cycle GHGs of 382 g CO_2 eq/km for a conventional HFCV and 254 g CO_2 eq/km for a CFRP-based HFCV, and 258.3 g CO_2 eq/km for a conventional BEV and 165.7 g CO_2 eq/km for a CFRP-based BEV. The city in summer scenario has the lowest GHG emissions, 107 g CO_2 eq/km for a conventional HFCV and 85 g CO_2 eq/km for a CFRP-based HFCV, and 93.0 g CO_2 eq/km for a conventional BEV and 72.7 g CO_2 eq/km for a CFRP-based BEV. The manufacturing phase emissions make up a significant portion of life cycle emissions, but fewer than the operations phase. The emission contribution of the assembly, maintenance, and end of life phases is negligible.

We observed that the use of CFRP-based BEVs and HFCVs provides a significant advantage in the locations considered in this study, such as Alberta, Canada, noted for its severe long winter season. Sensitivity and uncertainty analyses were conducted to determine the most sensitive metrics and compute a possible range of life cycle GHG emissions for every scenario. The life cycle GHG emissions of HFCVs range from 85^{+17}_{-12} g CO_2 eq/km for a CFRP-based HFCV in the city in summer scenario to 382^{+99}_{-65} g CO_2 eq/km for a conventional HFCV in the highway in severe winter scenario. The life cycle GHG emissions of BEVs range from 72^{+17}_{-12} g CO_2 eq/km for a CFRP-based HFCV in the city in summer scenario to 257^{+99}_{-65} g CO_2 eq/km for a conventional BEV in the highway in severe winter scenario.

The results and discussion of this research reflect guidelines for policy and decision makers on aspects of BEVs and HFCVs that need to be refined to significantly reduce GHG emissions at a

commercial scale. The results also provide insight on the applicability of fabricating asphaltene-based carbon fiber in Alberta, Canada.

Table 34: Operational phase emissions for both conventional and CFRP HFCVs [13, 14, 29, 35]

Scenarios	**Conventional (g CO2 eq/km)**	**CFRP (g CO2 eq/km)**
City_Summer	78	54
Highway_Severe_Winter	353	223

Table 35: Life cycle emissions for both conventional and CFRP HFCV vehicles [13, 14, 29, 35]

Scenarios	**Conventional (g CO2 eq/km)**	**CFRP (g CO2 eq/km)**
City_Summer	107	85
Highway_Severe_Winter	382	254

4.2. Recommendations for Future Work

Following are the future research can be performed based on the findings of this thesis.

1. Future research should analyze, in detail, battery production, replacement, and recycling and disposal to generate robust results.
2. Future research should be conducted to develop measures on how to meet consumer demand in terms of faster charging ability and better battery driving range.
3. A detailed optimization study needs to be performed to manage and strategize the increasing electricity needs related to the use of BEVs and to examine in depth the impact that

competing options like biofuel use could have on overall LCA comparison of ICEVs and BEVs.

4. Detailed research needs to be conducted on how the driving range of HFCVs can be increased through fuel cell optimization and modifications of on-board hydrogen storage systems.
5. All vehicle types can be considered and compared in terms of net energy consumption, life cycle GHG footprint, and investment cost, considering future changes in a regional power generation mix. The developed method can be implemented for other modes of road transport such as plug-in hybrid electric vehicles, hybrid electric vehicles, biofuel-fueled vehicles, heavy buses, and freight transport.
6. A system level assessment of the implementation of BEVs and HFCVs over a long term needs to be conducted, considering the potential penetration of these vehicles in the transportation sector.

Supporting Information (Section 2)

Table 36: Equations used to compute energy calculations [10, 13, 29]

Energy consuming parameters	Equation
Energy consumed by heater / AC	Max rating power of heater * % use of max rated power demand * operational time
Energy loss due to battery efficiency	(1 - ɳ) * Max storage capacity of battery
Energy consumed in lighting	Max rating power of lights * % use of max rated power demand * operational time
Energy consumed in radio, navigation	Max rating power of radio, navigation * % use of max rated power demand * operational time
Energy consumed in seat preheating	Max rating of preheater * time of preheating
Energy dissipated due to speed restrictions, braking	% dissipated energy (1 - ɳ Reg) * max storage capacity of battery
Energy required for driving on flat roads, along with energy consumed by drag and rolling friction	(m * a + (0.5 *Cd * A * V^2 * P) + Cr * m * g) * no of km travelled
Energy required for driving on hilly roads, along with energy consumed by drag and rolling friction	(0.5 * Cd * A * V^2 * P + Cr * m * g + (1 - f) * g * sin □) * no of km travelled
Energy lost due to inefficiency of motor and controller	(1 - ɳ motor * ɳ generator) *(((m * a + 0.5 *Cd * A * V^2 * P + Cr * m * g) * no of km's travelled) + (0.5 * Cd * A * V^2 * P + Cr * m * g + (1 - f) * g * sin □) * no of km travelled)
Energy lost due to transmission loss while transferring it to grid and battery	(1 - ɳ transmission) * max storage capacity of battery
Energy loss due to depth of discharge at 90 %	10 % * ɳ efficiency * max storage capacity of battery
Force equation	F = m * a + (0.5 *Cd * A * V^2 * P) + Cr * m * g
Energy	E = F * D
Energy loss due to depth of discharge at 80 %	20 % * ɳ efficiency * max storage capacity of battery

Supporting Information (Section 3)

Table 37: Battery replacement for each scenario for both conventional and CFRP BEVs [27, 29, 34, 37]

Scenario	Conventional	Battery Lifetime (Km)	Scenario	CFRP	Battery Lifetime (Km)
Battery_C_S_Con	2.00	100,000	Battery_C_S_CF	1.00	200,000
Battery_C_MW_Con	3.00	66,666	Battery_C_MW_CF	2.00	100,000
Battery_C_SW_Con	4.00	50,000	Battery_C_SW_CF	3.00	66,666
Battery_H_S_Con	5.00	40,000	Battery_H_S_CF	3.00	66,666
Battery_H_MW_Con	6.00	33,333	Battery_H_MW_CF	4.00	50,000
Battery_H_SW_Con	8.00	25,000	Battery_H_SW_CF	4.00	50,000
Battery_R_S_Con	2.00	100,000	Battery_R_S_CF	2.00	100,000
Battery_R_MW_Con	3.00	66,666	Battery_R_MW_CF	2.00	100,000
Battery_R_SW_Con	5.00	40,000	Battery_R_SW_CF	3.00	66,666

References

1. Lopez-Behar, D., et al., Putting electric vehicles on the map: A policy agenda for residential charging infrastructure in Canada. *Energy Research & Social Science*, 2019. **50**: p. 29-37.
2. Tagliaferri, C., et al., Life cycle assessment of future electric and hybrid vehicles: A cradle-to-grave systems engineering approach. *Chemical Engineering Research and Design*, 2016. **112**: p. 298-309.
3. Kittner, N., et al., Chapter 9 - Electric vehicles, in technological learning in the transition to a low-carbon energy system, M. Junginger and A. Louwen, Editors. 2020, *Academic Press*. p. 145-163.
4. Peterson, S.B., J.F. Whitacre, and J. Apt, Net air emissions from electric vehicles: The effect of carbon price and charging strategies. *Environmental Science and Technology*., 2011. **45**(5): p. 1792.
5. Frischknecht, R. and K. Flury, Life cycle assessment of electric mobility: answers and challenges—Zurich, April 6, 2011. *The International Journal of Life Cycle Assessment*, 2011. **16**(7): p. 691-695.
6. Granovskii, M., I. Dincer, and M.A. Rosen, Life cycle assessment of hydrogen fuel cell and gasoline vehicles. *International Journal of Hydrogen Energy*, 2006. **31**(3): p. 337-352.
7. Mahmoudzadeh Andwari, A., et al., A review of Battery Electric Vehicle technology and readiness levels. *Renewable and Sustainable Energy Reviews*, 2017. **78**: p. 414-430.
8. Intergovernmental Panel on Climate Change. Transport. [cited 2021 Jnauary 7]; Available from: https://www.ipcc.ch/site/assets/uploads/2018/02/ipcc_wg3_ar5_chapter8.pdf.
9. Hawkins, T.R., O.M. Gausen, and A.H. Strømman, Environmental impacts of hybrid and electric vehicles—a review. *The International Journal of Life Cycle Assessment*, 2012. **17**(8): p. 997-1014.
10. Del Duce, A., M. Gauch, and H.-J. Althaus, Electric passenger car transport and passenger car life cycle inventories in ecoinvent version 3. *The International Journal of Life Cycle Assessment*, 2014. **21**(9): p. 1314-1326.
11. Egede, P., et al., Life cycle assessment of electric vehicles – A framework to consider influencing factors. *Journal of Manufacturing Science and Technology*, 2015. **29**: p. 233-238.
12. Wager, G., J. Whale, and T. Braunl, Driving electric vehicles at highway speeds: The effect of higher driving speeds on energy consumption and driving range for electric vehicles in Australia. *Renewable and Sustainable Energy Reviews*, 2016. **63**: p. 158-165.
13. Ahmadi, P. and E. Kjeang, Comparative life cycle assessment of hydrogen fuel cell passenger vehicles in different Canadian provinces. *International Journal of Hydrogen Energy*, 2015. **40**(38): p. 12905-12917.
14. Alaswad, A., et al., Developments in fuel cell technologies in the transport sector. *International Journal of Hydrogen Energy*, 2016. **41**(37): p. 16499-16508.
15. Doluweera, G., et al., A scenario-based study on the impacts of electric vehicles on energy consumption and sustainability in Alberta. *Applied Energy*, 2020. **268**: p. 114961.
16. Salimi, S., et al., Lateral coefficient of friction for characterizing winter road conditions. *Canadian Journal of Civil Engineering*, 2015. **43**(1): p. 73-83.

17. Zhao, Y.-Q., et al., Estimation of road friction coefficient in different road conditions based on vehicle braking dynamics. *Chinese Journal of Mechanical Engineering*, 2017. **30**(4): p. 982-990.
18. Burnham, A., M.Q. Wang, and Y. Wu, Development and applications of GREET 2.7 - The transportation vehicle-cycle model. 2006, Argonne National Laboratory, Argonne: United States. [cited 2021 Jnauary 7]; Available from: https://www.osti.gov/biblio/898530
19. Czerwinski, F., Current trends in automotive lightweighting strategies and materials. *Materials*, 2021. **14**(21).
20. Ghosh, T., et al., Life cycle energy and greenhouse gas emissions implications of using carbon fiber reinforced polymers in automotive components: Front subframe case study. *Sustainable Materials and Technologies*, 2021. **28**: p. e00263.
21. Koffler, C., Life cycle assessment of automotive lightweighting through polymers under US boundary conditions. *The International Journal of Life Cycle Assessment*, 2014. **19**(3): p. 538-545.
22. Verma, A., et al., A techno-economic assessment of bitumen and synthetic crude oil transport (SCO) in the Canadian oil sands industry: Oil via rail or pipeline? *Energy*, 2017. **124**: p. 665-683.
23. Baritto, M., A.O. Oni, and A. Kumar, The development of a techno-economic model for the assessment of vanadium recovery from bitumen upgrading spent catalyst. *Journal of Cleaner Production*, 2022. **363**: p. 132376.
24. Khan, H., et al., Continuous, pilot-scale production of carbon fiber from a textile grade panacryonitrile polymer. *Materials Today Communications*, 2022. **31**: p. 103231.
25. Redelius, P., The structure of asphaltenes in bitumen. *Road Materials and Pavement Design*, 2006. **7**: p. 143-162.
26. Environmental assessment of plug-in hybrid electric vehicles, Volume 1: Nationwide greenhouse gas emissions. 2007. [cited 2021 Jnauary 7]; Available from: https://www.energy.gov/sites/prod/files/oeprod/DocumentsandMedia/EPRI-NRDC_PHEV_GHG_report.pdf
27. Campanari, S., G. Manzolini, and F. Garcia de la Iglesia, Energy analysis of electric vehicles using batteries or fuel cells through well-to-wheel driving cycle simulations. *Journal of Power Sources*, 2009. **186**(2): p. 464-477.
28. Canals Casals, L., et al., Sustainability analysis of the electric vehicle use in Europe for CO_2 emissions reduction. *Journal of Cleaner Production*, 2016. **127**: p. 425-437.
29. Del Duce, A., et al., eLCAr: Guidelines for the LCA of electric vehicles. *The International Journal of Life Cycle Assessment,* 2013.
30. Simons, A., Road transport: new life cycle inventories for fossil-fuelled passenger cars and non-exhaust emissions in ecoinvent v3. *The International Journal of Life Cycle Assessment*, 2013. **21**(9): p. 1299-1313.
31. Faria, R., et al., A sustainability assessment of electric vehicles as a personal mobility system. *Energy Conversion and Management*, 2012. **61**: p. 19-30.

32. Kintner-Meyer, M., K. Schneider, and R. Pratt, Impact assessment of plug-in hybrid vehicles on electric utilities and regional U.S. power grids. Part 1: Technical Analysis. 2006. [cited 2021 March 7]; Available from: https://grist.org/wp content/uploads/2010/05/5-24-07-technical-analy-wellinghoff.pdf?utm_source=syndication&utm_medium=rss&utm_campaign=offshore-wind-grist
33. Jochem, P., S. Babrowski, and W. Fichtner, Assessing CO_2 emissions of electric vehicles in Germany in 2030. *Transportation Research Part A: Policy and Practice*, 2015. **78**: p. 68-83.
34. Wang, H., et al., On-road vehicle emission inventory and its uncertainty analysis for Shanghai, China. *Science of the Total Environmental*, 2008. **398**(1-3): p. 60-7.
35. Wong, E.Y., et al., Life cycle assessment of electric vehicles and hydrogen fuel cell vehicles using the GREET model—A comparative study. Sustainability, 2021. **13**(9).
36. Huo, H., et al., Environmental implication of electric vehicles in China. *Environmental Science & Technology*, 2010. **44**(13): p. 4856-4861.
37. Greenswarak. The effect of depth of discharge on cycle life of a battery. [cited 2021 March 22]; Available from: https://greensarawak.com/wp-content/uploads/2017/12/deapthofdischargeandcyclelife.jpg.
38. Iclodean, C., et al., Comparison of different battery types for electric vehicles. conference series: *Materials Science and Engineering*, 2017. **252**: p. 012058.
39. Longo, S., et al., Life cycle assessment of storage systems: the case study of a sodium/nickel chloride battery. *Journal of Cleaner Production*, 2014. **85**: p. 337-346.
40. Marsh, R.A., P.G. Russell, and T.B. Reddy, Bipolar lithium-ion battery development. J. *Power Sources*. **65**(1−2): p. 133.
41. Hedegaard, K., et al., Effects of electric vehicles on power systems in Northern Europe. *Energy*, 2012. **48**(1): p. 356-368.
42. De Tena DL, P.T., Impact of electric vehicles on a future renewable energy-based power system in Europe with a focus on Germany. *International Journal of Energy Research*, 2018.
43. García Sánchez, J.A., et al., Comparison of Life Cycle energy consumption and GHG emissions of natural gas, biodiesel and diesel buses of the Madrid transportation system. *Energy*, 2012. **47**(1): p. 174-198.
44. Hawkins, T.R., et al., Comparative environmental life cycle assessment of conventional and electric vehicles. *Journal of Industrial Ecology*, 2012. **17**(1): p. 53-64.
45. Bellocchi, S., et al., Positive interactions between electric vehicles and renewable energy sources in CO_2-reduced energy scenarios: The Italian case. *Energy*, 2018. **161**: p. 172-182.
46. Faria, R., et al., Impact of the electricity mix and use profile in the life-cycle assessment of electric vehicles. *Renewable and Sustainable Energy Reviews*, 2013. **24**: p. 271-287.
47. McCarthy, R. and C. Yang, Determining marginal electricity for near-term plug-in and fuel cell vehicle demands in California: Impacts on vehicle greenhouse gas emissions. J. *Power Sources*, 2010. **195**(7): p. 2099.
48. Candelaresi, D., et al., Comparative life cycle assessment of hydrogen-fuelled passenger cars. *International Journal of Hydrogen Energy*, 2021. **46**(72): p. 35961-35973.
49. Teulon, H. and P. Osset, Life cycle analysis of a complex product, application of International Organization for Standardization 14040 to a complete car., *Society of Automotive Engineers International*, 1998.

50. Mehmeti, A., et al., Life cycle assessment and water footprint of hydrogen production methods: from conventional to emerging technologies. *Environments*, 2018. **5**(2).
51. Ptasinski, K.K., Efficiency analysis of hydrogen production methods from biomass. *International Journal of Alternative Propulsion*, 2008. **2**: p. 39-49.
52. Valente, A., et al., Using harmonised life-cycle indicators to explore the role of hydrogen in the environmental performance of fuel cell electric vehicles. *International Journal of Hydrogen Energy*, 2020. **45**(47): p. 25758-25765.
53. Pehnt, M. Life-cycle analysis of fuel cell system components. *International Journal of Hydrogen Energy* 2010.
54. De Cicco, D. and F. Taheri, Performances of magnesium- and steel-based 3D fiber-metal laminates under various loading conditions. *Composite Structures*, 2019. **229**: p. 111390.
55. Upadhyayula, V.K.K., et al., Lightweighting and electrification strategies for improving environmental performance of passenger cars in India by 2030: A critical perspective based on life cycle assessment. *Journal of Cleaner Production*, 2019. **209**: p. 1604-1613.
56. Schmidt, W.P., et al., Life cycle assessment of lightweight and end-of-life scenarios for generic compact class passenger vehicles. *The International Journal of Life Cycle Assessment* , 2004. **9**(6): p. 405.
57. Witik, R.A., et al., Assessing the life cycle costs and environmental performance of lightweight materials in automobile applications. *Composites Part A: Applied Science and Manufacturing*, 2011. **42**(11): p. 1694-1709.
58. Das, S., et al., Vehicle lightweighting energy use impacts in U.S. light-duty vehicle fleet. *Sustainable Materials and Technologies*, 2016. **8**: p. 5-13.
59. Belingardi, G., et al., Alternative lightweight materials and component manufacturing technologies for vehicle frontal bumper beam. *Composite Structures*, 2015. **120**: p. 483-495.
60. Patil, A., A.A. Patel, and R. Purohit, An overview of polymeric materials for automotive applications. *Materials Today: Proceedings*, 2017. **4**: p. 3807-3815.
61. Intergovernmnetal Panel on Climate Change, 2014: Synthesis report. Contribution of working groups I, II and III to the fifth assessment report of the Intergovernmental Panel on Climate Change, Core Writing Team, R.K. Pachauri, and L.A. Meyer, Editors. 2014: Geneva, Switzerland, [cited 2021 March 7]; Available from: https://www.ipcc.ch/report/ar5/syr/
62. Abraham, S., et al., Impact on climate change due to transportation sector – Research prospective. *Procedia Engineering*, 2012. **38**: p. 3869-3879.
63. Environment and climate change Canada, National inventory report 1990 - 2016: greenhouse gas sources and sinks in Canada. 1990 - 2016, Canada's Greenhouse gas inventory: Canada. [cited 2021 March 7]; Available from: https://publications.gc.ca/site/eng/9.506002/publication.html
64. United Nations Framework Convention on Climate Change. The paris agreement. 2016 [cited 2021 November 4]; Available from: https://unfccc.int/process-and-meetings/the-paris-agreement/the-paris-agreement#:~:text=The%20Paris%20Agreement%20is%20a%20legally%20binding%20international,to%201.5%20degrees%20Celsius%2C%20compared%20to%20pre-industrial%20levels.

65. Karaaslan, E., Y. Zhao, and O. Tatari, Comparative life cycle assessment of sport utility vehicles with different fuel options. *The International Journal of Life Cycle Assessment*, 2018. **23**(2): p. 333-347.
66. Bauer, C., et al., The environmental performance of current and future passenger vehicles: Life cycle assessment based on a novel scenario analysis framework. *Applied Energy*, 2015. **157**: p. 871-883.
67. Ramachandran, S. and U. Stimming, Well to wheel analysis of low carbon alternatives for road traffic. *Energy & Environmental Science*, 2015. **8**(11): p. 3313-3324.
68. Intergovernmental Panel on Climate Change, Global warming of 1.5°c.an Intergovernmental Panel on Climate Change special report on the impacts of global warming of 1.5°c above pre-industrial levels and related global greenhouse gas emission pathways, in the context of strengthening the global response to the threat of climate change, sustainable development, and efforts to eradicate poverty ed. v. masson-delmotte, et al. 2018: In Press [cited 2021 November 5]; Available from: https://www.ipcc.ch/sr15/
69. Rogelj, J., et al., Mitigation pathways compatible with 1.5°C in the context of sustainable development, in global warming of 1.5°C. an Intergovernmental Panel on Climate Change special report on the impacts of global warming of 1.5°c above pre-industrial levels and related global greenhouse gas emission pathways, in the context of strengthening the global response to the threat of climate change, sustainable development, and efforts to eradicate poverty v. masson-delmotte, et al., editors. 2018, [cited 2021 November 5]; Available from: https://www.ipcc.ch/sr15/
70. Zhang, R. and S. Fujimori, The role of transport electrification in global climate change mitigation scenarios. *Environmental Research Letters*, 2020. **15**(3): p. 034019.
71. Ellingsen, L.A.-W., B. Singh, and A.H. Strømman, The size and range effect: lifecycle greenhouse gas emissions of electric vehicles. *Environmental Research Letters,* 2016. **11**(5): p. 054010.
72. Ellingsen, L., C. Hung, and A. Strømman, Identifying key assumptions and differences in life cycle assessment studies of lithium-ion traction batteries with focus on greenhouse gas emissions. *Transportation Research Part D: Transport and Environment*, 2017. **55**: p. 82-90.
73. Streets, D.G., et al., Anthropogenic mercury emissions in China. *Atmospheric Environment*, 2005. **39**: p. 7789.
74. Czerwinski, F., Current trends in automotive lightweighting strategies and materials. *Materials (Basel, Switzerland)*, 2021. **14**(21): p. 6631.
75. Patil, A., A. Patel, and R. Purohit, An overview of polymeric materials for automotive applications. *Materials Today: Proceedings*, 2017. **4**(2, Part A): p. 3807-3815.
76. Osborne, J., Automotive composites – In touch with lighter and more flexible solutions. *Metal Finishing*, 2013. **111**(2): p. 26-30.
77. Baritto, M., A.O. Oni, and A. Kumar, Estimation of life cycle GHG emissions of asphaltene-based carbon fibers derived from oil sands bitumen. *Sustainable Materials and Technologies*, 2022.
78. Notter, D.A., et al., Contribution of Li-ion batteries to the environmental impact of electric vehicles. *Environmental Science & Technology*, 2010. **44**(17): p. 6550-6556.
79. Samaras, C. and K. Meisterling, Life cycle assessment of greenhouse gas emissions from plug-in hybrid vehicles: Implications for policy. *Environmental Science & Technology*, 2008. **42**(9): p. 3170-3176.

80. Garcia, R., J. Gregory, and F. Freire, Dynamic fleet-based life-cycle greenhouse gas assessment of the introduction of electric vehicles in the Portuguese light-duty fleet. *The International Journal of Life Cycle Assessment*, 2015. **20**(9): p. 1287-1299.
81. Ma, H., et al., A new comparison between the life cycle greenhouse gas emissions of battery electric vehicles and internal combustion vehicles. *Energy Policy*, 2012. **44**: p. 160-173.
82. Van Mierlo, J., M. Messagie, and S. Rangaraju, Comparative environmental assessment of alternative fueled vehicles using a life cycle assessment. *Transportation Research Procedia*, 2017. **25**: p. 3435-3445.
83. Glensor, K. and M.R. Muñoz B, Life-cycle assessment of Brazilian transport biofuel and electrification pathways. *Sustainability*, 2019. **11**(22).
84. Weis, A., et al., Emissions and cost implications of controlled electric vehicle charging in the u.s. pjm interconnection. *Environmental Science & Technology*, 2015. **49**(9): p. 5813-5819.
85. Onat, N.C., M. Kucukvar, and O. Tatari, Conventional, hybrid, plug-in hybrid or electric vehicles? State-based comparative carbon and energy footprint analysis in the United States. *Applied Energy*, 2015. **150**: p. 36-49.
86. Andersson, Ö. and P. Börjesson, The greenhouse gas emissions of an electrified vehicle combined with renewable fuels: Life cycle assessment and policy implications. *Applied Energy*, 2021. **289**: p. 116621.
87. International Organization for Standardization, 14040: 1997—Environmental management—Life cycle assessment-principles and framework. International Organization for Standardization, Switzerland, 2003. [cited 2021 November 5]; Available from: https://www.iso.org/standard/37456.html
88. International Organization for Standardization, 14040: Environmental management−Life cycle assessment−Requirements and guidelines. 2006. 54. [cited 2021 November 5]; Available from: https://www.iso.org/standard/37456.html
89. Koffler, C., et al., On the reporting and review requirements of International Organization for Standardization 14044. *The International Journal of Life Cycle Assessment*, 2020. **25**(3): p. 478-482.
90. International Organization for Standardization, 14040:2006 Environmental management -- Life cycle assessment -- Principles and framework. 2006, International Organization for Standardization: Geneva. [cited 2021 November 22]; Available from: https://www.iso.org/standard/37456.html
91. International Organization for Standardization, 14044:2006 Environmental management -- Life cycle assessment -- Requirements and guidelines. 2006, International Organization for Standardization (ISO): Geneva. [cited 2021 November 22]; Available from: https://www.iso.org/standard/37456.html
92. Fang, Y., et al. Modeling dynamic vehicle age distribution in Beijing. in Proceedings of the 2003. *IEEE International Conference on Intelligent Transportation Systems*, 2003.
93. Huo, H., et al., Projection of Chinese motor vehicle growth, oil demand, and CO_2 emissions through 2050. 69. [cited 2021 November 22]; Available from: https://www.researchgate.net/publication/270213183_Projection_of_Chinese_Motor_Vehicle_Growth_Oil_Demand_and_CO_2_Emissions_Through_2050

94. Amasawa, E., et al., Environmental performance of an electric vehicle composed of 47% polymers and polymer composites. *Sustainable Materials and Technologies*, 2020. **25**: p. e00189.
95. Bartolozzi, I., F. Rizzi, and M. Frey, Comparison between hydrogen and electric vehicles by life cycle assessment: A case study in Tuscany, Italy. *Applied Energy*, 2011. **101**: p. 103-111.
96. Balpreet Kukreja and University of British Columbia Sustainability Scholar, Life cycle analysis of electric vehicles: Quantifying the impact 2018, The University of British Columbia sustainability Vancouver, Canada. [cited 2021 November 22]; Available from: https://sustain.ubc.ca/sites/default/files/2018-63%20Lifecycle%20Analysis%20of%20Electric%20Vehicles_Kukreja.pdf
97. Government of Canada, Electric vehicles in Canada. [cited 2021 November 22]; Available from: https://tc.canada.ca/en/road-transportation/innovative-technologies/zero-emission-vehicles
98. Association, Canada. Government incentives for electirc vehicles. [cited 2021 November 26]; Available from: https://www.caa.ca/electric-vehicles/government-incentives/.
99. Canada, Alberta. New federal funding for zero emission vehicle purchase incentives and charging infrastructure in 2020 fall economic statement. Available from: https://electricautonomy.ca/2020/12/11/canada-federal-ev-rebate/.
100. Alberta, Climate change and transportation. 2018, Canada's offical greengouse gas inventory: Alberta, Canada. [cited 2021 November 26]; Available from: https://www.canada.ca/en/environment-climate-change/services/climate-change/greenhouse-gas-emissions/inventory.html
101. Alberta Innovates. Carbon Fibre Grand Challenge. 2021 [cited 2021 16 September]; Available from: https://albertainnovates.ca/programs/carbon-fibre-grand-challenge/.
102. Government of Canada, Alberta - Weather Conditions and forecast by locations. [cited 2021 16 September]; Available from: https://weather.gc.ca/forecast/canada/index_e.html?id=AB.
103. Pryshlakivsky, J. and C. Searcy, An uncertainty analysis of the energy intensity of 37 materials used in automobile manufacturing: Statistical methods and recommendations. *Sustainable Production and Consumption*, 2020. **24**: p. 12-25.
104. Nissan Intelligent Mobility. Nissan electric vehicle 2021 [cited 2021 July 15]; Available from: https://www.nissanusa.com/vehicles/electric-cars/leaf.html.
105. Wang, M., GREET 1.5 - Transportation fuel-cycle model, Vol. 1: Methodology, use, and results, and vol. 2, Detailed Results. 1999. [cited 2021 July 23]; Available from: https://www.osti.gov/biblio/14775
106. Wang, M., Development and use of GREET 1.6 fuel-cycle model for transportation fuels and vehicle technologies. 2001. [cited 2021 July 23]; Available from: https://www.researchgate.net/publication/236472582_Development_and_Use_of_GREET_16_fuel-cycle_model_for_transportation_fuels_and_vehicle_technologies
107. Alberta Utilities Commission. Annual electricity data. 2019 [cited 2021 13 September]; Available from: http://www.auc.ab.ca/pages/annual-electricity-data.aspx.
108. Davis, M., M. Ahiduzzaman, and A. Kumar, How will Canada's greenhouse gas emissions change by 2050? A disaggregated analysis of past and future greenhouse gas emissions using bottom-up energy modelling and Sankey diagrams. *Applied energy*, 2018. **220**: p. 754-786.

109. Davis, M., et al., Assessment of renewable energy transition pathways for a fossil fuel-dependent electricity-producing jurisdiction. *Energy for Sustainable Development*, 2020. **59**: p. 243-261.
110. TransportPolicy.net. International: Light-duty: Worldwide harmonized Light duty Vehicles Test Procedure. 2021 [cited 2021 November 15]; Available from: https://www.transportpolicy.net/standard/international-light-duty-worldwide-harmonized-light-vehicles-test-procedure-wltp/.
111. Group, J.D., Development of World-wide Light-duty Test Cycle. 2011: Stockholm, Sweden. [cited 2021 November 15]; Available from: https://unece.org/fileadmin/DAM/trans/doc/2015/wp29grpe/GRPE-72-02.pdf
112. Japan DHC Group. Development of World harmonized Light-duty Test Cycle. 2011 [cited 2021 July 15]; Available from: https://unece.org/fileadmin/DAM/trans/doc/2011/wp29grpe/WLTP-DHC-09-02e.pdf.
113. Governmnet of Canada. Alberta - Weather conditions and forecast by locations. 2021 [cited 2021 June 10]; Available from: https://weather.gc.ca/forecast/canada/index_e.html?id=AB.
114. Timmers, V.R.J.H. and P.A.J. Achten, Non-exhaust particulate matter emissions from electric vehicles. *Atmospheric Environment*, 2016. **134**: p. 10-17.
115. Müller, M., F. Biedenbach, and J. Reinhard, Development of an integrated simulation model for load and mobility profiles of private households. *Energies*, 2020. **13**(15).
116. Laboratory, A.N., Projection of Chinese motor vehicle growth, oil demand, and CO_2 emissions through 2050. 2006, U.S. department of energy: Tennessee. [cited 2021 June 10]; Available from: https://journals.sagepub.com/doi/10.3141/2038-09
117. Kawamoto, R., et al., Estimation of CO2 Emissions of Internal Combustion Engine Vehicle and Battery Electric Vehicle Using LCA. *Sustainability*, 2019. **11**(9): p. 2690.
118. 2001 National Household Travel Survey. 2004. [cited 2021 June 10]; Available from: https://nhts.ornl.gov/2001/usersguide/UsersGuide.pdf
119. Gao, L. and Z. Winfield, Life Cycle Assessment of Environmental and Economic Impacts of Advanced Vehicles. *Energies*, 2012. **5**.
120. Bakker, D., Battery electric vehicles performance, CO_2 emissions, lifecycle costs and advanced battery technology development 2010, Copernicus institute University of Utrecht. [cited 2021 June 10]; Available from: https://www.academia.edu/30578520/Battery_Electric_Vehicles_Performance_CO2_emissions_lifecycle_costs_and_advanced_battery_technology_development
121. Milligan, R., Drive cycles for battery electric vehicles and their fleet management. 2017: p. 489-555. [cited 2021 June 10]; Available from: https://www.researchgate.net/publication/322492597_Drive_cycles_for_battery_electric_vehicles_and_their_fleet_management
122. Greenswarak. The effect of depth of discharge on cycle life of a battery. 2017 [cited 2021 March 10]; Available from: https://greensarawak.com/wp-content/uploads/2017/12/deapthofdischargeandcyclelife.jpg.
123. Bartolozzi, I., F. Rizzi, and M. Frey, Comparison between hydrogen and electric vehicles by life cycle assessment: A case study in Tuscany, Italy. *Applied Energy*, 2013. **101**: p. 103-111.
124. Nemry, F., et al., Environmental Improvement of Passenger Cars. 2008. [cited 2021 March 10]; Available from: https://ec.europa.eu/environment/ipp/pdf/jrc_report.pdf

125. Jeff Staudinger and Gregory A. Keoleian, Management of End-of Life Vehicles (ELVs) in the US. 2001, Center for Sustainable System: University of Michigan: Michigan, U.S. [cited 2021 March 10]; Available from: https://css.umich.edu/publications/research-publications/management-end-life-vehicles-elvs-us
126. Mobility, NISSAN electrci vehicle 2021. [cited 2021 March 10]; Available from: https://www.nissanusa.com/vehicles/electric-cars/leaf.html.
127. Müller, M., F. Biedenbach, and J. Reinhard, Development of an integrated simulation model for load and mobility profiles of private households. *Energies*, 2020. **13**(15): p. 3843.
128. Perilhon, C., et al., Life cycle assessment applied to electricity generation from renewable biomass. *Energy Procedia*, 2012. **18**: p. 165-176.
129. Administration, U.S., 2009 National household travel survey: User's guide, Administration, Editor. 2011: U.S. [cited 2021 March 10]; Available from: https://www.nrel.gov/transportation/secure-transportation-data/assets/pdfs/2009-national-household-travel-survey-user-guide.pdf
130. Vancouver, Canada, Life cycle analysis of electric vehicles. 2018, The University of British Columbia, Sustainability: Vancouver, Canada. [cited 2021 March 10]; Available from: https://sustain.ubc.ca/sites/default/files/2018-63%20Lifecycle%20Analysis%20of%20Electric%20Vehicles_Kukreja.pdf
131. Brazil biofuels annual. 2020. [cited 2021 March 10]; Available from: https://apps.fas.usda.gov/newgainapi/api/Report/DownloadReportByFileName?fileName=Biofuels%20Annual_Sao%20Paulo%20ATO_Brazil_08-03-2020.
132. Vancouver, C.o., 2019 Vancouver panel survey report 2020, McElhanney: 200-858 Beatty street Vancouver BC. [cited 2021 March 10]; Available from: https://vancouver.ca/files/cov/2020-transportation-panel-survey.pdf
133. Province of British Columbia. The National Household Survey. [cited 2021 September 12]; Available from: https://www2.gov.bc.ca/gov/content/home/copyright.
134. Huijbregts, M.A., Application of uncertainty and variability in LCA. *The International Journal of Life Cycle Assessment*, 1998. **3**(5): p. 273-280.
135. Di Lullo, G., et al., Extending sensitivity analysis using regression to effectively disseminate life cycle assessment results. *The International Journal of Life Cycle Assessment*, 2020. **25**(2): p. 222-239.
136. Campolongo, F., J. Cariboni, and A. Saltelli, An effective screening design for sensitivity analysis of large models. *Environmental Modelling & Software*, 2007. **22**(10): p. 1509-1518.
137. Canadian Automobile Association . Electric vehicles. 2021 [cited 2021 June 12]; Available from: https://www.caa.ca/electric-vehicles/faq-electric-vehicles/.
138. Schweimer, G.W. and M. Levin, Life Cycle Inventory for the Golf A4. 2000. [cited 2021 June 12]; Available from: https://escholarship.org/content/qt3vh4v00t/qt3vh4v00t_noSplash_1c1c1684debd5c524f4a0904ed38d3fb.pdf?t=krn8rr
139. Forcellese, A., et al., Life cycle impact assessment of different manufacturing technologies for automotive carbon fiber reinforced plastic components. *Journal of Cleaner Production*, 2020. **271**: p. 122677.
140. Nissan Intelligent Mobility. Nissan electric vehicle 2021 [cited 2021 July 10]; Available from: https://www.nissanusa.com/vehicles/electric-cars/leaf.html.

141. United Nations, Climate Change Impacts and Adaption for Transport Network and Nodes. 2020, UNECE: Geneva, Switzerland. [cited 2021 July 10]; Available from: https://unece.org/sites/default/files/2021-01/ECE-TRANS-283e_web.pdf
142. Environment and climate change, Canada, National inventory report 1990 - 2016: Greenhouse gas sources and sinks in Canada. 1990 - 2016, Canada's greenhouse gas inventory: Canada. [cited 2021 July 10]; Available from: https://publications.gc.ca/site/eng/9.506002/publication.html
143. Santos, G., Road transport and CO_2 emissions: What are the challenges? *Transport Policy*, 2017. **59**: p. 71-74.
144. Nikolaidis, P. and A. Poullikkas, A comparative overview of hydrogen production processes. *Renewable and Sustainable Energy Reviews*, 2017. **67**: p. 597-611.
145. Bento, N., 15 - Investment in the infrastructure for hydrogen passenger cars—New hype or reality?, in Compendium of Hydrogen Energy, R.B. Gupta, A. Basile, and T.N. Veziroğlu, Editors. 2016, *Woodhead Publishin*g. p. 379-409.
146. Dincer, I., Environmental and sustainability aspects of hydrogen and fuel cell systems. *International Journal of Energy Research*, 2007. **31**(1): p. 29-55.
147. Moro, A. and L. Lonza, Electricity carbon intensity in European Member States: Impacts on GHG emissions of electric vehicles. *Transportation research. Part D, Transport and Environment*, 2018. **64**: p. 5-14.
148. Huang, Z. and X. Zhang, Well-to-wheels analysis of hydrogen based fuel-cell vehicle pathways in Shanghai. *Energy*, 2006. **31**(4): p. 471-489.
149. Hooftman, N., et al., A review of the European passenger car regulations – Real driving emissions vs local air quality. *Renewable and Sustainable Energy Reviews*, 2018. **86**: p. 1-21.
150. Lee, D.-Y., et al., Life-cycle implications of hydrogen fuel cell electric vehicle technology for medium- and heavy-duty trucks. *Journal of Power Sources*, 2018. **393**: p. 217-229.
151. Usai, L., et al., Life cycle assessment of fuel cell systems for light duty vehicles, current state-of-the-art and future impacts. *Journal of Cleaner Production*, 2021. **280**: p. 125086.
152. Hussain, M.M., I. Dincer, and X. Li, A preliminary life cycle assessment of fuel cell powered automobiles. *Applied Thermal Engineering*, 2007. **27**(13): p. 2294-2299.
153. Briguglio, N., et al., New simulation tool helping a feasibility study for renewable hydrogen bus fleet in Messina. *International Journal of Hydrogen Energy*, 2008. **33**(12): p. 3077-3084.
154. Nigro, N. and S. Jiang. Lifecycle greenhouse gas emissions from different light-duty vehicle and fuel pathways: A synthesis of recent research. 2013. [cited 2021 July 10]; Available from: https://www.c2es.org/document/lifecycle-greenhouse-gas-emissions-from-different-light-duty-vehicle-and-fuel-pathways-a-synthesis-of-recent-research/
155. Staffell, I., et al., The role of hydrogen and fuel cells in the global energy system. *Energy & Environmental Science*, 2019. **12**(2): p. 463-491.
156. Colella, W.G., M.Z. Jacobson, and D.M. Golden, Switching to a U.S. hydrogen fuel cell vehicle fleet: The resultant change in emissions, energy use, and greenhouse gases. *Journal of Power Sources*, 2005. **150**: p. 150-181.
157. Miotti, M., J. Hofer, and C. Bauer, Integrated environmental and economic assessment of current and future fuel cell vehicles. *The International Journal of Life Cycle Assessment*, 2017. **22**(1): p. 94-110.

158. Simons, A. and C. Bauer, A life-cycle perspective on automotive fuel cells. *Applied Energy*, 2015. **157**: p. 884-896.
159. An, F., et al., Passenger vehicle greenhouse gas and fuel economy standards: A global update. 2007. [cited 2021 July 10]; Available from: https://theicct.org/sites/default/files/publications/PV_standards_2007.pdf
160. Park, K.Y., J.H. Choi, and D.G. Lee, Delamination-free and high efficiency drilling of carbon fiber reinforced plastics. *Journal of Composite Materials*, 1995. **29**(15): p. 1988-2002.
161. Innovates, Alberta. bitumen beyond combustion. [cited 2021 July 10]; Available from: https://albertainnovates.ca/programs/bitumen-beyond-combustion/.
162. Luk, J.M., et al., Greenhouse gas emission benefits of vehicle lightweighting: Monte Carlo probabalistic analysis of the multi material lightweight vehicle glider. *Transportation Research Part D: Transport and Environment*, 2018. **62**: p. 1-10.
163. Athanasopoulou, L., H. Bikas, and P. Stavropoulos, Comparative well-to-wheel emissions assessment of internal combustion engine and battery electric vehicles. *Journal of Manufacturing Science and Technology*, 2018. **78**: p. 25-30.
164. Dai, Q., et al., Life Cycle Analysis of Lithium-Ion Batteries for Automotive Applications. *Batteries*, 2019. **5**(2): p. 48.
165. Peng, T., X. Ou, and X. Yan, Development and application of an electric vehicles life-cycle energy consumption and greenhouse gas emissions analysis model. *Chemical Engineering Research and Design*, 2018. **131**: p. 699-708.
166. Brodrick, C.-J., et al., Evaluation of fuel cell auxiliary power units for heavy-duty diesel trucks. *Transportation Research Part D: Transport and Environment*, 2002. **7**(4): p. 303-315.
167. Gemechu, E.D. and A. Kumar, Chapter 12 - The environmental performance of hydrogen production pathways based on renewable sources, in Renewable-Energy-Driven Future, J. Ren, Editor. 2021, Academic Press. p. 375-406. [cited 2021 July 10]; Available from: https://www.elsevier.com/books/renewable-energy-driven-future/ren/978-0-12-820539-6
168. Zhao, G. and A.S. Pedersen, Life cycle assessment of hydrogen production and consumption in an isolated territory. *Journal of Manufacturing Science and Technology*, 2018. **69**: p. 529-533.
169. Oni, A.O., et al., Comparative assessment of blue hydrogen from steam methane reforming, autothermal reforming, and natural gas decomposition technologies for natural gas-producing regions. *Energy Conversion and Management*, 2022. **254**: p. 115245.
170. Wang, M., et al., Projection of Chinese motor vehicle growth, oil demand, and CO2 emissions through 2050. 2006. [cited 2021 July 10]; Available from: https://journals.sagepub.com/doi/10.3141/2038-09
171. Wang, M., et al., Hydrogen production by methane steam reforming using metallic nickel hollow fiber membranes. *Journal of Membrane Science,* 2021. **620**: p. 118909.
172. Peng, X. and Q. Jin, Molecular simulation of methane steam reforming reaction for hydrogen production. *International Journal of Hydrogen Energy,* 2022. **47**(12): p. 7569-7585.
173. Vlieger, I.D., D.D. Keukeleere, and J. Kretzschmar, Environmental effects of driving behaviour and congestion related to passenger cars. *Atmospheric Environment*, 2000. **34**: p. 4649-4655.

174. Canadian Construction Association, Electric vehicles. [cited 2021 July 19]; Available from: https://www.caa.ca/electric-vehicles/faq-electric-vehicles/.

Appendix A

Operation phase calculations were done as per the equations given in Table A1.

Table A 1: Operation phase energy calculation equations

Energy consuming parameters	Equation
Energy consumed by heater / AC	Max rating power of heater * % use of max rated power demand * operational time
Energy loss due to battery efficiency	(1 - ɲ) * Max storage capacity of battery
Energy consumed in lighting	Max rating power of lights * % use of max rated power demand * operational time
Energy consumed in radio, navigation	Max rating power of radio, navigation * % use of max rated power demand * operational time
Energy consumed in seat preheating	Max rating of preheater * time of preheating
Energy dissipated due to speed restrictions, braking	% dissipated energy (1 - ɲ Reg) * max storage capacity of battery
Energy required for driving on flat roads, along with energy consumed by drag and rolling friction	(m * a + (0.5 *Cd * A * V^2 * P) + Cr * m * g) * no of km travelled
Energy required for driving on hilly roads, along with energy consumed by drag and rolling friction	(0.5 * Cd * A * V^2 * P + Cr * m * g + (1 - f) * g * sin □) * no of km travelled
Energy lost due to inefficiency of motor and controller	(1 - ɲ motor * ɲ generator) *(((m * a + 0.5 *Cd * A * V^2 * P + Cr * m * g) * no of km's travelled) + (0.5 * Cd * A * V^2 * P + Cr * m * g + (1 - f) * g * sin □) * no of km travelled)
Energy lost due to transmission loss while transferring it to grid and battery	(1 - ɲ transmission) * max storage capacity of battery
Energy loss due to depth of discharge at 90 %	10 % * ɲ efficiency * max storage capacity of battery
Force equation	F = m * a + (0.5 *Cd * A * V^2 * P) + Cr * m * g
Energy	E = F * D
Energy loss due to depth of discharge at 80 %	20 % * ɲ efficiency * max storage capacity of battery

Table A 2: Symbols for operation phase parameters

Symbol	Parameter
F	Force
m	Mass
a	Acceleration
Cd	Drag coefficient
A	Area
V	Velocity
P	Density
g	Acceleration due to gravity
E	Energy or work
□	Average slope of uphill roads
f	Regeneration energy
ɳ	Efficiency of battery
ɳ Reg	Regenerative efficiency